UNIVERSIDADE FEDERAL DE PERNAMBUCO
CENTRO DE INFORMÁTICA
PROGRAMA DE PÓS-GRADUAÇÃO EM CIÊNCIA DA COMPUTAÇÃO

DANIELA RAPOSO NUNES DE MELLO

Which is the most suitable scanner resolution for documents?

Recife

2025

DANIELA RAPOSO NUNES DE MELLO

Which is the most suitable scanner resolution for documents?

Dissertação de Mestrado apresentada ao Programa de Pós-graduação em Ciência da Computação do Centro de Informática da Universidade Federal de Pernambuco, como requisito parcial para obtenção do grau de Mestre em Ciência da Computação.

Área de Concentração: Processamento e Síntese de Mídias e Interação

Orientador: Prof. Dr. Rafael Dueire Lins

Coorientador: Prof. Dr. Raimundo Oliveira

Recife

2025

.Catalogação de Publicação na Fonte. UFPE - Biblioteca Central

Mello, Daniela Raposo Nunes de.
   Which is the most suitable scanner resolution for documents? / Daniela Raposo Nunes de Mello. - Recife, 2025.
   80f.: il.

   Dissertação (Mestrado) - Universidade Federal de Pernambuco, Centro de Informática, Programa de Pós-Graduação em Ciência da Computação, 2025.
   Orientação: Rafael Dueire Lins.
   Coorientação: Raimundo Corrêa de Oliveira.
   Inclui referências e apêndices.

   1. Image resolution; 2. Document digitization; 3. Nyquist-Shannon Theorem. I. Lins, Rafael Dueire. II. Oliveira, Raimundo Corrêa de. III. Título.

UFPE-Biblioteca Central

Daniela Raposo Nunes de Mello

“Which is the most suitable scanner resolution for documents?

Dissertação de mestrado apresentada ao Programa de Pós-Graduação em Ciência da Computação da Universidade Federal de Pernambuco, como requisito parcial para a obtenção do título de Mestre em Ciência da Computação. Área de Concentração: Mídia e Interação.

Aprovado em: 27/01/2025.

RESUMO

Definir a resolução correta de imagem para digitalização de documentos é essencial para garantir a preservação precisa de todas as informações necessárias e, ao mesmo tempo, otimizar a eficiência de aquisição, o tempo de processamento, a demanda de armazenamento e a largura de banda de transmissão. É fundamental que a resolução de digitalização garanta que o documento digitalizado, quando impresso em alta resolução nas dimensões originais, mantenha integralmente as informações do documento original, de forma a propiciar a preservação e manutenção da informação. Apesar de sua importância para a engenharia e preservação de documentos, os atuais padrões e recomendações de digitalização baseiam-se predominantemente em evidências experimentais e conhecimento empírico. Considerando esses parâmetros, a questão crucial "Qual é a resolução de digitalização mais adequada para documentos?" foi recentemente levantada pelo Professor George Nagy, um dos pesquisadores pioneiros na Engenharia de Documentos, destacando uma preocupação de longa data que não foi devidamente esclarecida pela comunidade de pesquisa. Este trabalho propõe uma resposta fundamentada nos princípios do teorema de Nyquist-Shannon da Teoria da Informação, esta abordagem tem por objetivo fornecer uma fundamentação teórica para a definição adequada da resolução na digitalização de documentos, de forma a assegurar a preservação das informações.

Palavras-chaves: Resolução de imagem. Digitalização de documentos. Teorema de Nyquist-Shannon

ABSTRACT

Defining the correct image resolution for document digitization is essential to ensure the accurate preservation of all necessary information while optimizing acquisition efficiency, processing time, storage demand, and the transmission bandwidth. It is crucial that the digitization resolution ensures that the digitized document, when printed in a high resolution at its original dimensions, fully retains the information from the original document, thus enabling the preservation and maintenance of the information. Despite its importance for document engineering and preservation, current digitization standards and recommendations are predominantly based on experimental evidence and empirical knowledge. Considering these parameters, the crucial question, "Which is the most suitable resolution for document digitization?" was recently raised by Professor George Nagy, one of the pioneers in Document Engineering, highlighting a long-standing concern that has not been adequately addressed by the research community. This work proposes an answer based on the principles of the Nyquist-Shannon theorem from Information Theory, this approach aims to provide a theoretical foundation for determining the appropriate resolution for document digitization, ensuring the preservation of information.

Keywords: Image resolution. Document digitization. Nyquist-Shannon Theorem.

LIST OF FIGURES

LIST OF CODES

LIST OF BOARDS

LIST OF TABLES

LIST OF ACRONYMS

BMP	Windows Bitmap
bpp	bits per pixel
cm	centimeters
DocEng'24	ACM Symposium on Document Engineering 2024
dpi	dots per inch
HF	Highest frequency
ICDAR	International Conference on Document Analysis and Recognition
in	inches
LD	Levenshtein Distance
lp/mm	line pairs per millimeter
MB	megabytes
mm	millimeters
OCR	Optical Character Recognition
PNG	Portable Networks Graphics
PSM	Page Segmentation Mode
pt	points
RGB	Red Green Blue
TIFF	Tagged Image Format

LIST OF SYMBOLS

Δ	Delta
σ	Sigma
μ	Mi
π	Pi

CONTENTS

1 INTRODUCTION

The correct determination of scanning resolution is essential to ensure that all information present in a document, especially in historical documents, is accurately captured. According to The Library of Congress (2014), the choice of spatial and tonal resolution directly impacts the quality of document preservation in digital images. If the scanning resolution is set too low, critical elements of the document may be lost, conversely, excessively high resolution drastically increases scanner acquisition time yielding too large images that are slow to process and claim unnecessary storage space and computer bandwidth for network transmission.

Back in 1991, Rafael Dueire Lins was challenged by Graziela Peregrino, head of the Documentation Department of the Joaquim Nabuco Foundation in Recife, Brazil, to find a way to preserve all the information on the rich file of letters of Joaquim Nabuco[1] to future generations Lins (2011). Using the only scanner available at the Universidade Federal de Pernambuco in Brazil then, Lins digitized several letters of Joaquim Nabuco in 75, 150, 200, 300, 500, and 700 dpi in true-color and printed the images using a high-quality color laser printer. The printed documents were handed to the documentation experts of the Joaquim Nabuco Foundation, who concluded that the 150 dpi images had good enough quality to preserve all the information of the original document. As there was a huge international interest in the letters of the Nabuco bequest by social science researchers from all over the world, the 200 dpi scanner resolution was adopted by then, as it was compatible with FAX-machine standards, the technology available to send documents via computer/phone networks.

Over the years, prominent institutions dedicated to document digitization and preservation, including The Digital Library Federation Benchmark Working Group (2002), The Library of Congress (2014) and Forschungsgemeinschaft (2016), have conducted empirical studies to identify and recommend optimal scanning resolutions for different document types. The technical guidelines provided by those institutions are primarily based on visual inspection of the images generated in which documents were scanned at different resolutions, with the optimal resolution selected based on the visual "quality" of the resulting images. Among the findings, it is possible to observe a consensus of approximately 300 dpi as the ideal minimum resolution for grayscale and RGB-mode documents. According to Puglia et al. (2004), this resolution can also serve as a baseline for other document types, such as illustrations, maps, plans, ma-

[1] Brazilian statesman, writer, and diplomat, the first Brazilian ambassador to the U.S.A, one of the key figures in the campaign for freeing black slaves in Brazil (b.1861-d.1910).

nuscripts, and large-format documents. Despite the agreement of using 300 dpi among those important institutions, there is no technical justification beyond empirical data analysis to support such recommendations.

During the welcome reception of the International Conference on Document Analysis and Recognition (ICDAR) 2023, Professor George Nagy asked Daniel Lopesti and Rafael Dueire Lins, the fundamental question: "Which is the most suitable scanner resolution for documents?". Rafael Dueire Lins promptly answered that the proper way to determine the resolution, considering the maintenance and preservation of information, would be through the Nyquist-Shannon theorem. Such answer was immediately acknowledged as providing the correct solution to the problem.

Whenever converting an analog signal into a digital representation two phases are involved. The first one is determining the number of samples one must take. As explained by Lathi (2005), the Nyquist-Shannon Theorem (1938) teaches that any (continuous) signal sampled with twice its maximum frequency may be re-constructed without losses. The second step in the digitization process is the quantization error, the maximum error tolerated in the representation of each sample.

Although the response given was immediately recognized as providing the solution to the question, as the theorem provides a theoretical basis for defining the minimum resolution required to capture all document details without information loss, ensuring that all the details of the document are retained whenever viewed or printed on the original size the validity of the solution had still to be proved. The suggested solution needed to be detailed and proved correct, which motivated the research developed in this dissertation.

The initial results of this dissertation Lins et al. (2024) was originally published in a short paper in the proceedings of the ACM Symposium on Document Engineering 2024 (DocEng'24), which was sent to Professors George Nagy, Daniel Lopesti, and Elisa Barney-Smith. Professor Nagy main feedback was:

> "... your experiments provide reassurance about the adequacy of generally accepted digitization parameters. Testing both bi-level and color scans, and using the spectral density for estimating the range of image frequencies, seem sound."

Professor Elisa Barney-Smith informed us that:

> "It is an interesting paper. It was the topic of a WG at the DAS 2002 workshop, but no detailed experiments were run, just a discussion and WG report paper (published in IJDAR in 2004)."

Besides that, Professor Barney-Smith listed some important papers of hers on image scanning Barney-Smith (1998), Barney-Smith and Andersen (2005) showing that the quality of scanner output has evolved drastically:

> "Some information about the scanner itself can be measured through the use of various test targets, including a simple knife edge (to return the step response of the optics). See several of my early papers where I spent a lot of time exploring this. Scanners today are much higher quality than scanners 30 years ago, we have the disk space and the processing power to process over-sampled images, so it isn't as critical today, but people still explore the scanner optics."

This point raised by Professor Barney-Smith is very important because the Shannon-Nyquist theorem does not address *quantization errors*. But it is also relevant to notice that such errors are device-dependent and that their effect would be more noticeable in higher-resolution images. Another concern raised by Professor Barney-Smith was:

> "Another point you should mention in future papers would be a discussion of WHAT information you want to extract from a scan of a document. You touched on this when you mentioned historical documents vs maps... If it is just the text content, it has a much lower frequency content than if one were looking at the paper fibers of the same document."

It is important to stress here that this paper aims to determine the "correct" scanner resolution to keep all the document information making a high-definition same-size print of the scanned document indistinguishable from the original. However, on two occasions scanning documents in 300 dpi was enough to distinguish the age of documents as described by Barboza, Lins and Jesus (2013) and even to detect frauds with latter-added strokes in hand-written documents as detailed by Barbosa et al. (2014).

This dissertation also widens the scope of Lins et al. (2024) in two ways. The first one was the inclusion of more complex and fine-detailed images that employ tiny fonts that would generate very high-frequency components. The second path uses Optical Character Recognition (OCR) to analyze how the resolution variation affects the recognition rate.

1.1 OBJECTIVES

The general objective in this dissertation is to bring a theoretical basis and show evidences that the most suitable resolution for document digitization are based on the principles of the Nyquist-Shannon theorem from Information Theory and ensure the accurate preservation of all necessary document information. Thus, this dissertation expands the scope of the study published in Lins et al. (2024), incorporating new experiments, additional images and detailed analyses.

Such target is reached by:

- Enlarging and evaluating the datasets of document used considering a diversity of detailed images, including those with tiny fonts and high-frequency components, at multiple resolutions to represent a much wider range of document types in the experiments performed.
- Investigating the effects of the binarization process in enhancing the recognition of text and fine details at different resolutions.
- Using OCR tools to evaluate the impact of resolution on recognition rates, using the Levenshtein Distance to analyze the effects of scanner resolution in the accuracy of the transcription of the texts.
- Experimentally validating the Nyquist-Shannon theorem as a basis for determining optimal scanner resolution, considering several practical implications.

2 THEORETICAL BACKGROUND

According to Gonzalez and Woods (2018), in the context of digital image processing, an image can be described as a two-dimensional function, *f(x,y)*, where *x* and *y* represent spatial coordinates of a plane and the amplitude of *f* is referred to as the intensity or gray level of that specific point. If *x, y* and the intensity values of f are all finite and discrete, the image is considered a digital image. The value of *f* at spatial coordinates *(x, y)* is regarded as a scalar quantity physically determined by the image source, with values being proportional to the energy of the image. Most images are acquired through the interaction between the lighting source falling on the scene and the reflection or absorption of energy carried out by the elements within the photographed scene. Thus, the function *f(x,y)* can be characterized as the outcome of the combination of the illumination and reflectance elements, defined respectively by *i(x,y)* and *r(x,y)*:

$$f(x,y) = i(x,y)r(x,y) \tag{2.1}$$

where

$$0 \leq i(x,y) < \infty \tag{2.2}$$

and

$$0 \leq r(x,y) \leq 1 \tag{2.3}$$

Gonzalez and Woods (2018) asserts that reflectance is determined by the properties of the imaged objects and constrained between 0 (indicating total absorption) and 1 (indicating total reflectance). In instances of images formed through transmission, like a chest X-ray, the function would rely on the transmissivity function rather than the reflectance function. However, the boundaries remain consistent, and the image function remains represented as the product in equation 2.1.

Reference Sonka, Hlavac and Boyle (2015) states that computerized image processing relies on digital image functions. Therefore, an image must be represented using suitable discrete data, such as a matrix. In Figure 1, there is a representation of a digital image acquisition process using array sensors. In such an example, the imaging system collects the incoming energy and focuses it onto an image plane. Since the array sensor coincides with the focal plane, the resulting outputs will be proportional to each sensor's integral of the light received.

These outputs are then converted to an analog signal by digital and analog circuitry, which is then digitized, resulting in a digital image.

Figure 1 – Representation of an digital image acquisition.

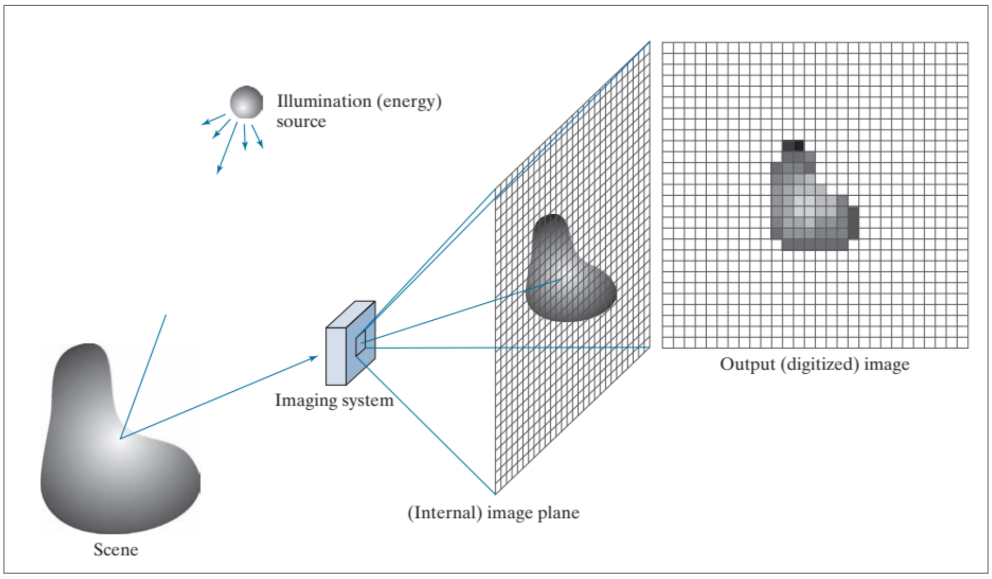

Source: GONZALEZ; WOODS (2018)

Considering the diversity of potential applications for digital image processing, Gonzalez and Woods (2018) highlights that images can be categorized by source, such as X-ray, visual, and infrared. The most prevalent energy source utilized today is the electromagnetic spectrum. This spectrum is grounded in the revelation that the resultant light beam is not white but comprises a continuous spectrum of colors extending from violet to red. Bushong (2013) describes that when sunlight passes through a prism, it becomes clear that white light consists of photons spanning a spectrum of wavelengths, and the prism functions to disperse and organize the emitted light into colors by refracting various wavelengths through distinct angles. Visible light comprises only a portion of the electromagnetic spectrum, extending over 25 orders of magnitude. Figure 2 illustrates the values of energy, frequency, and wavelength and identifies the three imaging windows of X-ray, visual, and MR imaging according to their associated values.

Figure 2 – Representation of different dimensions of pairs of lines.

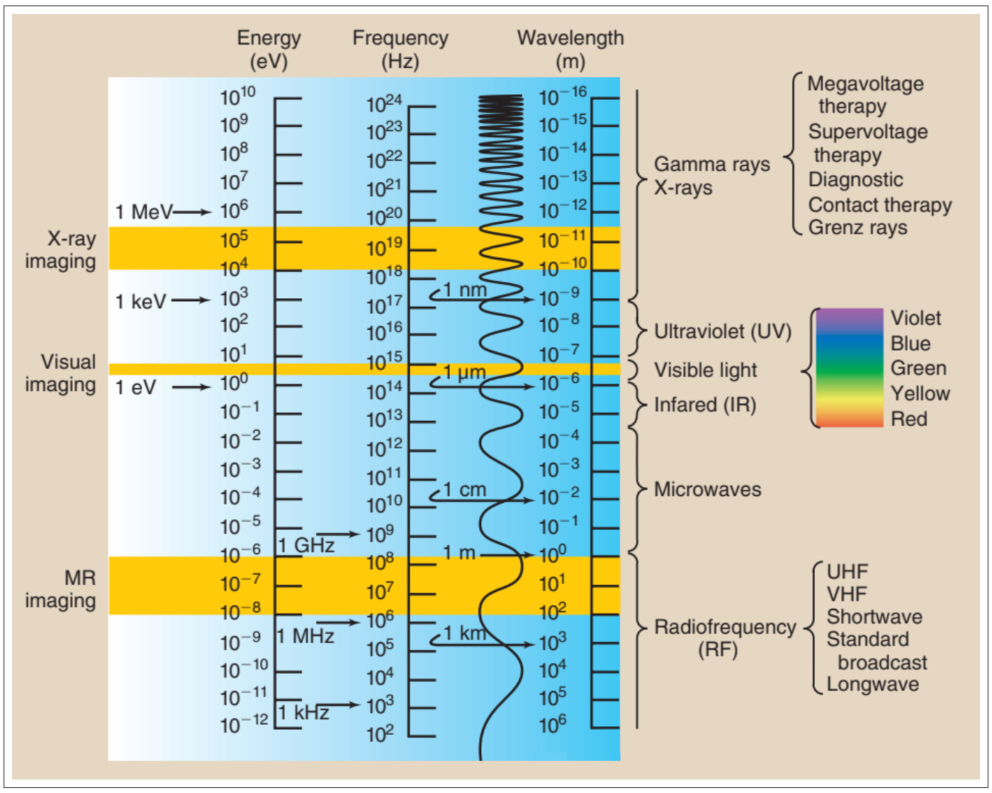

Source: BUSHONG (2013)

2.1 IMAGE RESOLUTION

Regarding the quality of a digital image, Sonka, Hlavac and Boyle (2015) emphasizes that it is directly proportional to its resolution. The author defines that the resolution of an image can be categorized into four main types: spatial resolution, spectral resolution, radiometric resolution and temporal resolution. This work will focus more specifically on spatial resolution and its impact on document scanning.

2.1.1 Spatial resolution

Bushberg (2012) states that spatial resolution refers to the ability of an imaging system to identify small details, that is, to distinguish small nearby elements that have different contrasts in an image. Sonka, Hlavac and Boyle (2015), highlights that the distance of the samples in the image plane determines this aspect. Therefore, the higher the spatial resolution, the better the visualization of details in an image.

Gonzalez and Woods (2018) add that, when considering the measurement of the smallest detail discernible in the image, the resolution in space is usually quantified in terms of line pairs per unit distance or dots (pixels) per unit distance. According to Bushong (2013), a line pair is defined by a high-contrast line separated by a space of width equal to that of the line. For radiological images, for example, it is common to use the unit line pairs per millimeter (lp/mm), referring to the lp/mm present in the image composition. According to Gonzalez and Woods (2018), one point per unit of distance refers to the size of the pixel present in the image composition. This measurement is generally used for printing files and is usually represented by the number of pixels in an inch, using the unit of dots per inch (dpi).

In Figures 3 and 4, respectively, representations of dimensions of pairs of lines and points (pixels) that can be applied concerning distance to determine spatial resolution are illustrated.

Figure 3 – Representation of different dimensions of pairs of lines.

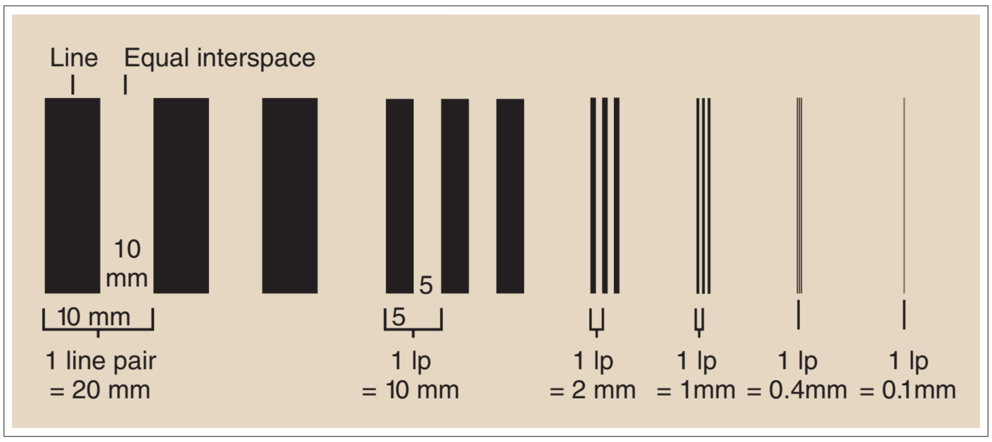

Source: BUSHONG (2013)

Figure 4 – Representation of different sizes of objects formed by points (pixels).

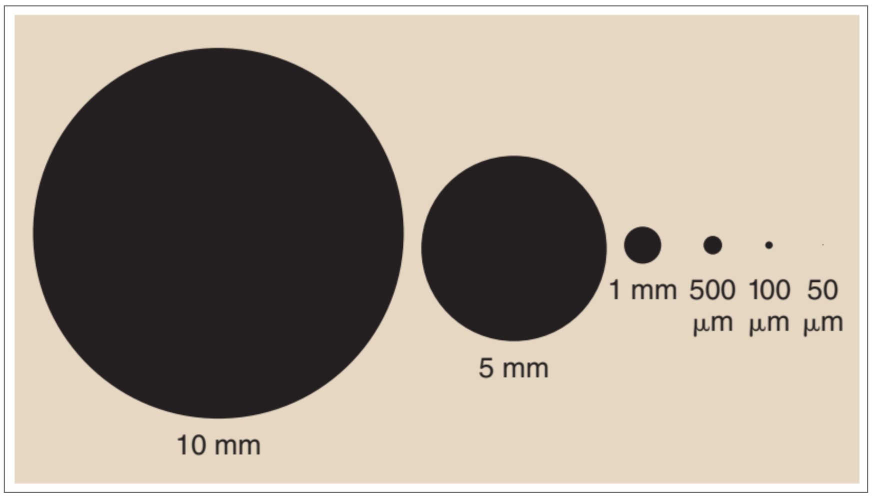

Source: BUSHONG (2013)

In figure 5 it is possible to see an example of the impact generated in an image at different spatial resolutions, considering the image at resolutions of 930 dpi, 300 dpi, 150 dpi, and 72 dpi. Gonzalez and Woods (2018), highlights that the difference in spatial resolution also affects the size of the image. However, in terms of comparing the impact of spatial resolution, the images were zoomed in for better visualization.

Figure 5 – Variation of spatial resolution in an image.

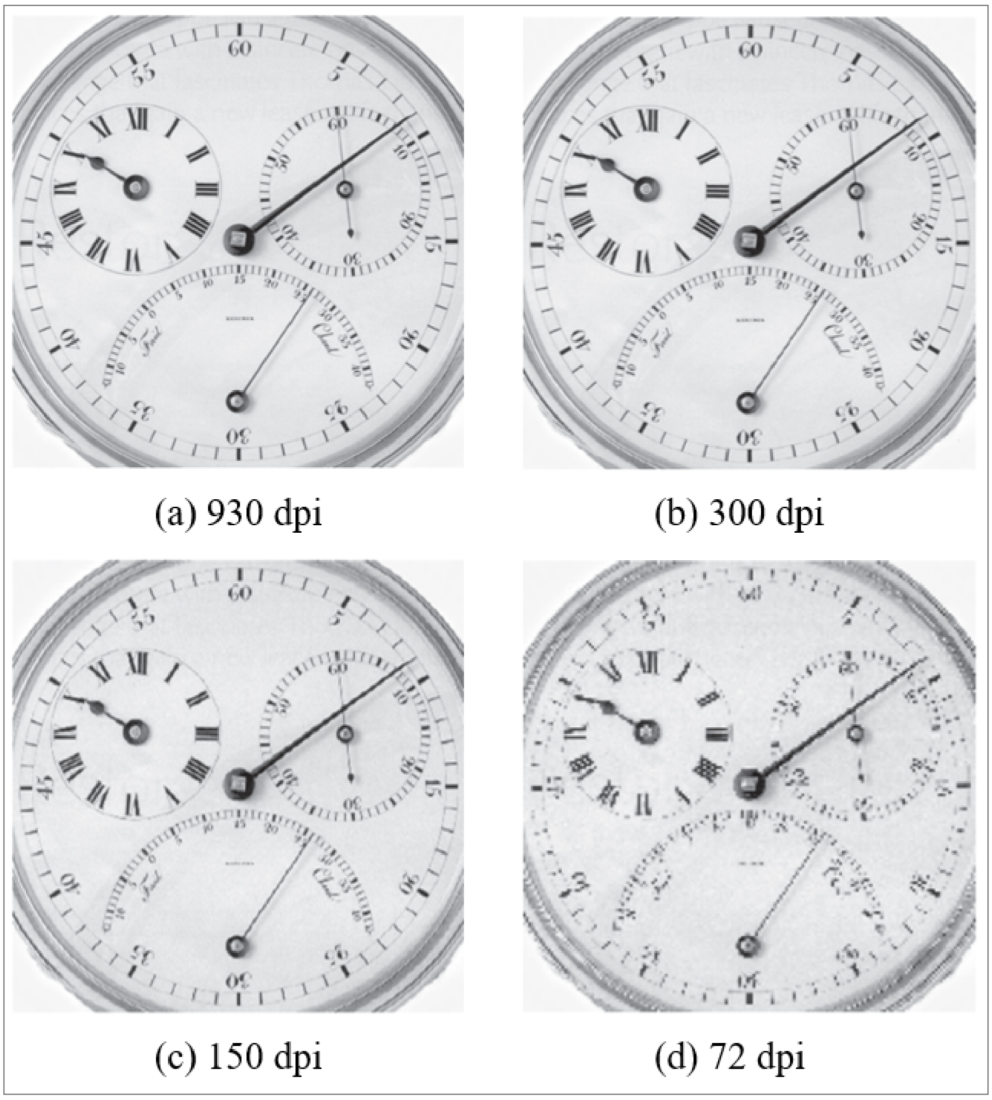

Source: GONZALEZ; WOODS (2018)

2.2 HISTORICAL DOCUMENTS IMAGE QUALITY

According to Kenney and Chapman (2001), determining image quality requirements depends on the characteristics of the type of document to be scanned. Capturing a finely detailed historical document written in pen and ink, for example, requires a higher resolution to correctly identify its elements. The author defines that, in general, documents can be classified into four identification categories as illustrated in table 1.

Table 1 – Documents Category

Document Category	Details
TEXTS/DASH	Can be produced manually, mechanographed or by machine. Usually in black and white. Includes books, manuscripts, newspapers, reports, typed or laser-printed documents, architectural plans, maps, line drawings, etchings, lithographs, and musical scores.
HALF TONE	In color or black and white. Reproductions, usually created from a photograph, made up of small dots or squares or lines, which are used to represent continuous tones. Most photographs in publications are halftones.
CONTINUOUS TONE	Color or black and white. Includes graphic illustrations in which all gray and color values can be reproduced: photographs, crayons, chalk and some pencil drawings, acrylics, watercolors and photographically reproduced facsimiles.
MIXED	Color or black and white. Refers to items containing halftone text and images or continuous tone text and images, such as newspapers, magazines, picture books, programs, and sheet music covers. Does not include text and line drawings together.

Source: Prepared by the author based on (KENNEY; CHAPMAN, 2001), 2024

Kenney and Chapman (2001) emphasizes, that in addition to document categories, other important factors to be considered in the scanning process are: level of detail, type of paper, level of contrast between ink and paper, sharpness, production process (machine-made or handmade) and quality of the document, considering if it is damaged, stained or incomplete. The quality of the digital image is inherently dependent on the quality of the source. For example, scanning a blurred image will result in a blurred digital copy, regardless of the resolution. In addition, the choice of hardware and software used in the digitization process can also influence the final output.

2.2.1 Historical documents resolution

According to Nagy and Seth (1984), the resolution applied by the scanner in the document scanning process is defined by the level of detail required in the image. When considering a two-level image (black and white), for example, 400 lines per inch would be considered an adequate value for spatial resolution.

The resolution for scanning documents for printing, according to Gonzalez and Woods (2018), is defined in terms of dpi. Table 2 contains different categories of documents followed by their spatial resolution information for printing provided by Gonzalez and Woods (2018) and Kenney and Chapman (2001).

Table 2 – Documents and their spatial resolutions. (**S.R.1** - Spatial Resolution provided by Gonzalez and Woods (2018), **S.R.2** - Spatial Resolution provided by Kenney and Chapman (2001))

Document	S. R. 1	S. R. 2
Newspapers	≈ 75	≈ 120 or 300
Magazines	≈ 133	–
Flyers	≈ 175	≈ 600
Books	≈ 2400	≈ 120 or 300
Monographs	–	≈ 600
Periodicals	–	≈ 600
Office documents	–	≈ 300
Tecnical draws	–	≈ 600
Maps	–	≈ 600
Handwritten materials	–	≈ 300

Source: Prepared by the author based on Gonzalez and Woods (2018) and Kenney and Chapman (2001), 2024

2.3 CONTINUOUS-TIME AND DISCRETE-TIME SIGNALS

Gonzalez and Woods (2018) explains that a continuous signal must be converted into a sequence of discrete values to be processed by a computer, a process that involves both sampling and quantization. Lathi (2005) emphasizes that continuous-time signals can be effectively analyzed by processing their discrete samples using discrete-time systems. To ensure accurate reconstruction of the original signal from its samples, the sampling rate must be sufficiently high, minimizing reconstruction errors. The sampling theorem provides the theoretical foundation for this process, defining the conditions under which continuous-time signals can be reliably sampled and reconstructed from their discrete sampled values.

Lathi (2005) further describes sampling theory as the connection between continuous-time and discrete-time representations. A continuous-time signal is expressed as a sequence of pulses and is specified in a continuum of time values t, while a discrete-time signal represents the same information numerically, as discrete values of t. Thus, both formats represent the same data, ensuring that each sample's information is equivalent, regardless of the representation. Some examples of continuous-time signals include outputs from telephones and analog cameras, while examples of discrete-time signals include monthly sales figures of a corporation and daily stock market averages. Figure 6(a) illustrates a continuous function $f(t)$ sampled at regular intervals ΔT, where each sample corresponds to a specific point on the continuous function. In contrast, Figure 6(b) represents these samples in the discrete x-domain, where the samples are indexed sequentially by integers (0, 1, 2, and 3) instead of their exact positions in time. This highlights that the sampled values at these points remain the same, ensuring information equivalence between the two domains.

Figure 6 – (a) *Left figure:* Continuous function $f(t)$ sampled ΔT units apart.
(b) *Right figure:* Samples in the x-domain, where x is discrete.

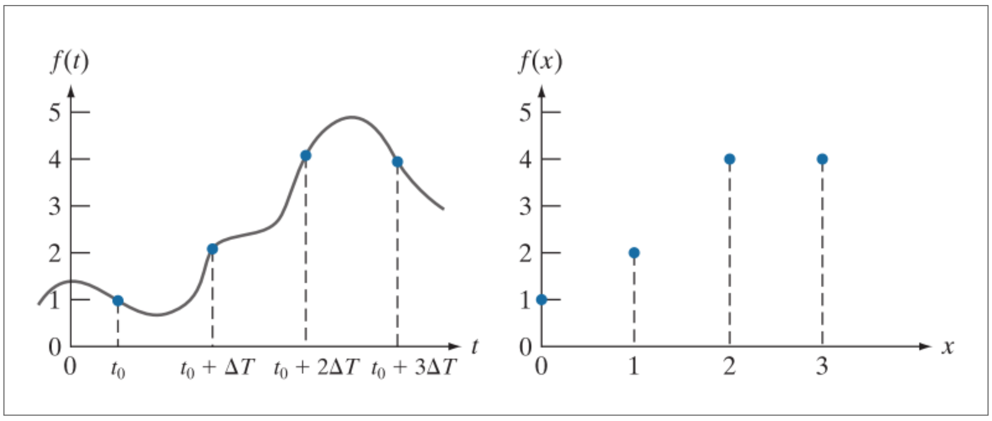

Source: GONZALEZ; WOODS (2018)

2.4 THE NYQUIST-SHANNON THEOREM

According to Lathi (2005), the basis of the Nyquist-Shannon Theorem is the Sampling Theorem, originally known as the "Interpolation Formula". Siebert (1986) describes that the general formulation of the "Sampling Theorem" was credited by H. S. Black to Cauchy in 1841 and around the 1920s, Nyquist, Carson, and Hartley revisited and refined the established concepts, laying the foundation for modern communication theory.

In 1948, the work of C. E. Shannon further formalized and popularized the theorem, Shannon (1949) even points out in his work that the theorem had already been portrayed previously by mathematicians in other forms, but had not appeared explicitly in the communication theory literature until Nyquist returned to work on the essential idea of the theorem and stated that, considering a $f(t)$ limited in bandwidth to a maximum frequency W and limited to the time interval T, with samples taken at intervals of $\frac{1}{2W}$ seconds apart, a total of $2TW$ samples will fully capture the information within the interval. Therefore, approximately $2TW$ numbers are enough to specify the function, based on a Fourier series expansion over the time interval T.

A band-limited function is defined as a function $f(t)$ whose Fourier transform is zero for frequency values outside a finite interval $[-\mu_{max}, \mu_{max}]$, as described by Gonzalez and Woods (2018). This restriction implies that, for a function to be confined within a specific time interval T, all frequency values outside this range must be zero, as stated by Shannon (1949).

Shannon articulated the theorem as follows:

> If a function of time $f(t)$ is limited to the band from 0 to W cycles per second, it is completely determined by giving its ordinates at a series of discrete points spaced $\frac{1}{2W}$ seconds apart (SHANNON, 1948, p. 34).

According to Lathi (2005), the samples can be taken arbitrarily at any instants, resulting in different intervals, as long as the sampling instants are recorded and on average of $2B$ samples per second. Gonzalez and Woods (2018) states that the term *Nyquist rate* defines a sampling rate equal to twice the highest frequency.

Based on Lee and Varaiya (2011), figure 7 illustrates an example of a signal sampling and reconstruction process based on The Nyquist-Shannon Theory in terms of its basis. Each line of pair graphs in the figure represents a step of the process as follows:

- **Step 1:** The left image represents the continuous-time original signal $x(t)$, and the right image shows its continuous Fourier transform $X(w)$, where the data is in terms of the frequency and band-limited to $[-\pi/T, \pi/T]$.

- **Step 2:** The signal $x(t)$ is sampled at intervals of T, resulting in the discrete signal $y(n)$. On the right, the discrete-time Fourier transform (DTFT) $Y(w)$ is shown, where the spectrum is periodically replicated with a period of $2\pi/T$.

- **Step 3:** The discrete-time signal $y(n)$ is converted into a train of impulses $w(t)$ by the Impulse Generator. In the frequency domain, $W(w)$ represents the scaled and periodic spectrum $1/T$.

- **Step 4:** The impulse train $w(t)$ is filtered by the $Sinc_T$ function, which is a scaled version of the sinus cardinalis function, defined as:

$$\text{sinc}_T(t) = \frac{\sin(\pi t/T)}{\pi t/T} \tag{2.4}$$

where:

- t = time
- T = the sampling period

This function acts as an interpolation kernel, ensuring that each sampled point contributes correctly to the reconstruction of the original signal. In frequency domain terms, $Sinc_T$, performs low-pass filtering, removing spectral replicas and preserving the original spectrum. Then, the inverse Fourier transform reconstructs the continuous-time signal $z(t)$, shown on the left, which matches the original signal $x(t)$.

Figure 7 – Steps in the Nyquist-Shannon sampling theorem.

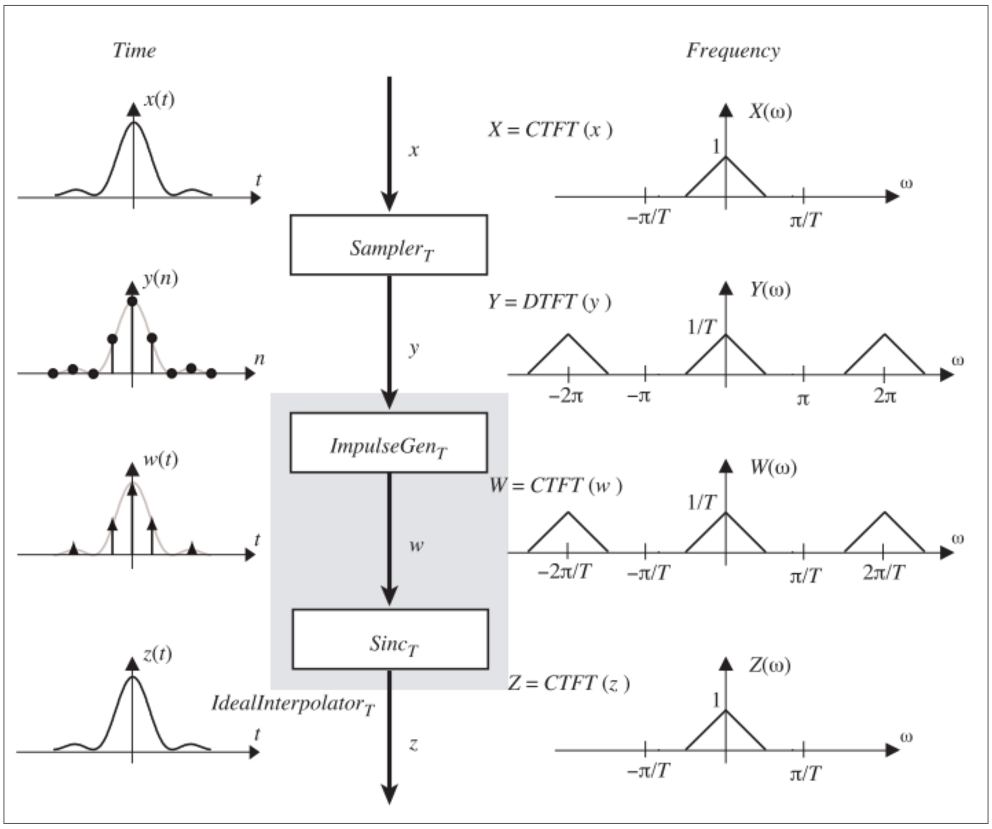

Source: LEE; VARAIYA (2011)

2.4.1 The Nyquist-Shannon Theorem applied to Images

In terms of a digital image, Sonka, Hlavac and Boyle (2015) describes that a continuous function $f(x, y)$ can be sampled by applying a discrete grid of sampling points in the plane, or the image function can also be expanded by applying an orthonormal function as a basis, such as the Fourier transform, resulting in coefficients of the expansion that represent the digitized image.

Colarusso et al. (1999) points out that the Nyquist-Shannon theorem is essential to direct imaging applications, as the signal is sampled through discrete pixel elements in an array. Sonka, Hlavac and Boyle (2015) also emphasizes that, there is a connection between the digital sampling density and the details that an image will contain. The Nyquist-Shannon principle implies that the sampling rate should be at least twice the highest spatial frequency to ensure accuracy. For example, Colarusso et al. (1999) describes that considering a diffraction-limited arrangement, the product of the lateral spatial resolution and the total magnification must be twice the pixel size of the image, as defined by Equation 2.5:

$$M_{tot}R_L \geq 2p \tag{2.5}$$

where:

- M_{tot}:total magnification
- R_L: lateral spatial resolution
- p: pixel size

Adhering to the Nyquist rate helps maintain the spatial fidelity of images and prevents sampling artifacts. In this context, oversampling does not provide additional information, resulting in a scenario commonly referred to as "empty magnification."Conversely, undersampling below the Nyquist-Shannon limit leads to distortions or artifacts, such as Moiré patterns, a phenomenon known as spatial aliasing Gonzalez and Woods (2018). Sonka, Hlavac and Boyle (2015) describes that aliasing happens when there is an overlapping of the periodically repeated results of the Fourier transform $f(u, v)$ of an image with band-limited spectrum, a result that can be prevented by choosing a sampling interval that it is less than half of the smallest interesting detail in the image.

Colarusso et al. (1999) explains that the resolution of an imaging device is primarily determined by its maximum capability. In terms of document scanning, Barney-Smith (1998) points out that the bitmap resulting from a two-level scan depends greatly on the parameters of the scanner used. The most common and simplest way to digitize a document in companies, or even at home, is through a flatbed scanner. Federal Agencies Digital Guidelines Initiative (2016) states that these models are easy to use, versatile and can achieve different resolution ranges, with values from 75 to 1200 dpi depending on the model used. Therefore, selecting the appropriate scanner resolution is essential to capture all document details effectively while avoiding the drawbacks of prolonged image acquisition and processing times, excessive storage requirements, and unnecessary network bandwidth usage.

2.5 EVALUATION MEASURE

2.5.1 Levenshtein Distance

Defined by Levenshtein (1966) in "*Binary codes capable of correcting deletions, insertions and reversals*", the Levenshtein Distance (LD) refers to the minimal number of insertions, deletions and replacements needed to to make two strings identical. The metric was proposed in the context of the code theory to solve problems in detecting and correcting transmission data. According to Navarro (2001) the Levenshtein distance is also known as *Edit distance* and, in a simplified definition, all the operations involved to guarantee the string matching are assigned as a cost of 1. The LD is widely used in applications such as evaluating spell-checkers, OCR systems, and DNA sequence analysis.

Shuwandy et al. (2020) defines that mathematically, the Levenshtein distance between two strings a, b with respectively length of $|a|$ and $|b|$ is given by $lev_{a,b}$ and detailed in Equation 2.6. The $lev_{a,b}(i, j)$ is the distance between the first i characters of a and the first j characters of b.

$$lev_{a,b}(i,j) = \begin{cases} \max(i,j) \text{ if} \min(i,j) = 0, \\ \min \begin{cases} lev_{a,b}(i-1,j)+1, & \text{(deletion)}, \\ lev_{a,b}(i,j-1)+1, & \text{(insertion)}, \\ lev_{a,b}(i-1,j-1)+1_{(a_i \neq b_j)}, & \text{(match or mismatch)}. \end{cases} \end{cases} \tag{2.6}$$

According to Shuwandy et al. (2020), the first element in the minimum refers to deletion, the second to insertion and the third refers to the match or mismatch of symbols, depending on their similarity. The $1_{(a_i \neq b_j)}$ is the indicator function in the match or mismatch elements, where:

$$\begin{cases} 1_{(a_i \neq b_j)} = 0 \text{ if } a_i = b_j \\ 1_{(a_i \neq b_j)} = 1 \text{ if } a_i \neq b_j \end{cases} \tag{2.7}$$

Shuwandy et al. (2020) reports an LD example between the words ‘GEEI’ and ‘GEELY’ to evaluate their similarity, considering ‘GEELY’ as the password of a system. Board 1 shows that the LD is 2, because of the two last characters.

Board 1 – Example of Levenshtein distance metric

G	E	E	I	
G	E	E	L	Y

Source: SHUWANDY et al. (2020)

3 MATERIALS AND METHODS

A distinct set of diversified files, representing the scope of document engineering, was selected to establish the optimal scanning resolution that balances image quality, processing time and storage space in document digitization. This selection was referred to as the “Test dataset"and is broadly divided into two main categories: text-only documents (“Text”) and documents containing both text and images (“General”). The test dataset includes twenty-eight distinct documents scanned at resolutions: 75, 150, 200, 300, 500, 700, and 1200 dpi. These documents are book pages and single paper files in different papers, font styles, sizes, formats and colors. The content includes:

- Typed Texts, in English, Portuguese and Spanish;
- Handwritten Texts in Portuguese;
- Maps;
- Architectural Plan,
- Images and Illustrations.

In figure 8 it is possible to observe samples of images from the text-only dataset followed by samples of images from the general dataset in figure 9.

Figure 8 – Samples of images from the Text-only Dataset

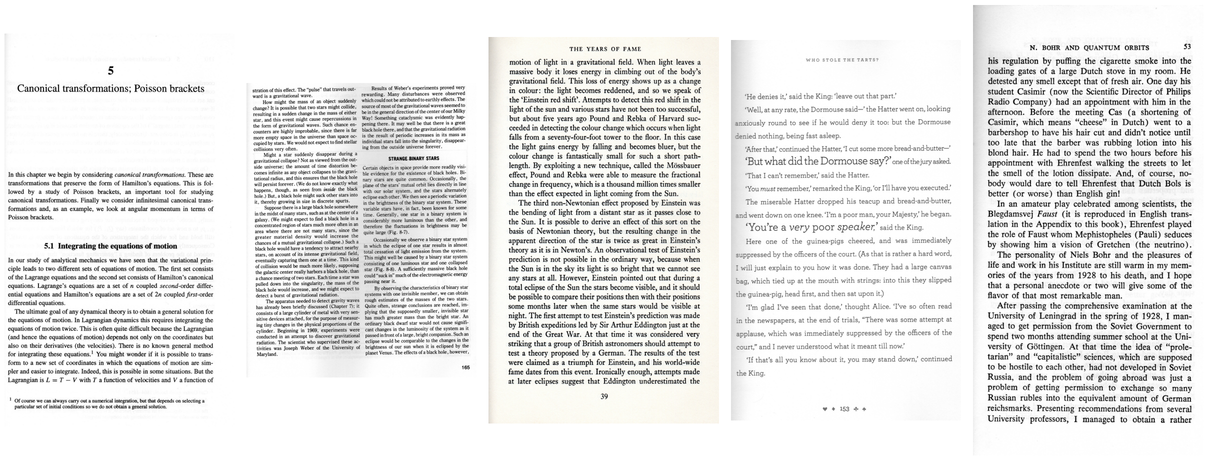

5

Canonical transformations; Poisson brackets

In this chapter we begin by considering *canonical transformations*. These are transformations that preserve the form of Hamilton’s equations. This is followed by a study of Poisson brackets, an important tool for studying canonical transformations. Finally we consider infinitesimal canonical transformations and, as an example, we look at angular momentum in terms of Poisson brackets.

5.1 Integrating the equations of motion

In our study of analytical mechanics we have seen that the variational principle leads to two different sets of equations of motion. The first set consists of the Lagrange equations and the second set consists of Hamilton’s canonical equations. Lagrange’s equations are a set of n coupled *second*-order differential equations and Hamilton’s equations are a set of $2n$ coupled *first*-order differential equations.

The ultimate goal of any dynamical theory is to obtain a general solution for the equations of motion. In Lagrangian dynamics this requires integrating the equations of motion twice. This is often quite difficult because the Lagrangian (and hence the equations of motion) depends not only on the coordinates but also on their derivatives (the velocities). There is no known general method for integrating these equations.[1] You might wonder if it is possible to transform to a new set of coordinates in which the equations of motion are simpler and easier to integrate. Indeed, this is possible in some situations. But the Lagrangian is $L = T - V$ with T a function of velocities and V a function of

[1] Of course we can always carry out a numerical integration, but that depends on selecting a particular set of initial conditions so we do not obtain a general solution.

stration of this effect. The “pulse” that travels outward is a gravitational wave.

How might the mass of an object suddenly change? It is possible that two stars might collide, resulting in a sudden change in the mass of either star, and this event might cause repercussions in the form of gravitational waves. Such chance encounters are highly improbable, since there is far more empty space in the universe than space occupied by stars. We would not expect to find stellar collisions very often.

Might a star suddenly disappear during a gravitational collapse? Not as viewed from the outside universe; the amount of time distortion becomes infinite as any object collapses to the gravitational radius, and this ensures that the black hole will persist forever. (We do not know exactly what happens, though, as seen from *inside* the black hole.) But, a black hole might suck other stars into it, thereby growing in size in discrete spurts.

Suppose there is a large black hole somewhere in the midst of many stars, such as at the center of a galaxy. (We might expect to find a black hole in a concentrated region of stars much more often in an area where there are not many stars, since the greater material density would increase the chances of a mutual gravitational collapse.) Such a black hole would have a tendency to attract nearby stars, on account of its intense gravitational field, eventually capturing them one at a time. This kind of collision would be much more likely, supposing the galactic center really harbors a black hole, than a chance meeting of two stars. Each time a star was pulled down into the singularity, the mass of the black hole would increase, and we might expect to detect a burst of gravitational radiation.

The apparatus needed to detect gravity waves has already been briefly discussed (Chapter 7); it consists of a large cylinder of metal with very sensitive devices attached, for the purpose of measuring tiny changes in the physical proportions of the cylinder. Beginning in 1969, experiments were conducted in an attempt to discover gravitational radiation. The scientist who supervised these activities was Joseph Weber of the University of Maryland.

Results of Weber’s experiments proved very rewarding. Many disturbances were observed which could not be attributed to earthly effects. The source of most of the gravitational waves seemed to be in the general direction of the center of our Milky Way! Something cataclysmic was evidently happening there. It may well be that there is a great black hole there, and that the gravitational radiation is the result of periodic increases in its mass as individual stars fall into the singularity, disappearing from the outside universe forever.

STRANGE BINARY STARS

Certain objects in space provide more readily visible evidence for the existence of black holes. Binary stars are quite common. Occasionally, the plane of the stars’ mutual orbit lies directly in line with our solar system, and the stars alternately eclipse each other. We then see a periodic variation in the brightness of the binary star system. These variable stars have, in fact, been known for some time. Generally, one star in a binary system is considerably more luminous than the other, and therefore the fluctuations in brightness may be quite large (Fig. 8-7).

Occasionally we observe a binary star system in which the eclipse of one star results in almost total cessation of light emission from the system. This might well be caused by a binary star system consisting of one luminous star and one collapsed star (Fig. 8-8). A sufficiently massive black hole could “suck in” much of the electromagnetic energy passing near it.

By observing the characteristics of binary star systems with one invisible member, we can obtain rough estimates of the masses of the two stars. Quite often, strange conclusions are reached, implying that the supposedly smaller, invisible star has much greater mass than the bright star. An ordinary black dwarf star would not cause significant changes in the luminosity of the system as it passed in front of a large, bright companion. Such an eclipse would be comparable to the changes in the brightness of our sun when it is eclipsed by the planet Venus. The effects of a black hole, however,

165

THE YEARS OF FAME

motion of light in a gravitational field. When light leaves a massive body it loses energy in climbing out of the body’s gravitational field. This loss of energy shows up as a change in colour: the light becomes reddened, and so we speak of the ‘Einstein red shift’. Attempts to detect this red shift in the light of the sun and various stars have not been too successful, but about five years ago Pound and Rebka of Harvard succeeded in detecting the colour change which occurs when light falls from a seventy-four-foot tower to the floor. In this case the light gains energy by falling and becomes bluer, but the colour change is fantastically small for such a short path-length. By exploiting a new technique, called the Mössbauer effect, Pound and Rebka were able to measure the fractional change in frequency, which is a thousand million times smaller than the effect expected in light coming from the Sun.

The third non-Newtonian effect proposed by Einstein was the bending of light from a distant star as it passes close to the Sun. It is possible to derive an effect of this sort on the basis of Newtonian theory, but the resulting change in the apparent direction of the star is twice as great in Einstein’s theory as it is in Newton’s. An observational test of Einstein’s prediction is not possible in the ordinary way, because when the Sun is in the sky its light is so bright that we cannot see any stars at all. However, Einstein pointed out that during a total eclipse of the Sun the stars become visible, and it should be possible to compare their positions then with their positions some months later when the same stars would be visible at night. The first attempt to test Einstein’s prediction was made by British expeditions led by Sir Arthur Eddington just at the end of the Great War. At that time it was considered very striking that a group of British astronomers should attempt to test a theory proposed by a German. The results of the test were claimed as a triumph for Einstein, and his world-wide fame dates from this event. Ironically enough, attempts made at later eclipses suggest that Eddington underestimated the

39

WHO STOLE THE TARTS?

‘He denies it,’ said the King: ‘leave out that part.’

‘Well, at any rate, the Dormouse said—’ the Hatter went on, looking anxiously round to see if he would deny it too: but the Dormouse denied nothing, being fast asleep.

‘After that,’ continued the Hatter, ‘I cut some more bread-and-butter—’

‘But what did the Dormouse say?’ one of the jury asked.

‘That I can’t remember,’ said the Hatter.

‘You *must* remember,’ remarked the King, ‘or I’ll have you executed.’

The miserable Hatter dropped his teacup and bread-and-butter, and went down on one knee. ‘I’m a poor man, your Majesty,’ he began.

‘You’re a *very* poor *speaker*,’ said the King.

Here one of the guinea-pigs cheered, and was immediately suppressed by the officers of the court. (As that is rather a hard word, I will just explain to you how it was done. They had a large canvas bag, which tied up at the mouth with strings: into this they slipped the guinea-pig, head first, and then sat upon it.)

‘I’m glad I’ve seen that done,’ thought Alice. ‘I’ve so often read in the newspapers, at the end of trials, “There was some attempt at applause, which was immediately suppressed by the officers of the court,” and I never understood what it meant till now.’

‘If that’s all you know about it, you may stand down,’ continued the King.

♥ ♦ 153 ♣ ♠

N. BOHR AND QUANTUM ORBITS 53

his regulation by puffing the cigarette smoke into the loading gates of a large Dutch stove in my room. He detested any smell except that of fresh air. One day his student Casimir (now the Scientific Director of Philips Radio Company) had an appointment with him in the afternoon. Before the meeting Cas (a shortening of Casimir, which means “cheese” in Dutch) went to a barbershop to have his hair cut and didn’t notice until too late that the barber was rubbing lotion into his blond hair. He had to spend the two hours before his appointment with Ehrenfest walking the streets to let the smell of the lotion dissipate. And, of course, nobody would dare to tell Ehrenfest that Dutch Bols is better (or worse) than English gin!

In an amateur play celebrated among scientists, the Blegdamsvej *Faust* (it is reproduced in English translation in the Appendix to this book), Ehrenfest played the role of Faust whom Mephistopheles (Pauli) seduces by showing him a vision of Gretchen (the neutrino).

The personality of Niels Bohr and the pleasures of life and work in his Institute are still warm in my memories of the years from 1928 to his death, and I hope that a personal anecdote or two will give some of the flavor of that most remarkable man.

After passing the comprehensive examination at the University of Leningrad in the spring of 1928, I managed to get permission from the Soviet Government to spend two months attending summer school at the University of Göttingen. At that time the idea of “proletarian” and “capitalistic” sciences, which are supposed to be hostile to each other, had not developed in Soviet Russia, and the problem of going abroad was just a problem of getting permission to exchange so many Russian rubles into the equivalent amount of German reichsmarks. Presenting recommendations from several University professors, I managed to obtain a rather

Source: The author (2024)

Figure 9 – Samples of images from the General Dataset.

Source: The author (2024)

The eighteen images of English texts were classified into the "Text Dataset", while the remaining ten images were organized into a separate group referred to as the "General Dataset". The flowchart in Figure 10 presents the process carried out to prepare each data set for the Fourier Transform application.

Figure 10 – Datasets Workflow

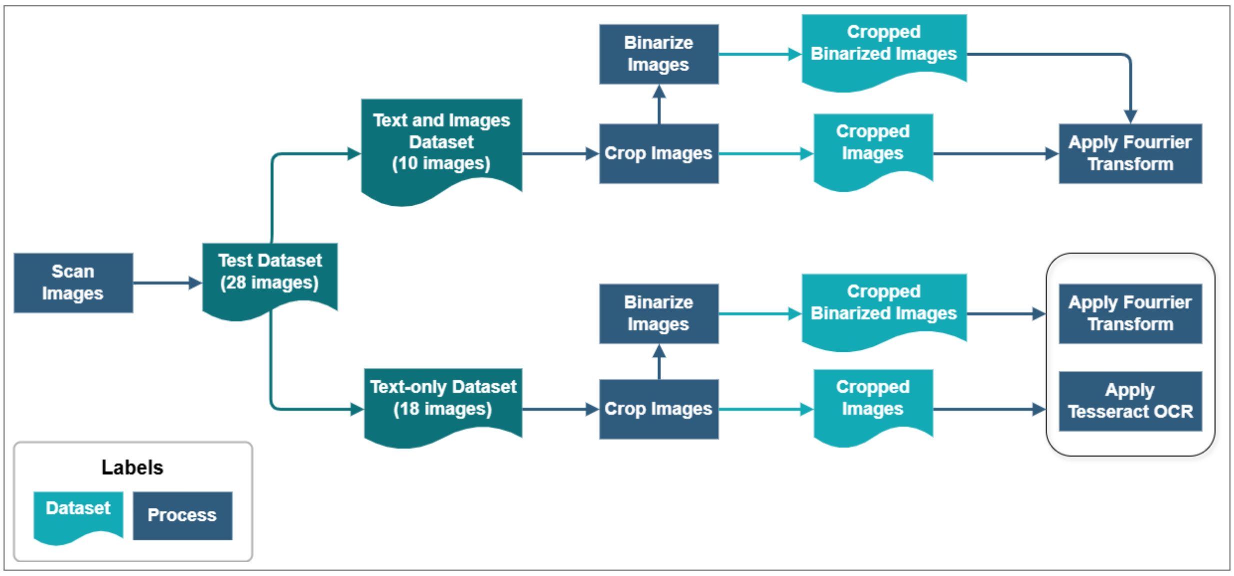

Source: The author (2024)

As mentioned in the previous section, the Nyquist-Shannon theorem applies to continuous signals that are bandwidth-limited. It is a principle in Fourier analysis that sharper signals (those with higher derivatives in the time or spatial domain) exhibit higher frequency components. When signals display "discontinuities" in time or space, a phenomenon known as "frequency overshooting" occurs, resulting in intense oscillations in the frequency domain. By closely examining a color document image, one observes that the pixel colors at boundaries transition smoothly, whereas binary images have sharp edges, which can introduce perceived signal discontinuities. The selected documents were examined in true-color and binary formats, to facilitate a more thorough frequency domain analysis.

To determine the optimal scanning resolution, the approach here involved analyzing the spectral density of various resolutions of the same image to locate the “maximum frequency”. The smallest resolution to yield such a frequency is considered the most efficient choice, balancing scanning time, storage requirements, network transmission bandwidth, and processing time, as processing time typically scales with file size. This study also evaluates the effect of different scanning resolutions on the transcription quality of text-only documents by comparing the Levenshtein distances between transcribed texts and their ground-truth counterparts.

3.1 SCANNING PROCESS

In this study, the first step in determining the optimal resolution for scanned documents was to digitize each document at 75, 150, 200, 300, 500, 700, and 1200 dpi. The files were scanned in color mode and saved in Portable Networks Graphics (PNG) format, a widely used raster format known for its efficient lossless compression and high bit-depth compatibility, as described by Puglia et al. (2004).

The scanning process was performed using three scanners: Epson EcoTank L4160, Epson EcoTank L8180, and HP LaserJet Pro Color M479FDW. The technical specifications of each device, as provided in their respective manuals, are summarized in Table 3. Based on these specifications, the first two scanners were capable of digitizing documents at all seven predefined resolutions. However, the HP LaserJet Pro Color M479FDW scanner was limited to the following resolutions: 75, 200, 300, and 1200 dpi.

Table 3 – Scanners specifications.

Specification	Epson L4160	Epson L8180	HP M479FDW
Scanner type	Flatbed	Flatbed	Flatbed
Photoelectric device	CIS	CIS	CIS
Effective pixels	10200 × 14040 pixels (1200 dpi)	-	-
Maximum document size	US letter or A4 (8.5 × 11.7 inches (in) or 216 × 297 millimeters (mm))	Legal (8.5 × 14 in or 216 × 356 mm)	Legal (8.5 × 14 in or 216 × 356 mm)
Optical resolution	1200 x 2.400 dpi	1.200 x 4.800 dpi	1200 x 1200 dpi
Output resolution	50 to 9600 dpi in 1 dpi increments	-	-
Image data	***Color:*** 48 bits per pixel (bpp) (internal), 24 bpp (external). ***Grayscale:*** 16 bpp (int.), 8 bpp (ext.). ***Black and White:*** 16 bpp (int.), 1 bpp (ext.)	***Color:*** 48 bpp (internal), 24 bpp (external). ***Grayscale:*** 16 bpp (int.), 8 bpp (ext.). ***Black and White:*** 16 bpp (int.), 1 bpp (ext.)	-
Light source	LED	LED	LED

Source: Prepared by the author based on EPSON (2019), EPSON (2021) and HP (2019), 2025.

3.2 CROPPING PROCESS

The Test Dataset was processed using a cropping algorithm, presented in Appendix A, to remove visible scanner edges and ensure a clear focus on the document page.

The Source Code 1 begins by selecting the image to be processed and defining its path. After verifying the existence of the image according to the specified path, the function “cv2.imread(path)” loads the found images and displays an error message if the image is not located. The cropping parameters are manually and individually adjusted for each image, considering its specific characteristics. The parameters ‘top‘, ‘bottom‘, ‘left‘, and ‘right‘ define the cropping percentages for the top, bottom, left, and right edges of the image, respectively. These values are stored in the dictionary “cut_values”, ensuring a clear mapping between cropping directions and their respective values.

The cropping function cut_and_save calculates the number of pixels to be cropped based on the defined percentages and performs the cropping operation using image[top:bottom, left:right]. This function takes the following parameters:

- image: the image to be cropped;
- output_path: the path to save the cropped image;
- resolution: the resolution of the image being processed;
- cut_percent: the cropping percentages.

It is important to highlight that the cropping percentages were applied across all different image resolutions, in line 43 of the Source Code 1, it is established as follows:

```
top, bottom, left, right = [int(p * max(image.shape) / 100) for p in
    cut_percent]
```

The line defines that, the cropping values are calculated as a percentage of the maximum image dimension (max(image.shape)). Thus, the cropping process is proportional to the image size, adapting to different resolutions. This approach helps maintain relative consistency in the visual content regardless of varying resolutions.

At the end of the process, the new cropped images are saved in PNG format and the applied cropping parameters are saved in an Excel file. An example of the cropping result for Image 01 across different resolutions is shown in Figure 11.

Figure 11 – Example of the different resolutions of Image 01 in the original scan size and after the cropping process.

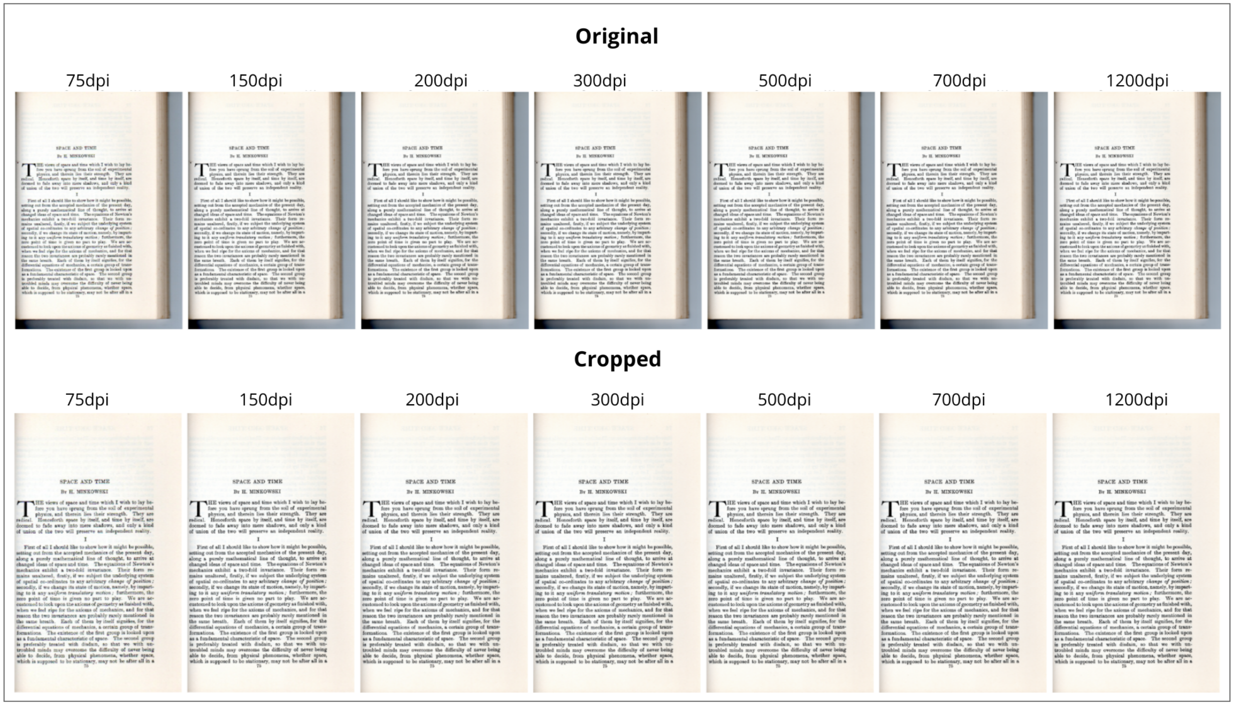

Source: The author (2025)

3.3 BINARIZATION PROCESS

After the cropping process, the images were subjected to binarization. According to Lins et al. (2021), the binarization of document images remains a significant research area, particularly due to its importance in processing stages of document analysis and optical character recognition (OCR). In this study, the Otsu binarization algorithm Otsu (1979) was applied to the test images due to its accessibility, ease of implementation, and consistent image quality. The implementation of this method can be found in Appendix B.

Initially, the Source Code 2 defines the specific image to be processed and sets its corresponding path. Subsequently, a validation step is performed to verify if the image exists. If the image is successfully found, it is loaded using the function `cv2.imread(path)` from the OpenCV library. In the event of an invalid path or missing image, an error message is displayed.

The main function responsible for the binarization process is `binarize_and_save`. This function begins by converting the original image to grayscale using the OpenCV function `cv2.cvtColor(image, cv2.COLOR_BGR2GRAY)`. This conversion is essential because Otsu's thresholding technique operates more effectively on grayscale images, where pixel intensities range from 0 (black) to 255 (white). According to the OpenCV documentation Doxygen

(2024), the use of the conversion code `cv2.COLOR_BGR2GRAY` ensures a reduction in computational complexity, facilitating the accurate application of the binarization technique.

As defines by Doxygen (2024), the subsequent step in line 30 of the Source Code 2, applies the Otsu thresholding method using the following OpenCV flags:

- `cv2.THRESH_BINARY`: Performs binary thresholding, where pixel values below the threshold are set to 0 (black) and values equal to or above the threshold are set to 255 (white);
- `cv2.THRESH_OTSU`: Automatically calculates the optimal global threshold for the image, minimizing the intra-class variance between the foreground and background pixel intensities.

Otsu's method is effective with images that exhibit a bimodal histogram, that presents two distinct peaks corresponding to the foreground and background, by automatically selecting the ideal threshold. It eliminates the subjectivity associated with manually determining a suitable threshold value, thus reducing the likelihood of misclassification.

Finally, the binarized image is saved to the specified path using the `cv2.imwrite(output_path, binarized_image)` function. This approach ensures that the resulting binarized images can be utilized for further analytical steps. Figure 12 presents an example of the binarized result for Image 01 in its different resolutions.

Figure 12 – Example of the different resolutions of Image 01 in the original scan color and after the binarization process.

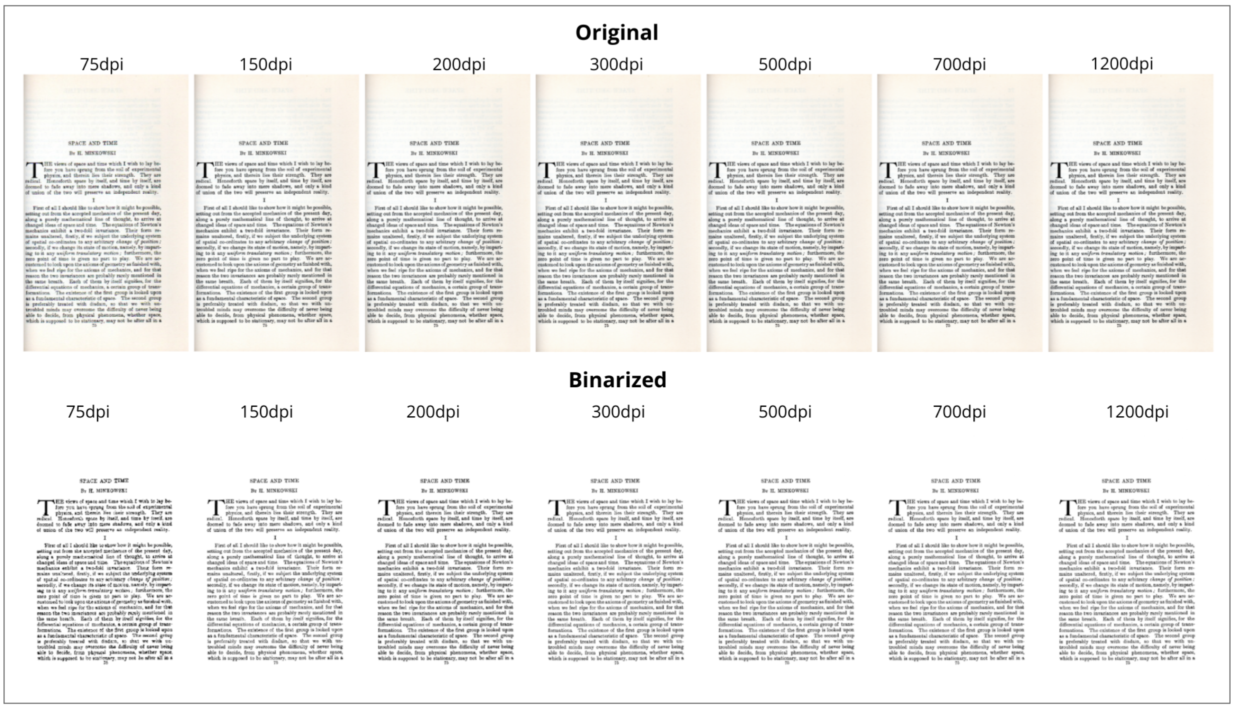

Source: The author (2025)

3.4 SPECTRAL ANALYSIS

The images were prepared as described previously and then the Fourier Transform was applied to each one using the NumPy library in Python, a tool widely used for scientific computing. The source code of the Fourier transform algorithm applied in the dataset is in Appendix C

The Source Code 3 starts locating the defined images, followed by checking for their existence. The images are loaded in grayscale mode using "`cv2.IMREAD_GRAYSCALE`", considering that Red Green Blue (RGB) images require separate transforms for each channel, the use of grayscale images reduces complexity, improving computational efficiency while still preserving meaningful frequency data based on the different intensities.

For each image, the Fourier Transform was applied considering the following code, located in lines 75-77 of the Source Code 3

```
transform_image = np.fft.fft2(image)
center_transform_image = np.fft.fftshift(transform_image)
magnitude_spectrum = np.log(np.abs(center_transform_image) + 1)
```

where:

- `np.fft.fft2(image)`: computes the 2D Fourier Transform, performing the calculation of the two-dimensional discrete Fourier transform across specified axes within an M-dimensional matrix;
- `np.fft.fftshift()`: moves to center the zero-frequency component within the spectrum, providing better visualization;
- `np.log(np.abs(center_transform_image) + 1)`: converts the frequency domain to a log scale for improved contrast, calculating the logarithm of the magnitude of the spectrum.

The function `calculate_max_frequency` finds the maximum frequency component in the transformed image, corresponding to the dominant structure in the image. The highest frequency was identified with the `numpy.argmax`, which finds the indices of maximum values and was used here to pinpoint the peak frequency within the magnitude spectrum as defined by Numpy (2024). With the magnitude spectrum results, it was possible to plot a frequency map and frequency range for each image resolution.

Following the same Fourier-based spectral analysis on the Source Code 3, the Source Code 4 shows the results in a Spectral Density Plot. The Spectral Density function $S(f)$ represents the distribution of energy across different frequency components and, as described by Oppenheim, Willsky and Nawab (1994), is defined as:

$$S(f) = |X(f)|^2 \tag{3.1}$$

where

- X(f) = Fourier transform of the signal x(t)

Considering that the signal has finite energy:

$$E = \int_{-\infty}^{\infty} |x(t)|^2 \, dt < \infty \tag{3.2}$$

To estimate the Spectral Density, the magnitude spectrum was calculated using the Fourier Transform, and then a normalized histogram of the frequency magnitudes was created. This histogram represents the relative occurrence of different frequencies in the image and the spectral analysis functions were defined as:

```python
def calculate_spectral_energy(magnitude_spectrum):
    return np.sum(magnitude_spectrum**2)
```

- `calculate_spectral_energy`: calculates the total spectral energy by summing the squares of the magnitude of the spectrum. This value represents the total energy of the signal in the analyzed frequency components;

```python
def calculate_max_frequency(magnitude_spectrum):
    row_center, col_center = np.unravel_index(np.argmax(magnitude_spectrum),
        magnitude_spectrum.shape)
    return magnitude_spectrum[row_center, col_center]
```

- `calculate_max_frequency`: finds the pixel with the highest frequency magnitude in the spectrum;

```python
def calculate_frequency_distribution(magnitude_spectrum):
    hist, bins = np.histogram(magnitude_spectrum.flatten(), bins=50, range
        =(0, magnitude_spectrum.max()))
    hist = hist / hist.sum()
    predominant_frequencies = bins[:-1][hist > 0.1]
    return hist, bins, predominant_frequencies
```

- `calculate_frequency_distribution`: creates a histogram of frequency magnitudes to identify the frequency distribution of the image. The relative frequency threshold above 0.1 was used, as defined by "`bins[:-1][hist > 0.1]`", which facilitated the generation of a frequency recurrence graph for the spectrum, normalizing the values so that the sum is 1 and considering values above 10% of occurrence according to Numpy (2024);

The frequencies in the resulting spectrum are based on the image resolutions and correspond to cycles per pixel. The Fourier Transform allowed the extraction of a frequency map, the identification of the frequency range, the determination of the highest frequency and the creation of a Spectral Density plot for each image, all using the Numpy library based on NumPy (2024) and subsequently visualized with the Matplotlib library as stated in the Matplotlib (2024) documentation.

Figures 13 to 19 show the frequency maps and ranges for Image 01 across different resolutions, accompanied by the Spectral Density graph. The maps are displayed using Matplotlib's jet colormap model described in Matplotlib (2024).

Figure 13 – Image 01, the frequency map and the Spectral Density of 75 dpi resolution.

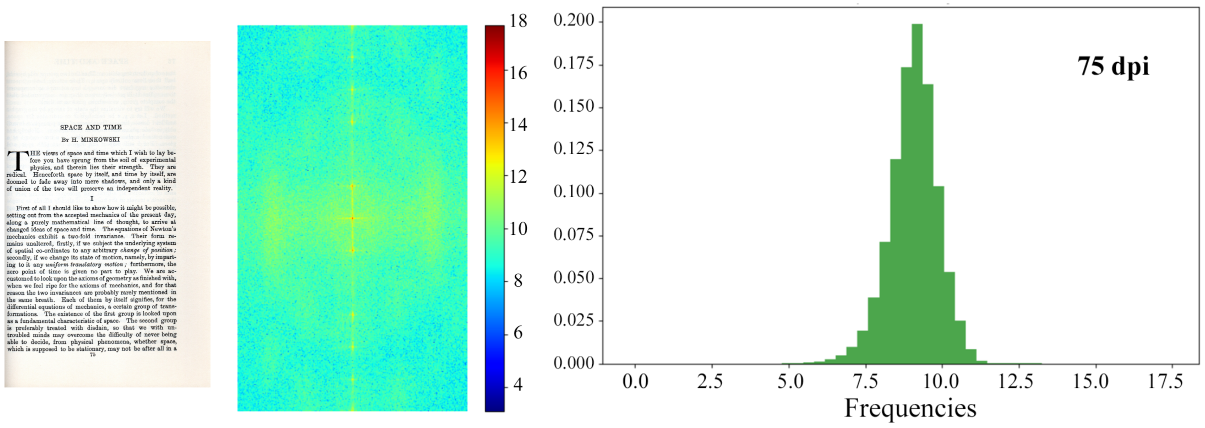

Source: The author (2024)

Figure 14 – Image 01, the frequency map and the Spectral Density of 150 dpi resolution.

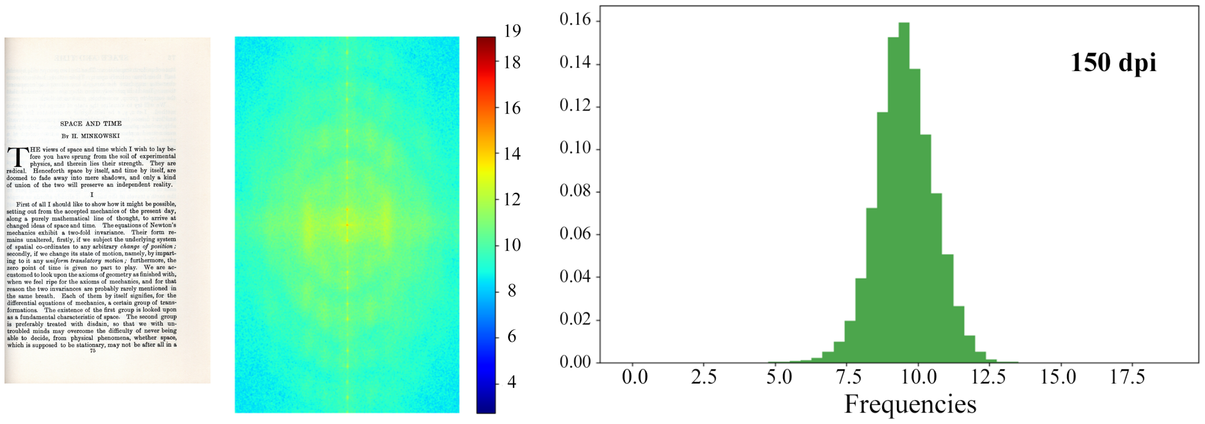

Source: The author (2024)

Figure 15 – Image 01, the frequency map and the Spectral Density of 200 dpi resolution.

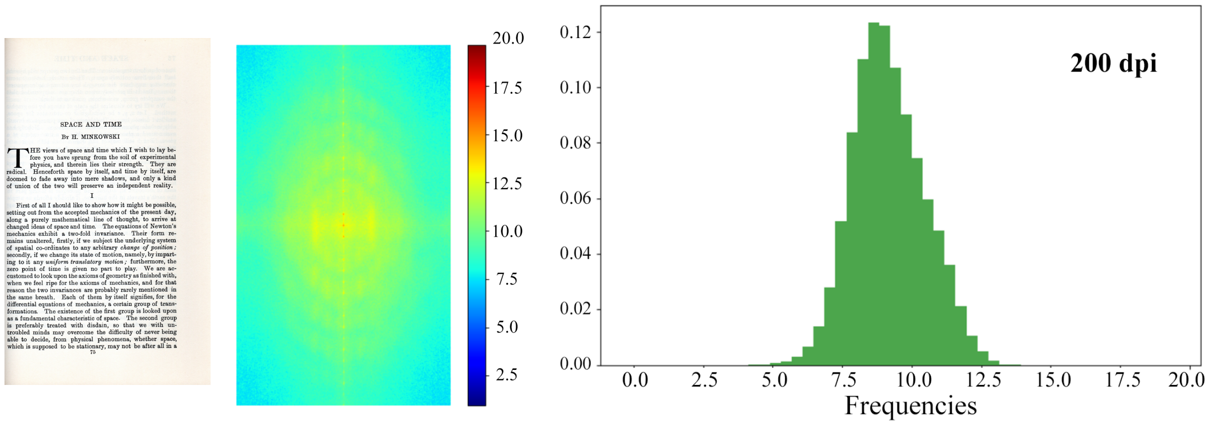

Source: The author (2024)

Figure 16 – Image 01, the frequency map and the Spectral Density of 300 dpi resolution.

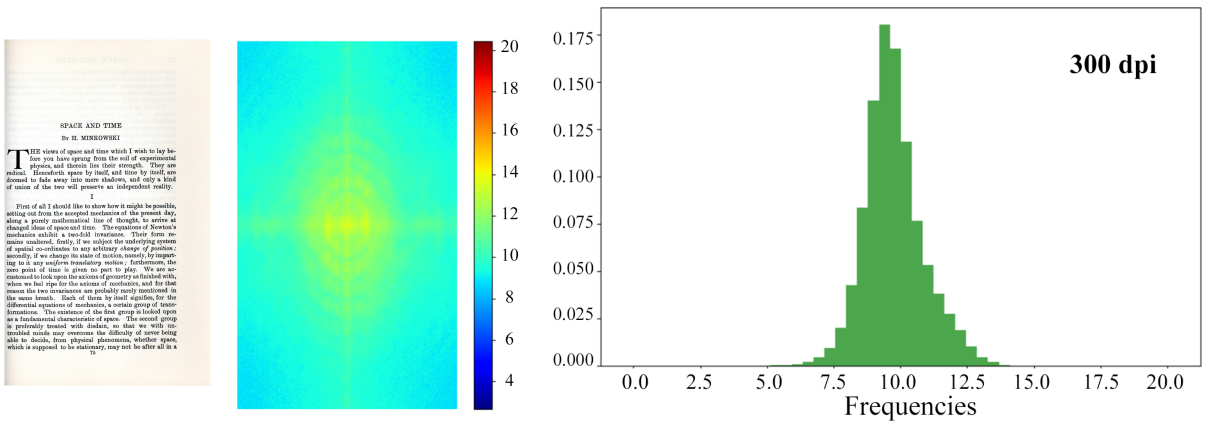

Source: The author (2024)

Figure 17 – Image 01, the frequency map and the Spectral Density of 500 dpi resolution.

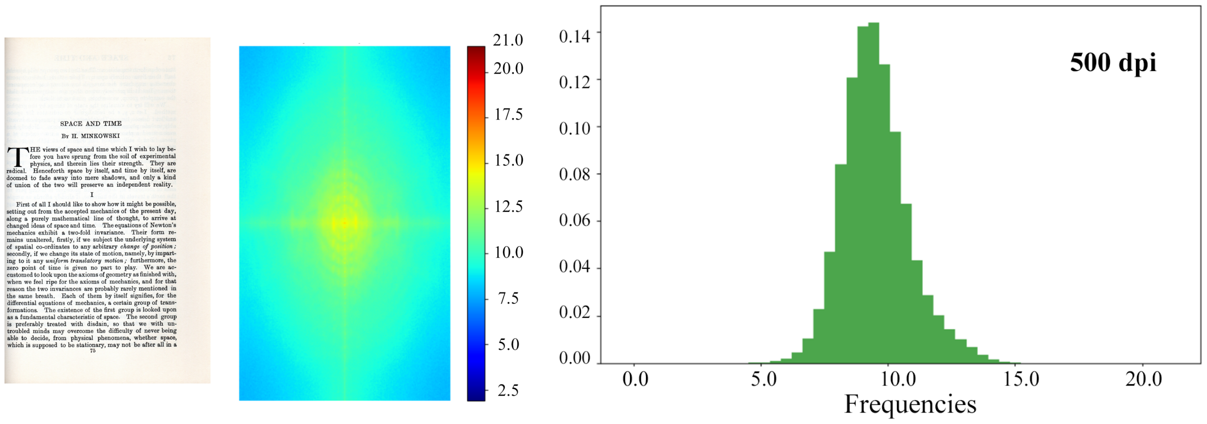

Source: The author (2024)

Figure 18 – Image 01, the frequency map and the Spectral Density of 700 dpi resolution.

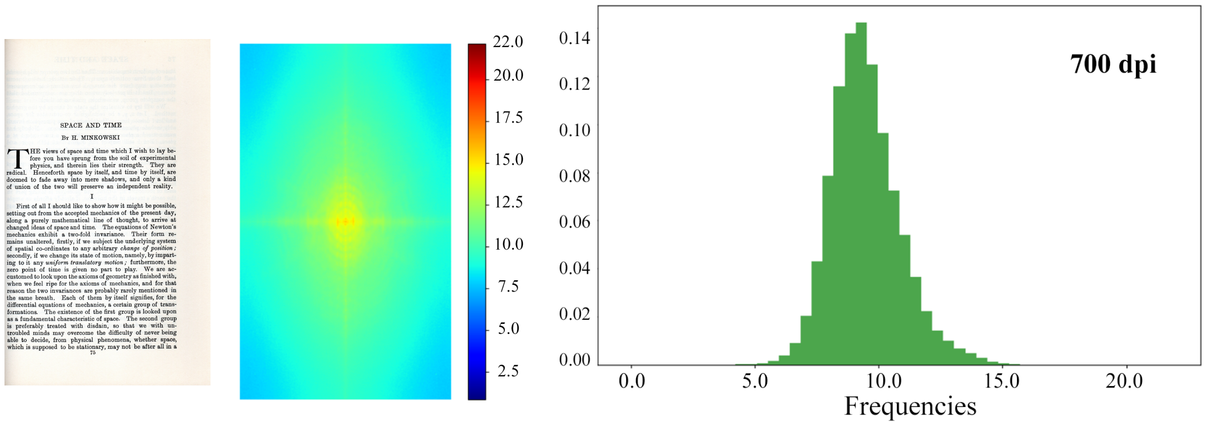

Source: The author (2024)

Figure 19 – Image 01, the frequency map and the Spectral Density of 1200 dpi resolution.

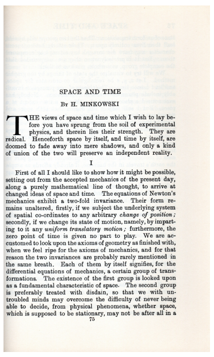

SPACE AND TIME

By H. MINKOWSKI

THE views of space and time which I wish to lay before you have sprung from the soil of experimental physics, and therein lies their strength. They are radical. Henceforth space by itself, and time by itself, are doomed to fade away into mere shadows, and only a kind of union of the two will preserve an independent reality.

I

First of all I should like to show how it might be possible, setting out from the accepted mechanics of the present day, along a purely mathematical line of thought, to arrive at changed ideas of space and time. The equations of Newton's mechanics exhibit a two-fold invariance. Their form remains unaltered, firstly, if we subject the underlying system of spatial co-ordinates to any arbitrary *change of position;* secondly, if we change its state of motion, namely, by imparting to it any *uniform translatory motion;* furthermore, the zero point of time is given no part to play. We are accustomed to look upon the axioms of geometry as finished with, when we feel ripe for the axioms of mechanics, and for that reason the two invariances are probably rarely mentioned in the same breath. Each of them by itself signifies, for the differential equations of mechanics, a certain group of transformations. The existence of the first group is looked upon as a fundamental characteristic of space. The second group is preferably treated with disdain, so that we with untroubled minds may overcome the difficulty of never being able to decide, from physical phenomena, whether space, which is supposed to be stationary, may not be after all in a

75

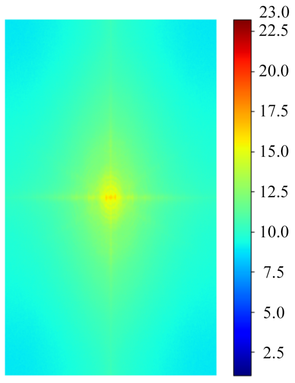

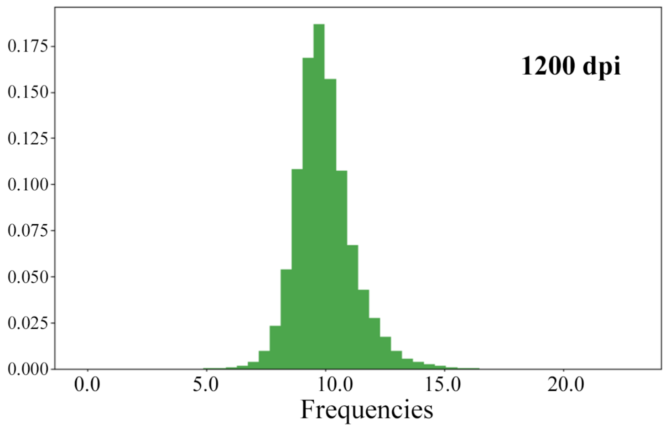

Source: The author (2024)

3.5 OPTICAL CHARACTER RECOGNITION (OCR)

According to Puglia et al. (2004), digital images must meet quality standards to ensure that OCR conversion achieves a certain level of accuracy. Barney-Smith and Andersen (2005) highlights that specific combinations of parameters governing scanning degradations can cause characters to appear either similar or significantly different when degraded. Beyond the influence of the optical resolution of the scanner on the document quality, factors such as contamination, manual underlining, or annotations can also pose challenges and interfere with the OCR process, as detailed by Forschungsgemeinschaft (2016).

Given the impact of document resolution on transcription accuracy, text-based documents were transcribed using optical character recognition (OCR), and the Levenshtein Distance was calculated for each resulting file. The implemented algorithm is presented in Appendix D.

The Source Code 5 begins by selecting the image to be processed and defining its path. After verifying the existence of the image according to the specified path, the function "`cv2.imread(path)`" loads the images and displays an error message if the image is not located. For the OCR process, Python-tesseract, a Python wrapper for the Google Tesseract-OCR Engine, was used, as referenced in PyPi (2024). Specifically, Tesseract OCR version 4.1.1 was applied and accessed by the pytesseract library (version 0.3.13) within the Python environment. The algorithm was executed without using the language dictionary or loading frequent words, this approach eliminates the influence of predefined words on OCRbased word recognition, prioritizing character-level identification for evaluating text element recognition. Based on doxygen (2015) and tesseract-ocr (2024), these settings were defined in line 60 of the Source Code 5, using the commands:

```
tesseract_config = --psm 6 load_system_dawg=0 load_freq_dawg=0]
```

where:

- `- -psm 6`: sets the Page Segmentation Mode (PSM) to assume a single uniform block of text;
- `load_system_dawg0̄ load_freq_dawg0̄`: disables the dictionary-based correction to allow a raw text extraction without auto-correction.

The OCR transcription of each document was saved in the correspondent TXT file format and the Python-Levenshtein library was employed by applying the code "`distance = levenshtein(reference_text, ocr_text)`" to calculate the Levenshtein distance between each transcribed text and the corresponding ground-truth text as described in PyPi (2024), the LD results were then saved in an Excel file and analyzed considering the OCR accuracy at the different image resolutions, based on measuring how many character changes (insertions, deletions, substitutions) were needed.

4 RESULTS

The data collected using the scanner Epson L4160 for the color and binary versions of the documents are summarized in four tables. Tables 4 and 5 contain data from the Text Dataset, while Tables 7 and 8 contain information from the General Dataset.

4.1 TEXT DATASET

Table 4 contains detailed information for the 18 images of the text dataset considering the colored images scanned with the Epson L4160 scanner. The information includes image size in centimeters (cm), text size in points (pt), resolution in dpi, file size for both PNG and Windows Bitmap (BMP) formats in megabytes (MB), the Highest frequency (HF) and Levenshtein distance measurements for each document across the seven previously defined resolution levels.

Table 4 – Text Dataset - Original images results (**Image size** in centimeters (cm), **Font size** in points (pt), **dpi** - image resolution in dots per inch, **png/bmp** - file size of the png/bmp image in megabytes (MB), **HF** - Highest frequency, **LD** - Levenshtein distance.)

Image	dpi	png	bmp	HF	LD	Image	png	bmp	HF	LD
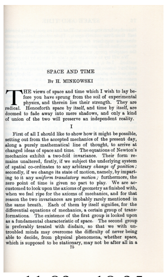	**75**	0.35	0.59	18	97	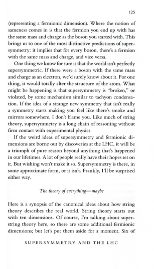	0.25	0.6	18	101
	150	1.28	2.37	19	12		0.75	2.4	19	11
	200	2.28	4.21	20	22		1.21	4.28	20	11
	300	5.12	9.47	20	21		2.39	9.61	21	9
	500	13.74	26.27	21	22		5.74	26.69	22	12
	700	25.82	51.49	22	24		9.91	52.27	22	11
11.89 x 18.95 Font size: 10	**1200**	69.81	151.27	23	28	11.45 x 21.00 Font size: 10	25.18	153.59	23	12
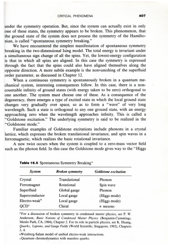	**75**	0.39	0.75	18	490	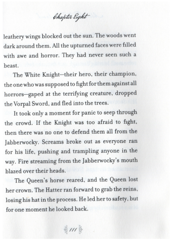	0.32	0.48	17	945
	150	1.29	2.98	19	164		1.18	1.92	19	912
	200	2.25	5.29	20	164		1.99	3.41	19	909
	300	4.51	11.9	21	170		4.76	7.66	20	912
	500	12.12	33.03	22	172		12.2	21.26	21	914
14.19 x 21.00	**700**	21.71	64.75	22	178	11.62 x 16.56	23.02	41.67	22	916
Font size: 10	**1200**	54.9	190.23	23	180	Font size: 12	59.57	122.44	23	913

SPACE AND TIME

By H. MINKOWSKI

THE views of space and time which I wish to lay before you have sprung from the soil of experimental physics, and therein lies their strength. They are radical. Henceforth space by itself, and time by itself, are doomed to fade away into mere shadows, and only a kind of union of the two will preserve an independent reality.

I

First of all I should like to show how it might be possible, setting out from the accepted mechanics of the present day, along a purely mathematical line of thought, to arrive at changed ideas of space and time. The equations of Newton's mechanics exhibit a two-fold invariance. Their form remains unaltered, firstly, if we subject the underlying system of spatial co-ordinates to any arbitrary *change of position;* secondly, if we change its state of motion, namely, by imparting to it any *uniform translatory motion;* furthermore, the zero point of time is given no part to play. We are accustomed to look upon the axioms of geometry as finished with, when we feel ripe for the axioms of mechanics, and for that reason the two invariances are probably rarely mentioned in the same breath. Each of them by itself signifies, for the differential equations of mechanics, a certain group of transformations. The existence of the first group is looked upon as a fundamental characteristic of space. The second group is preferably treated with disdain, so that we with untroubled minds may overcome the difficulty of never being able to decide, from physical phenomena, whether space, which is supposed to be stationary, may not be after all in a

75

125

(representing a fermionic dimension). Where the notion of sameness comes in is that the fermion you end up with has the same mass and charge as the boson you started with. This brings us to one of the most distinctive predictions of supersymmetry: it implies that for every boson, there's a fermion with the same mass and charge, and vice versa.

One thing we know for sure is that the world isn't perfectly supersymmetric. If there were a boson with the same mass and charge as an electron, we'd surely know about it. For one thing, it would totally alter the structure of the atom. What might be happening is that supersymmetry is "broken," or violated, by some mechanism similar to tachyon condensation. If the idea of a strange new symmetry that isn't really a symmetry starts making you feel like there's smoke and mirrors somewhere, I don't blame you. Like much of string theory, supersymmetry is a long chain of reasoning without firm contact with experimental physics.

If the weird ideas of supersymmetry and fermionic dimensions are borne out by discoveries at the LHC, it will be a triumph of pure reason beyond anything that's happened in our lifetimes. A lot of people really have their hopes set on it. But wishing won't make it so. Supersymmetry is there, in some approximate form, or it isn't. Frankly, I'll be surprised either way.

The theory of everything—maybe

Here is a synopsis of the canonical ideas about how string theory describes the real world. String theory starts out with ten dimensions. Of course, I'm talking about superstring theory here, so there are some additional fermionic dimensions; but let's put them aside for a moment. Six of

SUPERSYMMETRY AND THE LHC

CRITICAL PHENOMENA 407

under the symmetry operation. But, since the system can actually exist in only one of these states, the symmetry appears to be broken. This phenomenon, that the ground state of the system does not possess the symmetry of the Hamiltonian, is called "spontaneous symmetry breaking."

We have encountered the simplest manifestation of spontaneous symmetry breaking in the two-dimensional Ising model. The total energy is invariant under a simultaneous sign change of all the spins. Yet, the lowest-energy configuration is that in which all spins are aligned. In this case the symmetry is expressed through the fact that the spins could also have aligned themselves along the opposite direction. A more subtle example is the nonvanishing of the superfluid order parameter, as discussed in Chapter 12.

When a continuous symmetry is spontaneously broken in a quantum mechanical system, interesting consequences follow. In this case, there is a noncountable infinity of ground states (with energy taken to be zero) orthogonal to one another. The system must choose one of these. As a consequence of the degeneracy, there emerges a type of excited state in which the local ground state changes very gradually over space, so as to form a "wave" of very long wavelength. Such a state is orthogonal to any one ground state, with an energy approaching zero when the wavelength approaches infinity. This is called a "Goldstone excitation." The underlying symmetry is said to be realized in the "Goldstone mode."

Familiar examples of Goldstone excitations include phonons in a crystal lattice, which expresses the broken translational invariance, and spin waves in a ferromagnetic, which realizes the basic rotational invariance.

A new twist occurs when the system is coupled to a zero-mass vector field such as the photon field. In this case the Goldstone mode gives way to the "Higgs

Table 16.5 Spontaneous Symmetry Breaking[a]

System	*Broken symmetry*	*Goldstone excitation*
Crystal	Translational	Phonon
Ferromagnet	Rotational	Spin wave
Superfluid	Global gauge	Phonon
Superconductor	Local gauge	(Higgs mode)
Electro-weak[b]	Local gauge	(Higgs mode)
QCD[c]	Chiral	π mesons

[a]For a discussion of broken symmetry in condensed matter physics, see P. W. Anderson, *Basic Notions of Condensed Matter Physics* (Benjamin-Cummings, Menlo Park, CA, 1984), Chapter 2. For its role in particle physics, see K. Huang, *Quarks, Leptons, and Gauge Fields* (World Scientific, Singapore, 1982), Chapters 3, 4.

[b]Weinberg-Salam model of unified electro-weak interactions.

[c]Quantum chromodynamics with massless quarks.

Chapter Eight

leathery wings blocked out the sun. The woods went dark around them. All the upturned faces were filled with awe and horror. They had never seen such a beast.

The White Knight—their hero, their champion, the one who was supposed to fight for them against all horrors—gaped at the terrifying creature, dropped the Vorpal Sword, and fled into the trees.

It took only a moment for panic to seep through the crowd. If the Knight was too afraid to fight, then there was no one to defend them all from the Jabberwocky. Screams broke out as everyone ran for his life, pushing and trampling anyone in the way. Fire streaming from the Jabberwocky's mouth blazed over their heads.

The Queen's horse reared, and the Queen lost her crown. The Hatter ran forward to grab the reins, losing his hat in the process. He led her to safety, but for one moment he looked back.

111

Image	dpi	png	bmp	HF	LD	Image	png	bmp	HF	LD
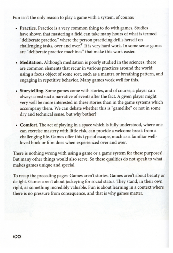	75	0.42	0.87	18	28	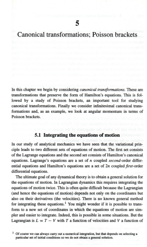	0.27	0.68	18	196
	150	1.44	3.49	19	14		0.87	2.71	19	6
	200	2.54	6.2	20	14		1.44	4.82	20	6
	300	5.47	13.94	21	18		2.84	10.85	21	9
	500	14.39	38.69	22	19		6.94	30.1	22	8
15.68 x 22.28	700	26.06	75.8	23	20	12.94 x 21.00	11.95	58.98	22	9
Font size: 12	1200	66.77	222.75	24	19	Font size: 11	30.5	173.31	23	12
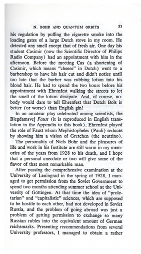	75	0.35	0.58	18	36	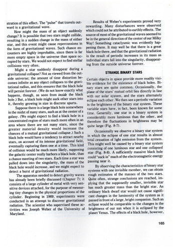	0.56	0.84	18	3071
	150	1.24	2.31	19	7		1.96	3.35	19	3110
	200	2.14	4.11	20	7		3.29	5.97	20	3104
	300	4.49	9.26	20	7		6.92	13.4	21	3205
	500	11.81	25.7	21	7		17.68	37.24	22	3211
11.04 x 21.00	700	21.68	50.35	22	7	15.10 x 22.28	31.94	72.95	22	3201
Font size: 12	1200	56.13	147.98	23	12	Font size: 10	81.99	214.32	24	3205
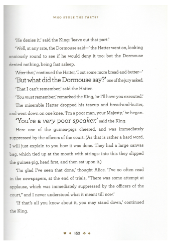	75	0.34	0.95	18	66	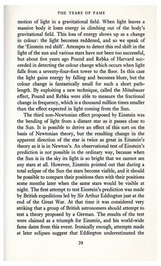	0.42	0.59	18	59
	150	1.06	3.81	20	23		1.43	2.37	19	1
	200	1.86	6.77	20	23		2.46	4.21	20	1
	300	3.9	15.23	21	25		5.36	9.47	20	1
	500	10.07	42.31	22	24		14.11	26.27	21	1
16.29 x 23.47	700	18.12	82.89	23	23	11.89 x 19.95	25.97	51.49	22	2
Font size: 12	1200	46.59	243.54	24	27	Font size: 12	68.84	151.27	23	4
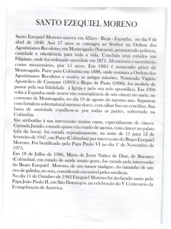	75	0.15	0.25	17	1638	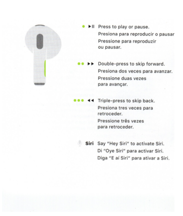	0.05	0.18	17	442
	150	0.53	1.01	18	55		0.18	0.71	18	48
	200	0.87	1.8	19	46		0.33	1.26	19	47
	300	1.87	4.05	20	44		0.74	2.83	19	39
	500	4.62	11.25	21	45		2	7.85	20	42
8.57 x 11.89	700	8.41	22.04	21	43	7.96 x 8.94	3.85	15.39	21	39
Font size: 7	1200	22.18	64.78	22	45	Font size: 7	10.33	45.2	22	44
	75	0.03	0.05	15	210		0.03	0.07	15	279
	150	0.11	0.21	16	56		0.12	0.27	17	71
	200	0.18	0.37	17	52		0.22	0.47	17	62
	300	0.43	0.84	18	39		0.5	1.07	18	32
	500	1.12	2.31	19	20		1.3	2.95	19	25
4.71 x 4.47	700	2.13	4.53	20	29	5.01 x 5.35	2.5	5.79	20	37
Font size: 5	1200	5.69	13.32	21	49	Font size: 5	6.66	17	21	54

Image	dpi	png	bmp	HF	LD	Image	png	bmp	HF	LD
Controles de canción Pulse la portada de un álbum y deslícese hacia la izquierda para que aparezcan los controles de canción Repetición, Genius y Aleatorio. Haga doble clic en el botón de reposo/activación para reproducir la pista siguiente. Alicia Keys Fallin' Songs in A Minor (10th Anni…	**75**	0.03	0.06	15	279	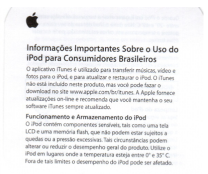 **Informações Importantes Sobre o Uso do iPod para Consumidores Brasileiros** O aplicativo iTunes é utilizado para transferir músicas, vídeo e fotos para o iPod, e para atualizar e restaurar o iPod. O iTunes não está incluído neste produto, mas você pode fazar o download no site www.apple.com/br/itunes. A Apple fornece atualizações on-line e recomenda que você mantenha o seu software iTunes sempre atualizado. **Funcionamento e Armazenamento do iPod** O iPod contém componentes sensíveis, tais como uma tela LCD e uma memória flash, que não podem estar sujeitos a quedas ou a pressão excessivas. Tais circunstâncias podem alterar ou reduzir o desempenho geral do produto. Utilize o iPod em lugares onde a temperatura esteja entre 0° e 35° C. Fora de tais limites o desempenho do iPod pode ser afetado.	0.03	0.07	16	786
	150	0.12	0.25	17	71		0.12	0.27	17	282
	200	0.21	0.45	17	62		0.2	0.47	17	41
	300	0.5	1	18	32		0.44	1.06	18	24
	500	1.3	2.78	19	25		1.11	2.94	19	20
4.71 x 5.38	**700**	2.45	5.44	20	37	5.59 x 4.78	2.04	5.76	20	21
Font size: 5	**1200**	6.51	15.99	21	54	Font size: 4	5.33	16.91	21	22
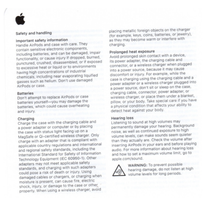	**75**	0.1	0.18	17	2586		0.87	1.14	18	4049
	150	0.4	0.74	18	1906		3.04	4.54	20	4152
	200	0.66	1.31	19	1960		5.12	8.09	20	4158
	300	1.44	2.94	19	1978		10.94	18.18	21	4153
	500	3.57	8.16	20	1982		27.47	50.5	22	4155
8.57 x 8.64	**700**	6.43	15.99	21	1976	18.05 x 25.26	50.1	98.93	23	4158
Font size: 5	**1200**	16.94	46.97	22	1978	Font size: 8	130.4	290.75	24	4169

Source: The author (2024)

Table 5 shows data for the 18 images in the Text Dataset considering the binarized images scanned with the Epson L4160 scanner. The information includes image size in cm, text size in pt, resolution in dpi, file size for PNG, BMP and Tagged Image Format (TIFF) formats in MB, the highest frequency and Levenshtein distance measurements for each document across the seven previously defined resolution levels.

Table 5 – Text Dataset - Binarized images results (**Image size** in centimeters (cm), **Font size** in points (pt), **dpi** - image resolution in dots per inch, **png/bmp/tiff** - file size of the png/bmp/tiff image in megabytes (MB), **HF** - Highest frequency, **LD** - Levenshtein distance).

Image	dpi	png	bmp	tiff	HF	LD	Image	png	bmp	tiff	HF	LD
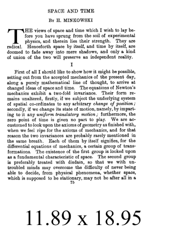	**75**	0.01	0.2	0.01	18	229	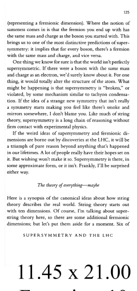	0.01	0.2	0.01	18	264
	150	0.04	0.79	0.02	19	16		0.04	0.8	0.02	19	12
	200	0.06	1.4	0.02	20	12		0.06	1.43	0.02	20	14
	300	0.12	3.16	0.03	20	10		0.11	3.21	0.03	21	13
	500	0.25	8.77	0.06	21	12		0.24	8.9	0.05	22	12
11.89 x 18.95	**700**	0.38	17.16	0.08	22	14	11.45 x 21.00	0.36	17.42	0.08	22	11
Font size: 10	**1200**	0.73	50.42	0.15	23	15	Font size: 10	0.68	51.22	0.14	23	12

Image	dpi	png	bmp	tiff	HF	LD	Image	png	bmp	tiff	HF	LD
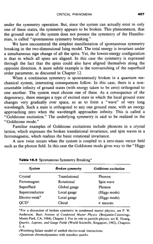	75	0.02	0.25	0.01	18	839	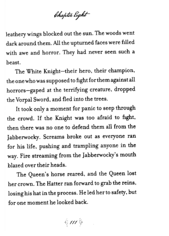	0.01	0.16	0.01	17	983
	150	0.05	0.99	0.03	19	172		0.03	0.64	0.01	19	912
	200	0.09	1.77	0.03	20	164		0.04	1.14	0.01	19	914
	300	0.17	3.97	0.05	21	166		0.08	2.55	0.02	20	911
	500	0.36	11.01	0.08	22	169		0.16	7.09	0.04	21	912
14.19 x 21.00	700	0.54	21.6	0.12	22	179	11.62 x 16.56	0.25	13.89	0.05	22	917
Font size: 10	1200	1.02	63.41	0.22	23	178	Font size: 12	0.48	40.81	0.1	23	915
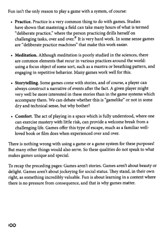	75	0.02	0.29	0.01	18	66	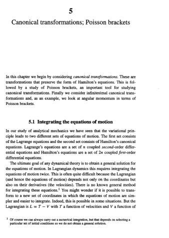	0.01	0.23	0.01	18	395
	150	0.05	1.17	0.02	19	14		0.04	0.9	0.02	19	10
	200	0.08	2.07	0.03	20	14		0.06	1.61	0.02	20	9
	300	0.16	4.65	0.04	21	21		0.12	3.62	0.03	21	7
	500	0.31	12.9	0.07	22	19		0.24	10.03	0.06	22	9
15.68 x 22.28	700	0.47	25.28	0.1	23	20	12.94 x 21.00	0.37	19.68	0.09	22	10
Font size: 12	1200	0.89	74.25	0.19	24	20	Font size: 11	0.71	57.77	0.16	23	14
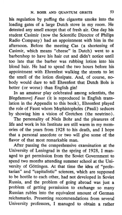	75	0.02	0.19	0.01	18	107	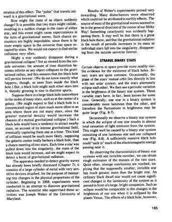	0.03	0.28	0.02	18	3090
	150	0.05	0.77	0.02	19	12		0.08	1.12	0.04	19	3187
	200	0.08	1.38	0.03	20	7		0.13	1.99	0.05	20	3163
	300	0.15	3.09	0.04	20	7		0.24	4.47	0.07	21	3204
	500	0.3	8.57	0.07	21	7		0.52	12.41	0.12	22	3208
11.04 x 21.00	700	0.45	16.78	0.1	22	7	15.10 x 22.28	0.78	24.32	0.18	22	3205
Font size: 12	1200	0.85	49.33	0.18	23	12	Font size: 10	1.47	71.44	0.32	24	3210
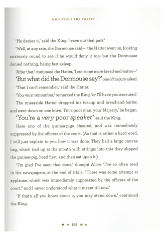	75	0.02	0.32	0.01	18	79	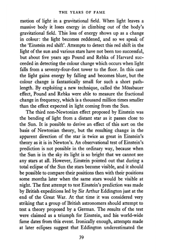	0.02	0.2	0.01	18	159
	150	0.05	1.27	0.02	20	29		0.05	0.79	0.02	19	2
	200	0.07	2.26	0.02	20	20		0.09	1.4	0.03	20	2
	300	0.12	5.09	0.03	21	25		0.17	3.16	0.04	20	1
	500	0.25	14.11	0.05	22	26		0.33	8.77	0.07	21	1
16.29 x 23.47	700	0.38	27.65	0.07	23	20	11.89 x 19.95	0.5	17.16	0.11	22	2
Font size: 12	1200	0.71	81.21	0.14	24	22	Font size: 12	0.94	50.42	0.19	23	3
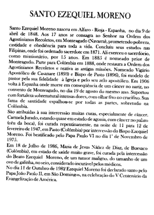	75	0.007	0.09	0.006	17	1602	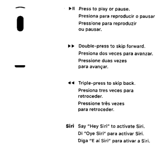	0.002	0.06	0.002	17	442
	150	0.02	0.34	0.01	18	107		0.006	0.24	0.003	18	49
	200	0.03	0.6	0.02	19	63		0.009	0.42	0.004	19	46
	300	0.06	1.36	0.02	20	47		0.02	0.94	0.005	19	41
	500	0.14	3.76	0.04	21	46		0.04	2.62	0.009	20	43
8.57 x 11.89	700	0.23	7.36	0.05	21	43	7.96 x 8.94	0.06	5.13	0.01	21	45
Font size: 7	1200	0.45	21.6	0.1	22	47	Font size: 7	0.14	15.08	0.04	22	58

Image	dpi	png	bmp	tiff	HF	LD	Image	png	bmp	tiff	HF	LD
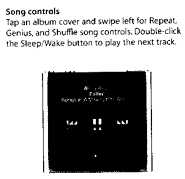	**75**	0.001	0.02	0.0004	15	210	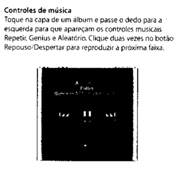	0.0008	0.02	0.0004	15	279
	150	0.003	0.07	0.001	16	85		0.004	0.09	0.002	17	104
	200	0.005	0.13	0.002	17	53		0.005	0.16	0.002	17	65
	300	0.009	0.28	0.004	18	43		0.01	0.36	0.004	18	53
	500	0.02	0.77	0.008	19	25		0.02	0.99	0.009	19	39
4.71 x 4.47 Font size: 5	**700**	0.04	1.51	0.01	19	24	5.01 x 5.35 Font size: 5	0.04	1.93	0.01	20	45
	1200	0.08	4.44	0.02	21	49		0.09	5.67	0.03	21	48
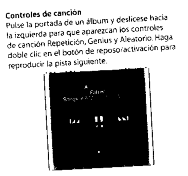	**75**	0.0008	0.02	0.0005	15	294	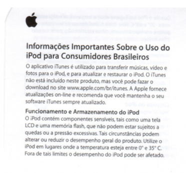	0.002	0.02	0.002	15	783
	150	0.004	0.09	0.002	17	116		0.005	0.09	0.004	17	360
	200	0.006	0.15	0.002	17	69		0.008	0.16	0.005	17	65
	300	0.01	0.34	0.005	18	47		0.02	0.35	0.007	18	32
	500	0.03	0.93	0.009	19	52		0.04	0.98	0.01	19	22
4.71 x 5.38 Font size: 5	**700**	0.04	1.82	0.01	20	48	5.59 x 4.78 Font size: 4	0.06	1.92	0.02	20	25
	1200	0.09	5.33	0.03	21	42		0.13	5.64	0.03	21	20
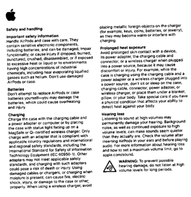	**75**	0.006	0.06	0.006	16	2586	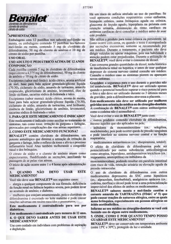	0.04	0.38	0.03	18	4066
	150	0.02	0.25	0.01	18	2325		0.11	1.52	0.05	20	4152
	200	0.03	0.44	0.02	18	1976		0.18	2.7	0.07	20	4153
	300	0.06	0.98	0.03	19	1981		0.35	6.06	0.11	21	4148
	500	0.13	2.72	0.04	20	1983		0.75	16.83	0.18	22	4156
8.57 x 8.64 Font size: 5	**700**	0.21	5.34	0.06	21	1979	18.05 x 25.26 Font size: 8	1.13	32.98	0.25	23	4150
	1200	0.45	15.66	0.1	22	1982		2.15	96.93	0.46	24	4162

Song controls
Tap an album cover and swipe left for Repeat, Genius, and Shuffle song controls. Double-click the Sleep/Wake button to play the next track.

Controles de música
Toque na capa de um álbum e passe o dedo para a esquerda para que apareçam os controles musicais Repetir, Genius e Aleatório. Clique duas vezes no botão Repouso/Despertar para reproduzir a próxima faixa.

Controles de canción
Pulse la portada de un álbum y deslícese hacia la izquierda para que aparezcan los controles de canción Repetición, Genius y Aleatorio. Haga doble clic en el botón de reposo/activación para reproducir la pista siguiente.

Informações Importantes Sobre o Uso do iPod para Consumidores Brasileiros
O aplicativo iTunes é utilizado para transferir músicas, vídeo e fotos para o iPod, e para atualizar e restaurar o iPod. O iTunes não está incluído neste produto, mas você pode fazar o download no site www.apple.com/br/itunes. A Apple fornece atualizações on-line e recomenda que você mantenha o seu software iTunes sempre atualizado.
Funcionamento e Armazenamento do iPod
O iPod contém componentes sensíveis, tais como uma tela LCD e uma memória flash, que não podem estar sujeitos a quedas ou a pressão excessivas. Tais circunstâncias podem alterar ou reduzir o desempenho geral do produto. Utilize o iPod em lugares onde a temperatura esteja entre 0° e 35° C. Fora de tais limites o desempenho do iPod pode ser afetado.

Safety and handling
Important safety information
Handle AirPods and case with care. They contain sensitive electronic components, including batteries, and can be damaged, impair functionality, or cause injury if dropped, burned, punctured, crushed, disassembled, or if exposed to excessive heat or liquid or to environments having high concentrations of industrial chemicals, including near evaporating liquified gasses such as helium. Don't use damaged AirPods or case.
Batteries
Don't attempt to replace AirPods or case batteries yourself—you may damage the batteries, which could cause overheating and injury.
Charging
Charge the case with the charging cable and a power adapter or computer or by placing the case with status light facing up on a MagSafe or Qi-certified wireless charger. Only charge with an adapter that is compliant with applicable country regulations and international and regional safety standards, including the International Standard for Safety of Information Technology Equipment (IEC 60950-1). Other adapters may not meet applicable safety standards, and charging with such adapters could pose a risk of death or injury. Using damaged cables or chargers, or charging when moisture is present, can cause fire, electric shock, injury, or damage to the case or other property. When using a wireless charger, avoid placing metallic foreign objects on the charger (for example, keys, coins, batteries, or jewelry), as they may become warm or interfere with charging.
Prolonged heat exposure
Avoid prolonged skin contact with a device, its power adapter, the charging cable and connector, or a wireless charger when plugged into a power source, because it may cause discomfort or injury. For example, while the case is charging using the charging cable and a power adapter or a wireless charger plugged into a power source, don't sit or sleep on the case, charging cable, connector, power adapter, or wireless charger, or place them under a blanket, pillow, or your body. Take special care if you have a physical condition that affects your ability to detect heat against your body.
Hearing loss
Listening to sound at high volumes may permanently damage your hearing. Background noise, as well as continued exposure to high volume levels, can make sounds seem quieter than they actually are. Check the volume after inserting AirPods in your ears and before playing audio. For more information about hearing loss and how to set a maximum volume limit, go to apple.com/sound.
WARNING: To prevent possible hearing damage, do not listen at high volume levels for long periods.

577395
PASTILHAS
Benalet®
cloridrato de difenidramina
cloreto de amônio
citrato de sódio
APRESENTAÇÕES
Embalagens com 12 pastilhas nos sabores mel-limão ou menta, ou embalagens contendo 52 pastilhas nos sabores mel-limão ou menta, contendo 5 mg de cloridrato de difenidramina, 50 mg de cloreto de amônio e 10 mg de citrato de sódio por pastilha.
USO ORAL
USO ADULTO E PEDIÁTRICO ACIMA DE 12 ANOS
COMPOSIÇÃO
Cada pastilha contém 5 mg de cloridrato de difenidramina (equivalente a 4,375 mg de difenidramina), 50 mg de cloreto de amônio e 10 mg de citrato de sódio.
Excipientes (sabor mel-limão): ácido cítrico, aroma artificial de mel, base para bala açúcar granulado/glicose líquida (70:30), ciclamato de sódio, amarelo de tartrazina, amarelo crepúsculo, glicirrizinato de amônio, levomentol, óleo de limão siciliano, sacarina sódica di-hidratada e talco.
Excipientes (sabor menta): ácido cítrico, aroma de menta, base para bala açúcar granulado/glicose líquida (70:30), ciclamato de sódio, amarelo de tartrazina, azul brilhante, essência de limão, glicirrizinato de amônio, levomentol, sacarina sódica di-hidratada e talco.
1. PARA QUE ESTE MEDICAMENTO É INDICADO?
Este medicamento é indicado como auxiliar no tratamento de sintomas, tais como tosse, irritação da garganta e faringite, provocados por complicações das vias aéreas superiores.
2. COMO ESTE MEDICAMENTO FUNCIONA?
BENALET® contém cloridrato de difenidramina, um potente antialérgico que diminui a sensação de irritação da garganta e faringe, inibe o reflexo da tosse e alivia o processo inflamatório local. Atua também melhorando a congestão nasal e dos brônquios.
O citrato de sódio e o cloreto de amônio atuam como expectorantes, fluidificando as secreções, auxiliando na passagem do ar pelas vias aéreas.
O início de ação ocorre entre 1 e 4 horas após administração oral.
3. QUANDO NÃO DEVO USAR ESTE MEDICAMENTO?
Você não deve usar **BENALET®** nos seguintes casos:
- alergia a qualquer componente de sua fórmula; deficiência da função renal ou falência hepática severa, pois podem levar ao acumulo de amônio; e diabetes;
- mulheres que estejam amamentando, pois o cloridrato de difenidramina é excretado no leite materno e pode causar reações adversas em recém-nascidos e prematuros;
Este medicamento é contraindicado para uso por diabéticos.
Este medicamento é contraindicado para menores de 12 anos.
4. O QUE DEVO SABER ANTES DE USAR ESTE MEDICAMENTO?
Use com cuidado em indivíduos com problemas de aspiração e deglutição.
Há um risco de asfixia atrelado ao uso de pastilhas. Se você apresenta condições respiratórias como enfisema, bronquite crônica, asma brônquica aguda ou crônica, glaucoma de ângulo agudo, hiperplasia na próstata com retenção urinária, diminuição do ritmo cardíaco ou arritmias cardíacas deve consultar o médico antes de usar este produto.
Não utilize o produto para tosse crônica ou persistente, tal como ocorre com asma, ou quando a tosse é acompanhada por secreções excessivas; somente se recomendado por um médico. Durante o tratamento, o paciente não deve dirigir veículos ou operar máquinas, pois sua habilidade e atenção podem estar prejudicadas. Durante a utilização de **BENALET®**, você deve evitar o consumo de álcool.
Caso consuma grandes quantidades de álcool, tenha histórico de insuficiência renal ou hepática, e antes de usar qualquer depressor do sistema nervoso central consulte um médico. Consulte o médico caso os sintomas piorem ou apareçam novos sintomas.
Gravidez: a segurança para o uso durante a gravidez não foi estabelecida. **BENALET®** deve ser utilizado apenas quando o potencial benefício superar o risco potencial para o feto e não deve ser utilizado durante os 3 últimos meses de gravidez, pois a difenidramina atravessa a placenta.
Este medicamento não deve ser utilizado por mulheres grávidas sem orientação médica ou do cirurgião-dentista.
A combinação de **BENALET®** com outros antitussígenos como a codeína não é aconselhável.
Você deve evitar o uso de **BENALET®** junto com:
- outros produtos contendo cloridrato de difenidramina, mesmo aqueles que são aplicados na pele;
- inibidores da monoaminoxidase (ex.: selegilina, moclobemida), pois pode ocorrer queda de pressão sanguínea e pode interferir no sistema nervoso central e na função respiratória;
- medicamentos antiarrítmicos (ex.: disopiramina, sotalol).
O efeito de cloridrato de difenidramina pode ser potencializado por outras substâncias anticolinérgicas como atropina, biperideno, antidepressivos tricíclicos (ex.: imipramina, amitriptilina) ou inibidores da monoaminoxidase, podendo resultar em paralisia intestinal com risco de vida, retenção urinária ou elevação aguda da pressão intraocular.
O uso de cloridrato de difenidramina com outros medicamentos depressores do SNC como hipnóticos (ex.: alprazolam, fenobarbital), analgésicos opiáceos (ex.: codeína, morfina) e álcool pode levar a uma potencialização imprevisível dos efeitos de ambos os medicamentos.
BENALET® sabores menta e mel-limão contêm o corante amarelo de TARTRAZINA (FD&C nº 5) que pode causar reações de natureza alérgica, entre as quais asma brônquica, especialmente em pessoas alérgicas ao ácido acetilsalicílico.
Informe ao seu médico ou cirurgião-dentista se você está fazendo uso de algum outro medicamento.
5. ONDE, COMO E POR QUANTO TEMPO POSSO GUARDAR ESTE MEDICAMENTO?
BENALET® deve ser conservado em temperatura ambiente (entre 15°C e 30°C), protegido da luz e umidade.

Source: The author (2024)

The analysis of the images in the Text Dataset shows that applying a low scan resolution, such as 75 dpi, leads to very poor OCR performance, with minimal document details preserved. In these cases, the Levenshtein distances were significantly higher than those at 150 dpi, highlighting that low resolutions hinder accurate recognition of document features, including finer character details. For binarized images, low resolution further exacerbates this issue, especially in images with small details. For instance, a small image from the dataset is illustrated in Figure 20, measuring 4.71 x 4.47 centimeters and with a font size of 5 pt. The figure shows that during binarization all text content was lost, resulting in an illegible image.

At higher resolutions, when analyzing the density of frequencies exceeding the maximum frequency obtained at 300 dpi, the difference in spectral densities observed approaches the level of scanning noise, with values typically below 0.001. This suggests that increasing the resolution beyond

Figure 20 – Small image, measuring 4.71 x 4.47 centimeters, in the resolution of 75 dpi.

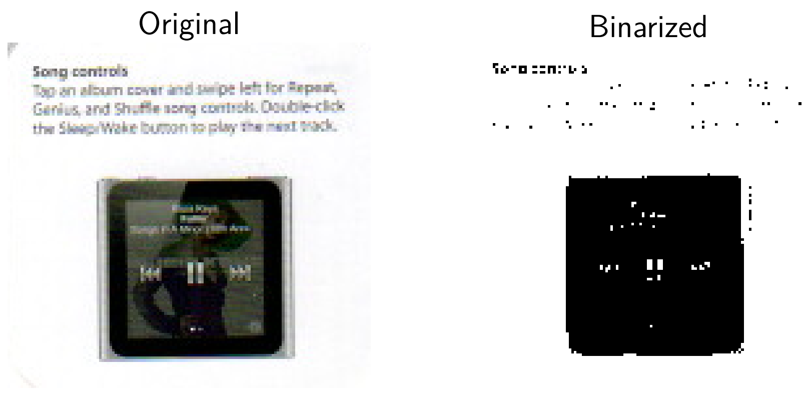

Song controls
Tap an album cover and swipe left for Repeat, Genius, and Shuffle song controls. Double-click the Sleep/Wake button to play the next track.

Source: The author (2024)

300 dpi adds minimal useful detail, as the spectral density for such high frequencies does not significantly contribute to document clarity.

The maximum frequency observed in the 200 to 300 dpi range tends to be consistent, generally falling between 19 and 21. This stability in maximum frequency across these resolutions indicates that further increases in resolution yield diminishing returns in terms of detail capture. Consequently, the maximum frequency difference between 300 dpi and even higher resolutions is minor, with a maximum discrepancy of about three units. Such findings imply that 300 dpi may be an optimal balance point, as higher resolutions lead to larger file sizes without substantial improvements in detail discernment or spectral information.

Table 6 presents the percentage of frequency density exceeding the maximum frequencies obtained at 200 dpi and 300 dpi for the original text images. The results show that the use of different scanners did not result in significant changes in the frequency results, and the observed difference in density values can be considered a scanning error of the device.

Table 6 – Proportion of highest frequency density above the maximum frequency of 200 and 300 dpi in the General dataset - Original images

Image	**dpi**	**Epson L4160**		**Epson L8180**		**HP M479FDW**	
		200dpi	**300dpi**	**200dpi**	**300dpi**	**200dpi**	**300dpi**
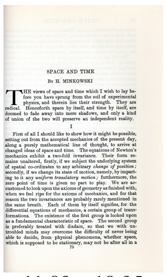 11.89 x 18.95 Font size: 10	**75**	0.0000%	0.0000%	0.0000%	0.0000%	0.0000%	0.0000%
	150	0.0000%	0.0000%	0.0000%	0.0000%	-	-
	200	0.0000%	0.0000%	0.0000%	0.0000%	0.0000%	0.0000%
	300	0.1761%	0.0000%	0.1832%	0.0000%	0.3225%	0.0000%
	500	0.5880%	0.1843%	0.5502%	0.1455%	-	-
	700	0.9939%	0.4210%	0.8421%	0.3093%	-	-
	1200	1.2763%	0.7350%	0.9576%	0.3971%	1.7536%	0.8336%
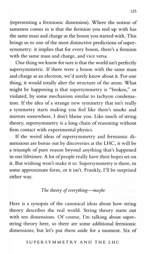 11.45 x 21.00 Font size: 10	**75**	0.0000%	0.0000%	0.0000%	0.0000%	0.0000%	0.0000%
	150	0.0000%	0.0000%	0.0000%	0.0000%	-	-
	200	0.0000%	0.0000%	0.0000%	0.0000%	0.0000%	0.0000%
	300	0.2400%	0.0000%	0.1377%	0.0000%	0.1707%	0.0000%
	500	1.2415%	0.4823%	0.6000%	0.2044%	-	-
	700	1.7568%	0.8456%	0.8859%	0.3397%	-	-
	1200	1.8204%	1.0146%	1.2866%	0.6932%	1.7131%	0.8698%
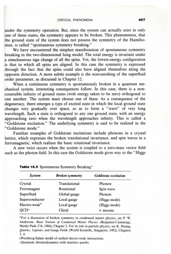 14.19 x 21.00 Font size: 10	**75**	0.0000%	0.0000%	0.0000%	0.0000%	0.0000%	0.0000%
	150	0.0000%	0.0000%	0.0000%	0.0000%	-	-
	200	0.0000%	0.0000%	0.0000%	0.0000%	0.0000%	0.0000%
	300	0.0000%	0.0000%	0.1362%	0.0000%	0.4593%	0.0000%
	500	0.4851%	0.1886%	0.5081%	0.1905%	-	-
	700	0.8319%	0.3965%	0.7758%	0.3259%	-	-
	1200	1.0326%	0.7835%	1.1232%	0.6761%	1.8980%	0.4013%
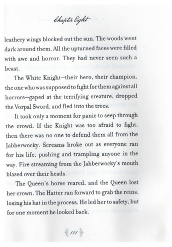 11.62 x 16.56 Font size: 12	**75**	0.0000%	0.0000%	0.0000%	0.0000%	0.0000%	0.0000%
	150	0.0000%	0.0000%	0.0000%	0.0000%	-	-
	200	0.0000%	0.0000%	0.0000%	0.0000%	0.0000%	0.0000%
	300	0.1707%	0.0000%	0.1447%	0.0000%	0.1925%	0.0000%
	500	0.7210%	0.1802%	0.4661%	0.1687%	-	-
	700	0.9952%	0.4215%	0.7909%	0.3424%	-	-
	1200	1.1225%	0.6127%	0.9789%	0.5623%	1.0115%	0.5206%
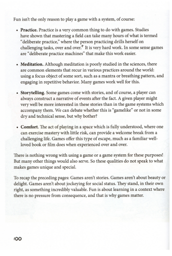 15.68 x 22.28 Font size: 12	**75**	0.0000%	0.0000%	0.0000%	0.0000%	0.0000%	0.0000%
	150	0.0000%	0.0000%	0.0000%	0.0000%	-	-
	200	0.0000%	0.0000%	0.0000%	0.0000%	0.0000%	0.0000%
	300	0.1576%	0.0000%	0.1611%	0.0000%	0.1615%	0.0000%
	500	0.6866%	0.2405%	0.7174%	0.1990%	-	-
	700	0.8531%	0.3534%	0.9929%	0.4385%	-	-
	1200	1.0343%	0.6024%	1.2005%	0.7363%	1.3622%	0.7875%

Image	dpi	Epson L4160		Epson L8180		HP M479FDW	
		200dpi	300dpi	200dpi	300dpi	200dpi	300dpi
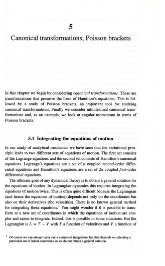	75	0.0000%	0.0000%	0.0000%	0.0000%	0.0000%	0.0000%
	150	0.0000%	0.0000%	0.0000%	0.0000%	-	-
	200	0.0000%	0.0000%	0.0000%	0.0000%	0.0000%	0.0000%
	300	0.0000%	0.0000%	0.4237%	0.0000%	0.1810%	0.0000%
	500	0.2566%	0.1633%	1.1932%	0.1792%	-	-
	700	0.3839%	0.3000%	1.5859%	0.3264%	-	-
12.94 x 21.00 Font size: 11	1200	0.6848%	0.3939%	1.6612%	0.5077%	1.5448%	0.8194%
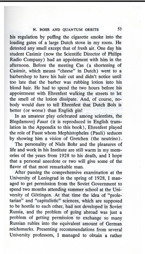	75	0.0000%	0.0000%	0.0000%	0.0000%	0.0000%	0.0000%
	150	0.0000%	0.0000%	0.0000%	0.0000%	-	-
	200	0.0000%	0.0000%	0.0000%	0.0000%	0.0000%	3.8212%
	300	0.0000%	0.0000%	0.2335%	0.0000%	0.1679%	8.0493%
	500	0.1417%	0.1417%	0.7729%	0.2639%	-	-
	700	0.1387%	0.1387%	1.0906%	0.5209%	-	-
11.04 x 21.00 Font size: 12	1200	0.0000%	0.0000%	1.2987%	0.8255%	0.8636%	14.3764%
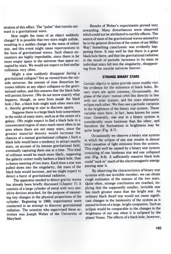	75	0.0000%	0.0000%	0.0000%	0.0000%	0.0000%	0.0000%
	150	0.0000%	0.0000%	0.0000%	0.0000%	-	-
	200	0.0000%	0.0000%	0.0000%	0.0000%	0.0000%	0.0000%
	300	0.1622%	0.0000%	0.2316%	0.0000%	0.1615%	0.0000%
	500	0.5178%	0.1711%	0.7481%	0.2823%	-	-
	700	1.0329%	0.4078%	1.1366%	0.4747%	-	-
15.10 x 22.28 Font size: 10	1200	1.1921%	0.6618%	1.3727%	0.7650%	0.9998%	0.4669%
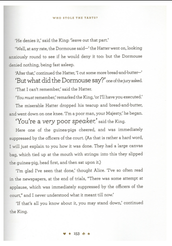	75	0.0000%	0.0000%	0.0000%	0.0000%	0.0000%	0.0000%
	150	0.0000%	0.0000%	0.0000%	0.0000%	-	-
	200	0.0000%	0.0000%	0.0000%	0.0000%	0.0000%	0.0000%
	300	0.2068%	0.0000%	0.4196%	0.0000%	0.1668%	0.0000%
	500	1.1964%	0.4877%	1.2297%	0.1695%	-	-
	700	1.5840%	0.8494%	1.7359%	0.3271%	-	-
16.29 x 23.47 Font size: 12	1200	1.3543%	0.9224%	1.4636%	0.5573%	1.1400%	0.7245%
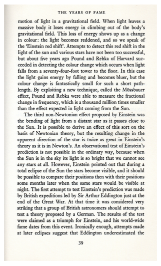	75	0.0000%	0.0000%	0.0000%	0.0000%	0.0000%	0.0000%
	150	0.0000%	0.0000%	0.0000%	0.0000%	-	-
	200	0.0000%	0.0000%	0.0000%	0.0000%	0.0000%	0.0000%
	300	0.4489%	0.0000%	0.2411%	0.0000%	0.1794%	0.0000%
	500	0.9904%	0.1568%	0.9393%	0.4603%	-	-
	700	1.3210%	0.2917%	1.2009%	0.6165%	-	-
11.89 x 19.95 Font size: 12	1200	1.4147%	0.4168%	1.3511%	0.7556%	1.3881%	0.7763%

Image	dpi	Epson L4160		Epson L8180		HP M479FDW	
		200dpi	300dpi	200dpi	300dpi	200dpi	300dpi
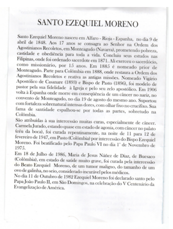	**75**	0.0000%	0.0000%	0.0000%	0.0000%	0.0000%	0.0000%
	150	0.0000%	0.0000%	0.0000%	0.0000%	-	-
	200	0.0000%	0.0000%	0.0000%	0.0000%	0.0000%	0.0000%
	300	0.8463%	0.0000%	0.1748%	0.0000%	0.3930%	0.0000%
	500	2.5246%	0.2690%	1.0470%	0.2753%	-	-
8.57 x 11.89	**700**	3.4287%	0.6810%	1.7451%	0.6810%	-	-
Font size: 7	**1200**	3.7217%	1.1440%	2.3127%	1.2318%	3.8615%	1.6708%
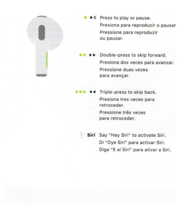	**75**	0.0000%	0.0000%	0.0000%	0.0000%	0.0000%	0.0000%
	150	0.0000%	0.0000%	0.0000%	0.0000%	-	-
	200	0.0000%	0.0000%	0.0000%	0.0000%	0.0000%	0.0000%
	300	0.0099%	0.0000%	0.0095%	0.0000%	0.1924%	0.0000%
	500	0.5667%	0.5317%	0.5033%	0.4721%	-	-
7.96 x 8.94	**700**	1.2616%	1.1879%	1.0458%	0.9786%	-	-
Font size: 7	**1200**	1.8711%	1.8147%	1.5301%	1.4701%	2.0657%	0.9401%
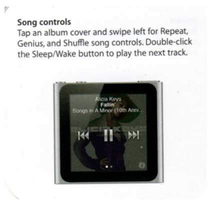	**75**	0.0000%	0.0000%	0.0000%	0.0000%	0.0000%	0.0000%
	150	0.0000%	0.0872%	0.0000%	0.0795%	-	-
	200	0.0000%	0.1244%	0.0000%	0.1796%	0.0000%	0.0000%
	300	0.0000%	0.0000%	0.0000%	0.0000%	0.0442%	0.0000%
	500	0.0000%	0.0636%	0.0000%	0.0629%	-	-
4.71 x 4.47	**700**	0.0000%	0.1703%	0.0000%	0.1939%	-	-
Font size: 5	**1200**	0.1592%	0.5337%	0.1721%	0.6931%	1.9900%	1.7066%
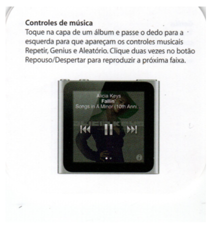	**75**	0.0000%	0.0113%	0.0000%	0.0000%	0.0000%	0.0000%
	150	0.0000%	0.1026%	0.0000%	0.0939%	-	-
	200	0.0000%	0.0807%	0.0000%	0.1832%	0.0000%	0.0000%
	300	0.0000%	0.0000%	0.0000%	0.0000%	0.2167%	0.0000%
	500	0.0941%	0.1968%	0.0000%	0.0617%	-	-
5.01 x 5.35	**700**	0.0605%	0.1967%	0.0000%	0.1907%	-	-
Font size: 5	**1200**	0.3266%	0.7406%	0.1496%	0.6592%	2.2168%	0.7389%
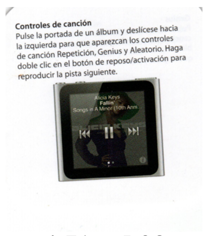	**75**	0.0000%	0.0000%	0.0000%	0.0000%	0.0000%	0.0000%
	150	0.0000%	0.1087%	0.0000%	0.2236%	-	-
	200	0.0000%	0.0815%	0.0000%	0.1731%	0.0000%	0.0000%
	300	0.0000%	0.0000%	0.0000%	0.0000%	0.0543%	0.0000%
	500	0.0872%	0.2101%	0.0000%	0.0710%	-	-
4.71 x 5.38	**700**	0.1865%	0.3763%	0.0000%	0.2615%	-	-
Font size: 5	**1200**	0.4501%	0.9327%	0.1572%	0.8157%	1.0271%	0.8403%

SANTO EZEQUIEL MORENO

Santo Ezequiel Moreno nasceu em Alfaro - Rioja - Espanha, no dia 9 de abril de 1848. Aos 17 anos se consagra ao Senhor na Ordem dos Agostinianos Recoletos, em Monteagudo (Navarra), prometendo pobreza, castidade e obediência para toda a vida. Concluiu seus estudos nas Filipinas, onde foi ordenado sacerdote em 1871. Ali exerceu o sacerdócio, como missionário, por 15 anos. Em 1885 é nomeado prior de Monteagudo. Parte para Colômbia em 1888, onde restaura a Ordem dos Agostinianos Recoletos e reativa as antigas missões. Nomeado Vigário Apostólico de Casanare (1893) e Bispo de Pasto (1896), foi modelo de pastor pela sua fidelidade à Igreja e pelo seu zelo apostólico. Em 1906 volta à Espanha onde morre em conseqüência de um câncer no nariz, no convento de Monteagudo, no dia 19 de agosto do mesmo ano. Suportou com fortaleza sobrenatural intensas dores, com olhar fixo no crucifixo. Sua fama de santidade espalhou-se por todas as partes, sobretudo na Colômbia.

São atribuídas à sua intercessão muitas curas, especialmente de câncer. Carmela Jurado, estando quase em estado de agonia, com câncer no palato (céu da boca), foi curada repentinamente, na noite de 11 para 12 de fevereiro de 1947, em Pasto (Colômbia) por intercessão do Bispo Ezequiel Moreno. Foi beatificado pelo Papa Paulo VI no dia 1° de Novembro de 1975.

Em 18 de Julho de 1986, Maria de Jesus Náñez de Diaz, de Buesaco (Colômbia), em estado de saúde muito grave, foi curada pela intercessão do Beato Ezequiel Moreno, de um tumor maligno, do tamanho de um ovo de galinha, no seio, considerado incurável pelos médicos.

No dia 11 de Outubro de 1982 Ezequiel Moreno foi declarado santo pelo Papa João Paulo II, em São Domingos, na celebração do V Centenário da Evangelização de América.

Press to play or pause.
Presiona para reproducir o pausar
Pressione para reproduzir ou pausar.

Double-press to skip forward.
Presiona dos veces para avanzar.
Pressione duas vezes para avançar.

Triple-press to skip back.
Presiona tres veces para retroceder.
Pressione três vezes para retroceder.

Siri Say "Hey Siri" to activate Siri.
Di "Oye Siri" para activar Siri.
Diga "E aí Siri" para ativar a Siri.

Song controls
Tap an album cover and swipe left for Repeat, Genius, and Shuffle song controls. Double-click the Sleep/Wake button to play the next track.

Controles de música
Toque na capa de um álbum e passe o dedo para a esquerda para que apareçam os controles musicais Repetir, Genius e Aleatório. Clique duas vezes no botão Repouso/Despertar para reproduzir a próxima faixa.

Controles de canción
Pulse la portada de un álbum y deslícese hacia la izquierda para que aparezcan los controles de canción Repetición, Genius y Aleatorio. Haga doble clic en el botón de reposo/activación para reproducir la pista siguiente.

Image	dpi	Epson L4160		Epson L8180		HP M479FDW	
		200dpi	**300dpi**	**200dpi**	**300dpi**	**200dpi**	**300dpi**
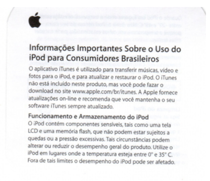	**75**	0.0000%	0.0000%	0.1722%	0.3560%	0.0000%	0.0000%
	150	0.0107%	0.0000%	0.0000%	0.1598%	-	-
	200	0.0000%	0.0000%	0.0000%	0.1164%	0.0000%	0.0000%
	300	0.2360%	0.0000%	0.0000%	0.0000%	0.2684%	0.0000%
	500	1.2629%	0.3359%	0.0000%	0.0000%	-	-
5.59 x 4.78	**700**	2.7519%	0.8205%	0.0000%	0.0000%	-	-
Font size: 4	**1200**	3.9866%	2.0043%	0.0000%	0.0000%	4.7040%	2.0457%
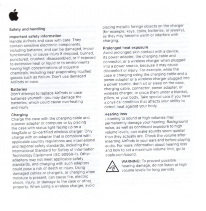	**75**	0.0000%	0.0000%	0.0000%	0.0000%	0.0000%	0.0000%
	150	0.0000%	0.0000%	0.0000%	0.0000%	-	-
	200	0.0000%	0.0000%	0.0000%	0.0000%	0.0000%	0.0000%
	300	0.1662%	0.0000%	0.1666%	0.0000%	0.3770%	0.0000%
	500	0.7108%	0.1727%	0.7647%	0.1858%	-	-
8.57 x 8.64	**700**	1.8023%	0.5432%	2.0381%	0.6429%	-	-
Font size: 5	**1200**	3.4152%	1.7602%	3.4642%	1.7633%	6.0758%	2.7101%
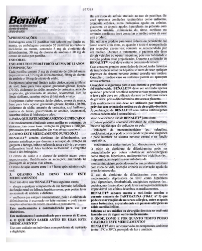	**75**	0.0000%	0.0000%	0.0000%	0.0000%	0.0000%	0.0000%
	150	0.0000%	0.0000%	0.0000%	0.0000%	-	-
	200	0.0000%	0.0000%	0.0000%	0.0000%	0.0000%	0.0000%
	300	0.1725%	0.0000%	0.1515%	0.0000%	0.1584%	0.0000%
	500	0.6136%	0.1534%	0.5106%	0.1687%	-	-
18.05 x 25.26	**700**	0.9497%	0.3855%	0.8566%	0.3639%	-	-
Font size: 8	**1200**	1.2721%	0.6811%	1.2115%	0.6637%	0.8021%	0.3238%

Source: The author (2024)

Informações Importantes Sobre o Uso do iPod para Consumidores Brasileiros
O aplicativo iTunes é utilizado para transferir músicas, vídeo e fotos para o iPod, e para atualizar e restaurar o iPod. O iTunes não está incluído neste produto, mas você pode fazer o download no site www.apple.com/br/itunes. A Apple fornece atualizações on-line e recomenda que você mantenha o seu software iTunes sempre atualizado.

Funcionamento e Armazenamento do iPod
O iPod contém componentes sensíveis, tais como uma tela LCD e uma memória flash, que não podem estar sujeitos a quedas ou a pressão excessivas. Tais circunstâncias podem alterar ou reduzir o desempenho geral do produto. Utilize o iPod em lugares onde a temperatura esteja entre 0° e 35° C. Fora de tais limites o desempenho do iPod pode ser afetado.

Safety and handling

Important safety information
Handle AirPods and case with care. They contain sensitive electronic components, including batteries, and can be damaged, impair functionality, or cause injury if dropped, burned, punctured, crushed, disassembled, or if exposed to excessive heat or liquid or to environments having high concentrations of industrial chemicals, including near evaporating liquified gasses such as helium. Don't use damaged AirPods or case.

Batteries
Don't attempt to replace AirPods or case batteries yourself—you may damage the batteries, which could cause overheating and injury.

Charging
Charge the case with the charging cable and a power adapter or computer or by placing the case with status light facing up on a MagSafe or Qi-certified wireless charger. Only charge with an adapter that is compliant with applicable country regulations and international and regional safety standards, including the International Standard for Safety of Information Technology Equipment (IEC 60950-1). Other adapters may not meet applicable safety standards, and charging with such adapters could pose a risk of death or injury. Using damaged cables or chargers, or charging when moisture is present, can cause fire, electric shock, injury, or damage to the case or other property. When using a wireless charger, avoid placing metallic foreign objects on the charger (for example, keys, coins, batteries, or jewelry), as they may become warm or interfere with charging.

Prolonged heat exposure
Avoid prolonged skin contact with a device, its power adapter, the charging cable and connector, or a wireless charger when plugged into a power source, because it may cause discomfort or injury. For example, while the case is charging using the charging cable and a power adapter or a wireless charger plugged into a power source, don't sit or sleep on the case, charging cable, connector, power adapter, or wireless charger, or place them under a blanket, pillow, or your body. Take special care if you have a physical condition that affects your ability to detect heat against your body.

Hearing loss
Listening to sound at high volumes may permanently damage your hearing. Background noise, as well as continued exposure to high volume levels, can make sounds seem quieter than they actually are. Check the volume after inserting AirPods in your ears and before playing audio. For more information about hearing loss and how to set a maximum volume limit, go to apple.com/sound.

WARNING: To prevent possible hearing damage, do not listen at high volume levels for long periods.

577395

PASTILHAS **Benalet**®
cloridrato de difenidramina
cloreto de amônio
citrato de sódio

APRESENTAÇÕES
Embalagens com 12 pastilhas nos sabores mel-limão ou menta, ou embalagens contendo 52 pastilhas nos sabores mel-limão ou menta, contendo 5 mg de cloridrato de difenidramina, 50 mg de cloreto de amônio e 10 mg de citrato de sódio por pastilha.
USO ORAL
USO ADULTO E PEDIÁTRICO ACIMA DE 12 ANOS
COMPOSIÇÃO
Cada pastilha contém 5 mg de cloridrato de difenidramina (equivalente a 4,375 mg de difenidramina), 50 mg de cloreto de amônio e 10 mg de citrato de sódio.
Excipientes (sabor mel-limão): ácido cítrico, aroma artificial de mel, base para bala açúcar granulado/glicose líquida (70:30), ciclamato de sódio, amarelo de tartrazina, amarelo crepúsculo, glicirrizinato de amônio, levomentol, óleo de limão siciliano, sacarina sódica di-hidratada e talco.
Excipientes (sabor menta): ácido cítrico, aroma de menta, base para bala açúcar granulado/glicose líquida (70:30), ciclamato de sódio, amarelo de tartrazina, azul brilhante, essência de limão, glicirrizinato de amônio, levomentol, sacarina sódica di-hidratada e talco.
1. PARA QUE ESTE MEDICAMENTO É INDICADO?
Este medicamento é indicado como auxiliar no tratamento de sintomas, tais como tosse, irritação da garganta e faringite, provocados por complicações das vias aéreas superiores.
2. COMO ESTE MEDICAMENTO FUNCIONA?
BENALET® contém cloridrato de difenidramina, um potente antialérgico que diminui a sensação de irritação da garganta e faringe, inibe o reflexo da tosse e alivia o processo inflamatório local. Atua também melhorando a congestão nasal e dos brônquios.
O citrato de sódio e o cloreto de amônio atuam como expectorantes, fluidificando as secreções, auxiliando na passagem do ar pelas vias aéreas.
O início de ação ocorre entre 1 e 4 horas após administração oral.
3. QUANDO NÃO DEVO USAR ESTE MEDICAMENTO?
Você não deve usar **BENALET®** nos seguintes casos:
- alergia a qualquer componente de sua fórmula; deficiência da função renal ou falência hepática severa, pois podem levar ao acúmulo de amônio; e diabetes;
- mulheres que estejam amamentando, pois o cloridrato de difenidramina é excretado no leite materno e pode causar reações adversas em recém-nascidos e prematuros;
Este medicamento é contraindicado para uso por diabéticos.
Este medicamento é contraindicado para menores de 12 anos.
4. O QUE DEVO SABER ANTES DE USAR ESTE MEDICAMENTO?
Use com cuidado em indivíduos com problemas de aspiração e deglutição.
Há um risco de asfixia atrelado ao uso de pastilhas. Se você apresenta condições respiratórias como enfisema, bronquite crônica, asma brônquica aguda ou crônica, glaucoma de ângulo agudo, hiperplasia na próstata com retenção urinária, diminuição do ritmo cardíaco ou arritmias cardíacas deve consultar o médico antes de usar este produto.
Não utilize o produto para tosse crônica ou persistente, tal como ocorre com asma, ou quando a tosse é acompanhada por secreções excessivas; somente se recomendado por um médico. Durante o tratamento, o paciente não deve dirigir veículos ou operar máquinas, pois sua habilidade e atenção podem estar prejudicadas. Durante a utilização de **BENALET®**, você deve evitar o consumo de álcool.
Caso consuma grandes quantidades de álcool, tenha histórico de insuficiência renal ou hepática, e antes de usar qualquer depressor do sistema nervoso central consulte um médico. Consulte o médico caso os sintomas piorem ou apareçam novos sintomas.
Gravidez: a segurança para o uso durante a gravidez não foi estabelecida. **BENALET®** deve ser utilizado apenas quando o potencial benefício superar o risco potencial para o feto e não deve ser utilizado durante os 3 últimos meses de gravidez, pois a difenidramina atravessa a placenta.
Este medicamento não deve ser utilizado por mulheres grávidas sem orientação médica ou do cirurgião-dentista.
A combinação de **BENALET®** com outros antitussígenos como a codeína não é aconselhável.
Você deve evitar o uso de **BENALET®** junto com:
- outros produtos contendo cloridrato de difenidramina, mesmo aqueles que são aplicados na pele;
- inibidores da monoaminoxidase (ex.: selegilina, moclobemida), pois pode ocorrer queda de pressão sanguínea e pode interferir no sistema nervoso central e na função respiratória;
- medicamentos antiarrítmicos (ex.: disopiramina, sotalol).
O efeito de cloridrato de difenidramina pode ser potencializado por outras substâncias anticolinérgicas como atropina, biperideno, antidepressivos tricíclicos (ex.: imipramina, amitriptilina) ou inibidores da monoaminoxidase, podendo resultar em paralisia intestinal com risco de vida, retenção urinária ou elevação aguda da pressão intraocular.
O uso de cloridrato de difenidramina com outros medicamentos depressores do SNC como hipnóticos (ex.: alprazolam, fenobarbital), analgésicos opiáceos (ex.: codeína, morfina) e álcool pode levar a uma potencialização imprevisível dos efeitos de ambos os medicamentos.
BENALET® sabores menta e mel-limão contêm o corante amarelo de TARTRAZINA (FD&C nº 5) que pode causar reações de natureza alérgica, entre as quais asma brônquica, especialmente em pessoas alérgicas ao ácido acetilsalicílico.
Informe ao seu médico ou cirurgião-dentista se você está fazendo uso de algum outro medicamento.
5. ONDE, COMO E POR QUANTO TEMPO POSSO GUARDAR ESTE MEDICAMENTO?
BENALET® deve ser conservado em temperatura ambiente (entre 15ºC e 30ºC), protegido da luz e umidade.

The results shown in Table 6 indicate that increasing the resolution does not lead to a significant rise in higher frequencies. The slight increase in higher frequency density observed is likely due to digitization noise.

Figure 21 depicts how often each resolution achieved the minimum Levenshtein Distance value, indicating the optimal Levenshtein Distance performance across various resolutions for each image. Notably, the 1200 dpi resolution did not achieve the best results for any of the 18 images assessed. In contrast, the 150 dpi resolution achieved the best outcomes in terms of the minimum Levenshtein Distance for 8 of the 18 images examined.

In some cases, as demonstrated in Figure 22, the identical Levenshtein distance outcomes were achieved across a range of five different resolutions. Specifically, the resolutions 150, 200, 300, 500, and 700 dpi all yielded the same text recognition results.

Therefore, in terms of choosing the best resolution equalizing all the digitizing aspects, it could be said that 200 dpi was the optimal resolution in this case, considering the identification of image

Figure 21 – Quantitative of image resolutions with minimal Levenshtein distance - 18 images (μ: mean, σ^2: variance).

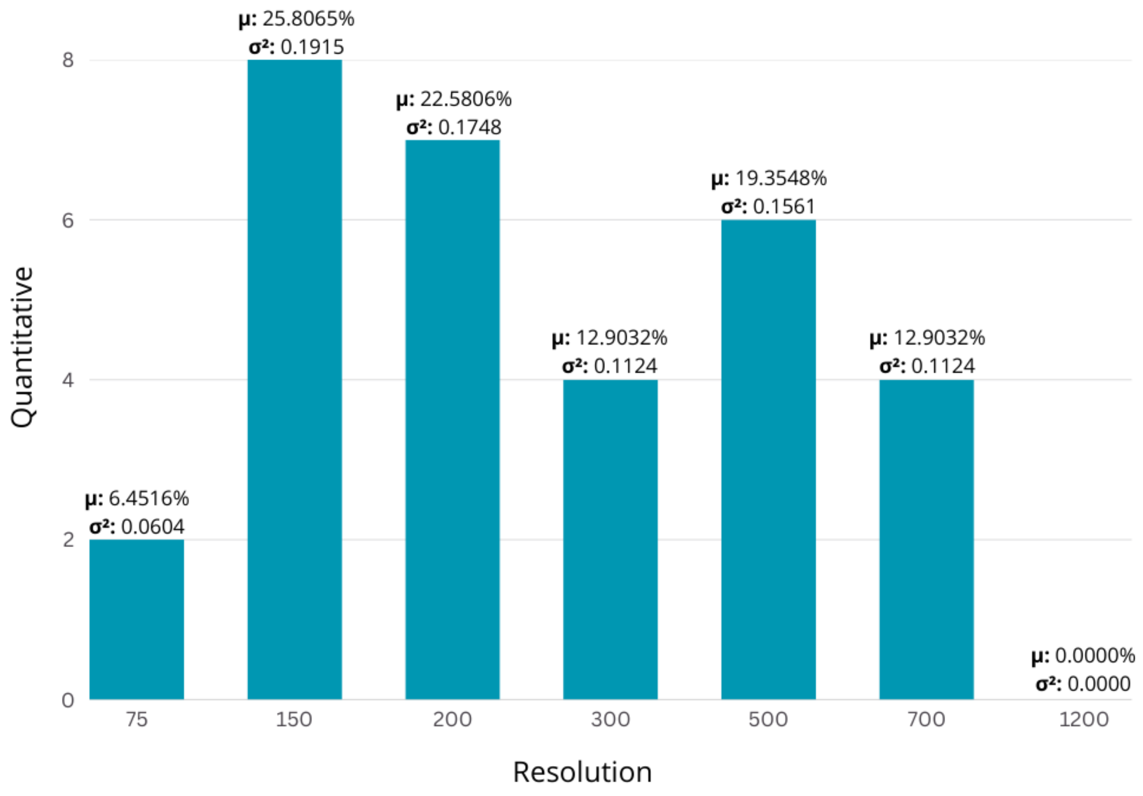

Source: The author (2024)

Figure 22 – Image illustrating the same Levenshtein Distance results to different resolutions.

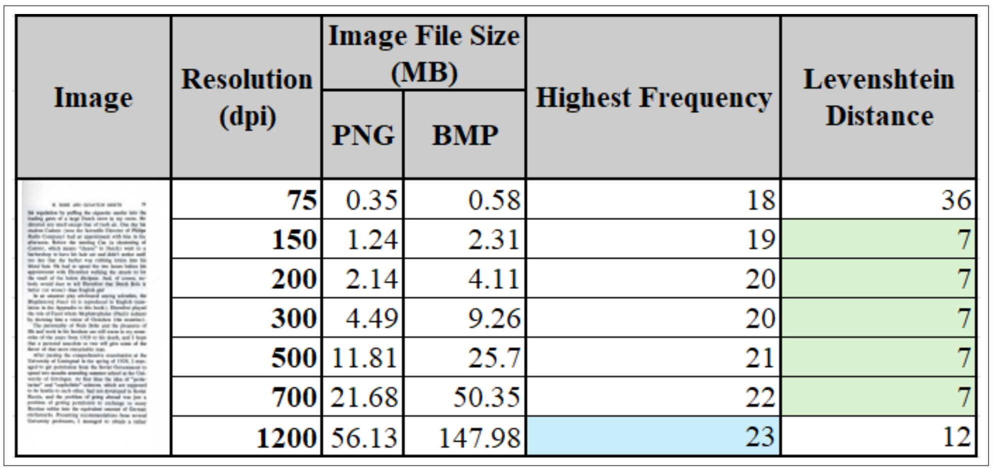

Image	Resolution (dpi)	Image File Size (MB)		Highest Frequency	Levenshtein Distance
		PNG	BMP		
	75	0.35	0.58	18	36
	150	1.24	2.31	19	7
	200	2.14	4.11	20	7
	300	4.49	9.26	20	7
	500	11.81	25.7	21	7
	700	21.68	50.35	22	7
	1200	56.13	147.98	23	12

Source: The author (2024)

details, file size and processing time linked.

The complete text dataset contains images with varying font sizes, ranging from 4 to 12 pt. When analyzing only the first ten images with a standard font size of 10 to 12 pt, Figure 23 shows that the best Levenshtein distance was generally achieved at 150 or 200 dpi. This suggests that these resolutions are likely aligned with the OCR training data. Notably, even for images with smaller text sizes, 150 and 200 dpi remained the best resolutions. Moreover, these results remain optimal even when evaluating all eighteen images, as illustrated in Figure 23, where the performance is more balanced across all resolutions.

However, the results may vary depending on the use of a dictionary in the OCR process and the structural characteristics of the pages, such as whether they contain single or double columns. In general, the best Levenshtein distance was consistently found at 150 or 200 dpi, demonstrating that these resolutions already provide good results in terms of information retention and preservation.

Figure 23 – Quantitative of image resolutions with minimal Levenshtein distance - 10 images (μ: mean, σ^2: variance).

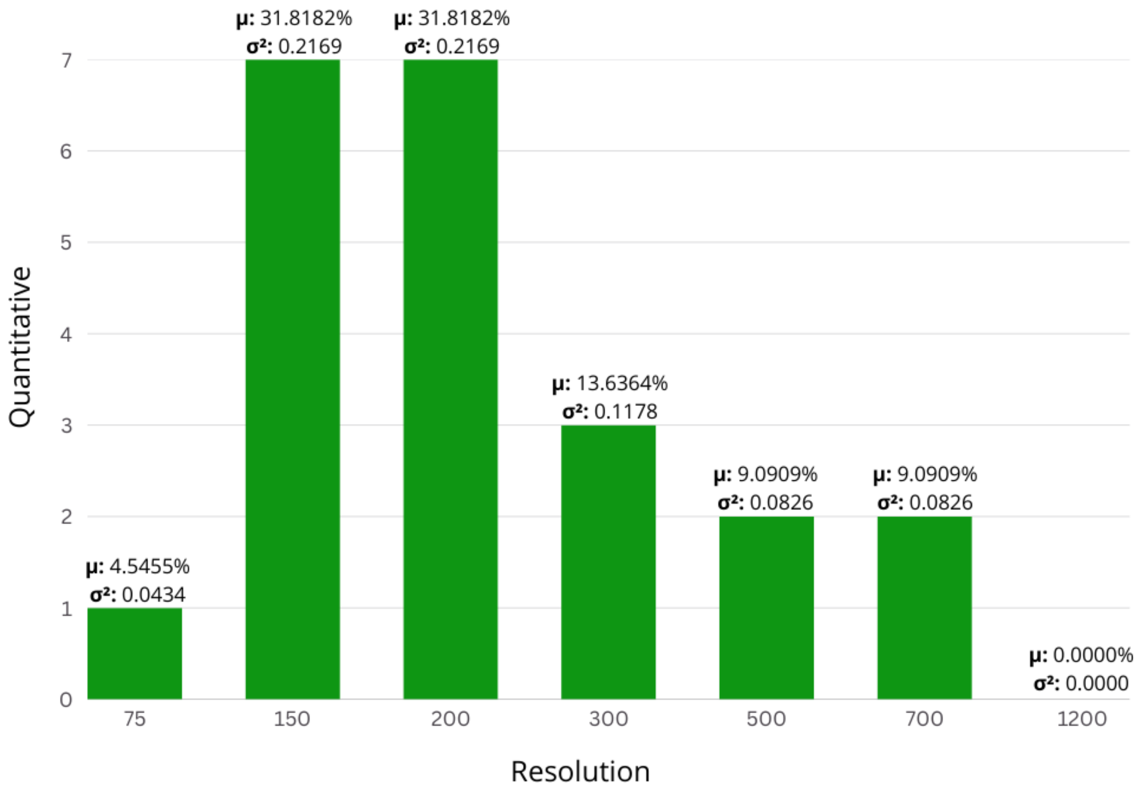

Source: The author (2024)

4.2 GENERAL DATASET

Table 7 display the results obtained using the scanner Epson L4160 for the colored images in the General Dataset. The information includes image size in cm, resolution in dpi, file size for both PNG and BMP formats in MB and the highest frequency for each image across the seven resolution levels.

Table 7 – General Dataset - Original images results. (**Image size** in centimeters (cm), **Font size** in points (pt), **dpi** - image resolution in dots per inch, **png/bmp** - file size of the png/bmp image in megabytes (MB), **HF** - Highest frequency).

Image	dpi	png	bmp	HF	Image	png	bmp	HF
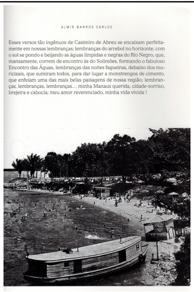	**75**	0.47	0.72	17	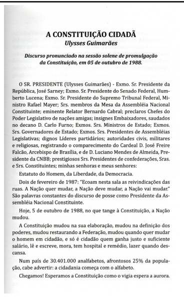	0.36	0.67	18
	150	1.75	2.88	19		1.18	2.66	19
	200	3.04	5.13	19		1.97	4.74	20
	300	7.23	11.54	20		4.01	10.66	21
	500	19.3	32.05	21		10.03	29.62	22
	700	36.61	62.8	22		17.38	58.03	22
13.75 x 21.00	**1200**	99.61	184.55	23	12.70 x 21.00	44.3	170.47	23
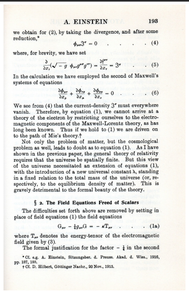	**75**	0.35	0.59	18	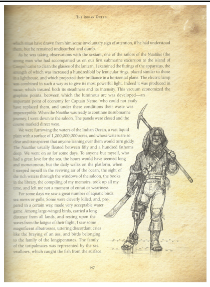	0.69	0.98	18
	150	1.25	2.37	19		2.54	3.9	19
	200	2.22	4.22	20		4.4	6.93	20
	300	4.91	9.48	20		11.78	15.59	21
	500	13.27	26.34	21		31.04	43.3	22
	700	24.71	51.64	22		60.25	84.83	23
12.29 x 19.34	**1200**	65.27	151.69	23	16.90 x 23.16	162.8	249.23	24
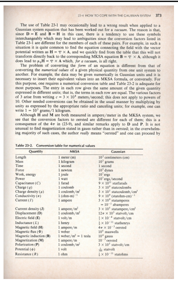	**75**	0.62	0.95	18	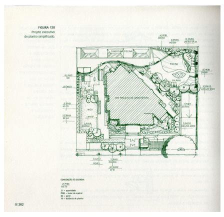	0.62	1	18
	150	2.23	3.78	20		2.48	3.99	20
	200	3.76	6.73	20		4.29	7.1	20
	300	8.5	15.12	21		10.4	15.97	21
	500	22.11	42.02	22		27.18	44.36	22
	700	41.49	82.31	23	20.49 x 19.54	52.34	86.92	23
15.41 x 24.65	**1200**	111.64	241.84	24		137.95	255.43	24
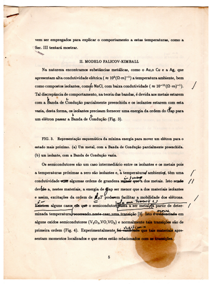	**75**	0.79	1.55	19		1.17	1.55	19
	150	2.89	6.22	20		4.28	6.22	20
	200	5.21	11.07	21		7.28	11.07	20
	300	12.22	24.89	21		16.61	24.89	21
	500	32.88	69.17	22		43.1	69.17	22
	700	62.73	135.52	23		79.64	135.52	23
21.00 x 29.67	**1200**	175.47	398.27	24	21.00 x 29.67	214.77	398.27	24

Image	dpi	png	bmp	HF	Image	png	bmp	HF
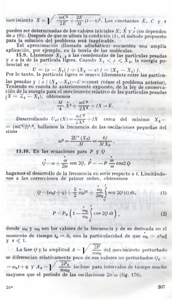	**75**	0.32	0.5	18		0.78	1.28	18
	150	1.12	2	19	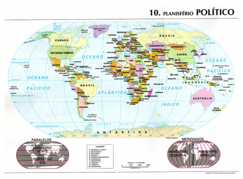	2.73	5.14	20
	200	1.91	3.56	19		4.91	9.13	20
	300	4.16	8.01	20		12.67	20.51	21
	500	10.81	22.25	21		33.31	56.97	22
	700	19.92	43.61	22	26.75 x 19.24	61.64	111.64	23
10.60 x 18.90	**1200**	52.31	128.08	23		166.26	328.13	24

Source: The author (2024)

Table 8 show the results obtained using the scanner Epson L4160 to digitize the binarized images in the General Dataset, presenting the same information present in Table 7 for each image across the seven resolution levels but with the tiff file size beyond the PNG and BMP formats.

Table 8 – General Dataset - Binarized images results (**Image size** in centimeters (cm), **Font size** in points (pt), **dpi** - image resolution in dots per inch, **png/bmp/tiff** - file size of the png/bmp/tiff image in megabytes (MB), **HF** - Highest frequency).

Image	dpi	png	bmp	tiff	HF	Image	png	bmp	tiff	HF
	75	0.01	0.24	0.01	17	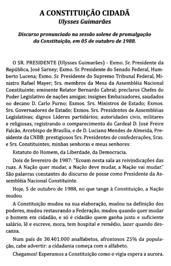	0.02	0.22	0.01	18
	150	0.04	0.96	0.02	19		0.05	0.89	0.02	19
	200	0.06	1.71	0.03	19		0.08	1.58	0.03	20
	300	0.15	3.85	0.08	20		0.15	3.56	0.04	21
	500	0.34	10.7	0.19	21		0.29	9.88	0.06	22
	700	0.61	20.94	0.31	22		0.44	19.35	0.09	22
13.75 x 21.00	**1200**	1.46	61.52	0.65	23	12.70 x 21.00	0.81	56.82	0.16	23
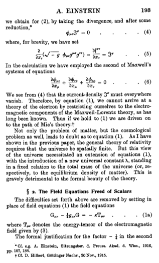	**75**	0.01	0.2	0.01	18	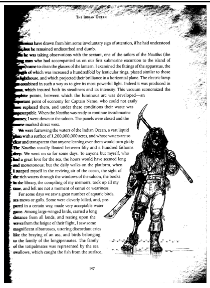	0.03	0.33	0.02	18
	150	0.04	0.79	0.02	19		0.08	1.3	0.04	19
	200	0.06	1.41	0.02	20		0.13	2.31	0.06	20
	300	0.12	3.16	0.03	20		0.3	5.2	0.19	21
	500	0.24	8.78	0.05	21		0.69	14.44	0.38	22
	700	0.37	17.21	0.08	22		1.3	28.29	0.7	23
12.29 x 19.34	**1200**	0.7	50.58	0.14	23	16.90 x 23.16	3.34	83.11	1.52	24

Image	dpi	png	bmp	tiff	HF	Image	png	bmp	tiff	HF
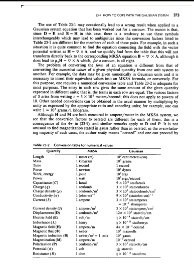	**75**	0.02	0.32	0.02	18	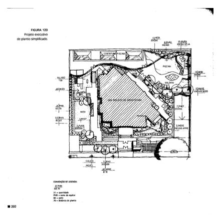	0.01	0.23	0.01	18
	150	0.07	1.26	0.03	20		0.02	0.34	0.01	18
	200	0.11	2.24	0.04	20		0.06	1.33	0.02	20
	300	0.2	5.04	0.06	21		0.08	2.37	0.03	20
	500	0.42	14.01	0.09	22		0.35	14.79	0.14	22
	700	0.64	27.44	0.14	23	20.49 x 19.54	0.59	28.98	0.22	23
15.41 x 24.65	**1200**	1.2	80.61	0.25	24		1.32	85.14	0.42	24
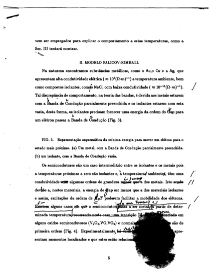	**75**	0.02	0.52	0.01	19	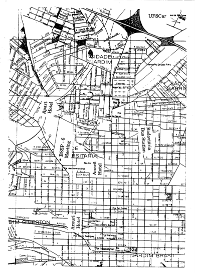	0.05	0.52	0.03	19
	150	0.06	2.07	0.02	20		0.14	2.07	0.05	20
	200	0.09	3.69	0.03	21		0.21	3.69	0.07	21
	300	0.18	8.31	0.06	21		0.37	8.31	0.12	21
	500	0.36	23.06	0.1	22		0.75	23.06	0.21	22
	700	0.56	45.2	0.16	23		1.15	45.2	0.31	23
21.00 x 29.67	**1200**	1.19	132.76	0.36	24	21.00 x 29.67	2.28	132.76	0.6	24
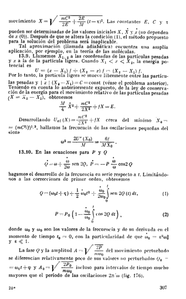	**75**	0.01	0.17	0.01	18	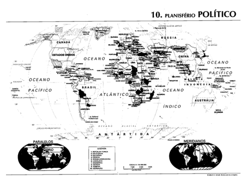	0.02	0.43	0.01	18
	150	0.03	0.67	0.02	19		0.07	1.71	0.04	20
	200	0.05	1.19	0.02	20		0.11	3.04	0.06	20
	300	0.1	2.68	0.03	20		0.31	6.84	0.22	21
	500	0.22	7.43	0.05	21		0.72	19	0.37	22
	700	0.33	14.55	0.07	22	26.75 x 19.24	1.27	37.22	0.53	23
10.60 x 18.90	**1200**	0.62	42.69	0.13	23		2.98	109.4	0.98	24

Source: The author (2024)

When analyzing the General Dataset, similar trends were observed regarding maximum frequency variation and spectral density as in the Text Dataset. For example, Figures 4 to 10 in Table 7 illustrate the spectral density across frequencies, showing that the density beyond the 200 or 300 dpi cutoff is minimal, a pattern consistent across all images tested in the dataset. Table 9 also illustrates the percentage of frequencies higher than the maximum frequencies obtained in 200dpi and 300dpi, demonstrating that higher resolutions do not result in a significant amount of higher frequencies.

Based on the observations, non-historically significant files can be digitized at 200 dpi, which results in raster file sizes 2.25 times smaller than those at 300 dpi and offers over twice the file size reduction in PNG format.

Table 9 – Proportion of highest frequency density above the maximum frequency of 200 and 300 dpi in the Text dataset - Original images

Image	dpi	Epson L4160		Epson L8180		HP M479FDW	
		200dpi	300dpi	200dpi	300dpi	200dpi	300dpi
	75	0.0000%	0.0000%	0.0000%	0.0000%	0.0000%	0.0000%
	150	0.0000%	0.0000%	0.0000%	0.0000%	-	-
	200	0.0000%	0.0000%	0.0000%	0.0000%	0.0000%	0.0000%
	300	0.0000%	0.0000%	0.0000%	0.0000%	0.1829%	0.0000%
	500	0.1739%	0.1739%	0.1991%	0.1991%	-	-
	700	0.3401%	0.3401%	0.3627%	0.3627%	-	-
13.75 x 21.00	**1200**	0.4561%	0.4561%	0.7504%	0.7504%	1.4719%	0.6643%
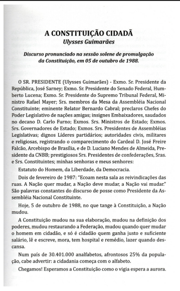	**75**	0.0000%	0.0000%	0.0000%	0.0000%	0.0000%	0.0000%
	150	0.0000%	0.0000%	0.0000%	0.0000%	-	-
	200	0.0000%	0.0000%	0.0000%	0.0000%	0.0000%	0.0000%
	300	0.1567%	0.0000%	0.1400%	0.0000%	0.1653%	0.0000%
	500	0.5437%	0.1614%	0.5848%	0.1904%	-	-
	700	0.8412%	0.3623%	0.8718%	0.3346%	-	-
12.70 x 21.00	**1200**	1.0642%	0.5784%	0.9640%	0.5272%	0.6736%	0.3319%
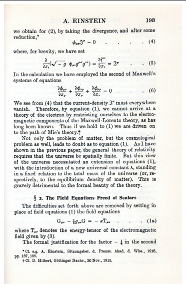	**75**	0.0000%	0.0000%	0.0000%	0.0000%	0.0000%	0.0000%
	150	0.0000%	0.0000%	0.0000%	0.0000%	-	-
	200	0.0000%	0.0000%	0.0000%	0.0000%	0.0000%	0.0000%
	300	0.1658%	0.0000%	0.1392%	0.0000%	0.2803%	0.0000%
	500	0.6387%	0.2244%	0.5532%	0.2114%	-	-
	700	0.9439%	0.4204%	0.8171%	0.3416%	-	-
12.29 x 19.34	**1200**	1.2231%	0.7238%	1.1250%	0.6915%	1.6518%	0.8943%
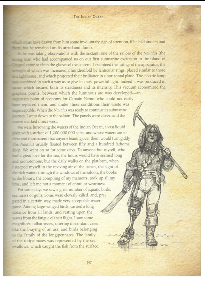	**75**	0.0000%	0.0000%	0.0000%	0.0000%	1.2229%	0.0000%
	150	0.0000%	0.0000%	0.0000%	0.0000%	-	-
	200	0.0000%	0.0000%	0.0000%	0.0000%	0.0000%	0.0000%
	300	0.1750%	0.0000%	0.2145%	0.0000%	4.5415%	0.0000%
	500	0.7548%	0.2599%	0.8297%	0.2478%	-	-
	700	1.4052%	0.5967%	1.5002%	0.5903%	-	-
16.90 x 23.16	**1200**	1.6978%	0.8975%	0.1737%	0.0000%	15.6025%	0.9139%
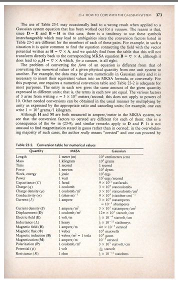	**75**	0.0000%	0.0000%	0.0000%	0.0000%	0.0000%	0.0000%
	150	0.0000%	0.0000%	0.0000%	0.0000%	-	-
	200	0.0000%	0.0000%	0.0000%	0.0000%	0.0000%	0.0000%
	300	0.2299%	0.0000%	0.2531%	0.0000%	0.2568%	0.0000%
	500	0.9183%	0.3665%	1.0455%	0.4420%	-	-
	700	1.3367%	0.6662%	1.5035%	0.7234%	-	-
15.41 x 24.65	**1200**	1.2570%	0.6966%	1.3554%	0.7342%	1.7939%	0.9430%

Image	dpi	Epson L4160		Epson L8180		HP M479FDW	
		200dpi	300dpi	200dpi	300dpi	200dpi	300dpi
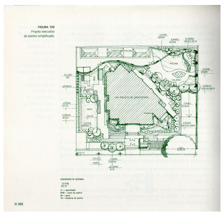	75	0.0000%	0.0000%	0.0000%	0.0000%	0.0000%	0.0000%
	150	0.0000%	0.0000%	0.0000%	0.0000%	-	-
	200	0.0000%	0.0000%	0.0000%	0.0000%	0.0000%	0.0000%
	300	0.1870%	0.0000%	0.0135%	0.0000%	0.1891%	0.0000%
	500	0.3562%	0.1450%	0.2116%	0.1864%	-	-
20.49 x 19.54	700	0.3787%	0.0958%	0.4905%	0.4638%	-	-
	1200	0.7148%	0.3492%	0.7261%	0.6995%	0.8922%	0.4309%
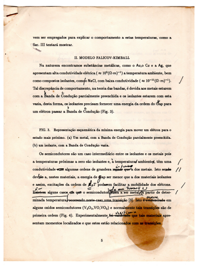	75	0.0000%	0.0000%	0.0000%	0.0000%	0.0000%	0.0000%
	150	0.0000%	0.0000%	0.0000%	0.0000%	-	-
	200	0.0000%	0.0000%	0.0000%	0.0000%	0.0000%	0.0000%
	300	0.1520%	0.0000%	0.1537%	0.0000%	0.1560%	0.0000%
	500	0.5009%	0.1817%	0.5374%	0.1549%	-	-
	700	0.6664%	0.3228%	0.7438%	0.3294%	-	-
21.00 x 29.67	1200	0.8160%	0.5120%	0.1691%	0.0000%	0.6554%	0.3202%
	75	0.0000%	0.0000%	0.0000%	0.0000%	0.0000%	0.0000%
	150	0.0000%	0.0000%	0.0000%	0.0000%	-	-
	200	0.0000%	0.0000%	0.0000%	0.0000%	0.0000%	0.0000%
	300	0.1652%	0.0000%	0.1521%	0.0000%	0.1327%	0.0000%
	500	0.3020%	0.1656%	0.2983%	0.1591%	-	-
	700	0.3620%	0.1034%	0.3502%	0.0973%	-	-
21.00 x 29.67	1200	0.4672%	0.2773%	0.4971%	0.2937%	0.6587%	0.3190%
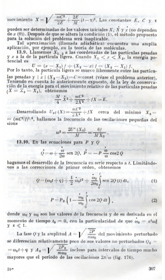	75	0.0000%	0.0000%	0.0000%	0.0000%	0.0000%	0.0000%
	150	0.0000%	0.0000%	0.0000%	0.0000%	-	-
	200	0.0000%	0.0000%	0.0000%	0.0000%	0.0000%	0.0000%
	300	0.2295%	0.0000%	0.1542%	0.0000%	0.1591%	0.0000%
	500	1.1176%	0.4638%	0.7368%	0.2220%	-	-
	700	1.4892%	0.7468%	1.0632%	0.4667%	-	-
10.60 x 18.90	1200	1.5833%	0.8906%	1.2826%	0.7881%	1.1653%	0.5329%
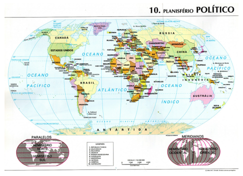	75	0.0000%	0.0000%	0.0000%	0.0000%	0.0000%	0.0000%
	150	0.0000%	0.0000%	0.0000%	0.0000%	-	-
	200	0.0000%	0.0000%	0.0000%	0.0000%	0.0000%	0.0000%
	300	0.1722%	0.0000%	0.1572%	0.0000%	2.0679%	0.0000%
	500	0.1495%	0.0093%	0.1572%	0.0196%	-	-
26.75 x 19.24	700	0.3703%	0.0994%	0.3599%	0.1028%	-	-
	1200	0.7404%	0.3279%	0.7280%	0.3697%	7.7849%	0.5799%

Source: The author (2024)

5 CONCLUSIONS

Professor George Nagy's inquiry regarding the most suitable scanner resolution for capturing all details and information from a document can be addressed by considering the optimal balance between quality and efficiency, particularly through the lens of the Nyquist-Shannon theorem. The analysis of spectral density and frequency maps of images is essential in determining the ideal digitization resolution, as it highlights the primary frequencies present in each image and reinforces the importance of operating within the limits established by this theorem.

As demonstrated in this study, scanning at 150 or 200 dpi generally captures all the essential details required for accurate OCR transcription of standard documents. These resolutions align well with the principles outlined by the Nyquist theorem, ensuring that necessary frequencies are adequately represented while maintaining manageable file sizes. This efficiency makes 150 dpi and 200 dpi the optimal minimum resolutions for storage and transmission, allowing for excellent lossless compression using formats like PNG for color images and TIFF-G4 for binary files.

Scanning at 300 dpi provides an additional "safety margin"by capturing finer details, which may be relevant for historical documents or those with very small text. While modern storage capacities and processing power can accommodate this higher resolution, it comes with trade-offs, including longer scanning times, increased storage requirements, greater network bandwidth usage, and extended processing durations. Notably, even with this increase in resolution, the primary frequency ranges of each image remain unchanged, as observed in the frequency maps and spectral density analyses. A comparative analysis with different scanners also confirms that increasing the resolution does not lead to a significant rise in higher frequency density. The slight increase observed is likely due to digitization noise rather than additional meaningful details.

Furthermore, this study has shown that binarizing document images does not significantly affect the maximum frequency captured, suggesting that increasing the digitization resolution beyond 300 dpi is generally unnecessary. Higher resolutions do not necessarily translate into proportional improvements in image quality and can lead to inefficiencies, such as increased scanning time, excessive storage and bandwidth consumption, and longer processing durations due to larger raster file sizes.

Thus, the findings suggest that resolutions between 150 and 300 dpi provide the best balance between quality and efficiency for most digitization needs, ensuring accurate OCR transcription and effective digital storage without unnecessary computational overhead.

REFERENCES

BARBOSA, R. d. S.; LINS, R. D.; LIRA, E. D. F. D.; CAMARA, A. C. A. Later added strokes or text - fraud detection in documents written with ballpoint pens. In: *2014 14th International Conference on Frontiers in Handwriting Recognition*. [S.l.: s.n.], 2014. p. 517–522.

BARBOZA, R. d. S.; LINS, R. D.; JESUS, D. M. d. A color-based model to determine the age of documents for forensic purposes. In: *2013 12th International Conference on Document Analysis and Recognition*. [S.l.: s.n.], 2013. p. 1350–1354.

BARNEY-SMITH, E. H. Characterization of image degradation caused by scanning. *Pattern Recognition Letters*, 1998.

BARNEY-SMITH, E. H.; ANDERSEN, T. Text degradations and ocr training. *Eighth International Conference on Document Analysis and Recognition, 2005. Proceedings*, 2005.

BUSHBERG, J. T. *The essential physics of medical imaging*. [S.l.]: Bushberg, Jerrold T., 2012.

BUSHONG, S. C. *Radiologic science for technologists: Physics, biology and protection*. [S.l.]: Elsevier, 2013.

COLARUSSO, P. et al. Raman and infrared microspectroscopy. *Encyclopedia of Spectroscopy and Spectrometry*, Elsevier, p. 1945–1954, 1999.

doxygen. *tesseract::Dict Class Reference*. 2015. Last accessed 29 Jan 2025. Available at: <https://tesseract-ocr.github.io/tessapi/3.x/a00362.html#aa94c8519d79413969cbf94c9a9efcbd1>.

DOXYGEN. *OpenCV: Open Source Computer Vision. In: Image Processing in OpenCV: Image Thresholding*. 2024. Last accessed Jan 09, 2024. Available at: <https://docs.opencv.org/3.4/d7/d4d/tutorial_py_thresholding.html>.

EPSON. *L4160 User's Guide*. [S.l.], 2019.

EPSON. *L8180 User's Guide*. [S.l.], 2021.

Federal Agencies Digital Guidelines Initiative. *Technical Guidelines for Digitizing Cultural Heritage Materials - Creation of Raster Image Files*. [S.l.], 2016.

FORSCHUNGSGEMEINSCHAFT, D. *DFG-Praxisregeln, „Digitalisierung“*. [S.l.], 2016.

GONZALEZ, R. C.; WOODS, R. E. *Digital image processing*. fourth. [S.l.]: Pearson, 2018.

HP. *MFP HP Color LaserJet Pro série M478-M479*. [S.l.], 2019.

KENNEY, A. R.; CHAPMAN, S. *Requisitos de resolucao digital para textos : metodos para o estabelecimento de criterios de qualidade de imagem*. Rio de Janeiro: Projeto Conservação Preventiva em Bibliotecas e Arquivos, 2001. Caderno temático produzido pelo Projeto Conservação Preventiva em Bibliotecas e Arquivos.

LATHI, B. P. *Linear Systems and Signals*. Second. [S.l.]: Oxford University Press, 2005.

LEE, E. A.; VARAIYA, P. *Structure and Interpretation of Signals and Systems*. Second. [S.l.]: Pearson Education, 2011.

LEVENSHTEIN, V. I. Binary codes capable of correcting deletions, insertions and reversals. *Soviet Physics - Doklady*, 1966.

LINS, R. D. Two decades of document processing in latin america. *Journal of Universal Computer Science*, v. 17, n. 1, p. 151–161, 2011.

LINS, R. D.; MELLO; DE, D. R. N.; OLIVEIRA, R. C. d. Which is the most suitable scanner resolution for documents? Detailing the answer given to the question raised by Professor George Nagy. *DocEng '24: Proceedings of the ACM Symposium on Document Engineering 2024*, 2024.

LINS, R. D. et al. ICDAR 2021 Competition on Time-Quality Document Image Binarization. In: *ICDAR 2021*. [S.l.: s.n.], 2021. p. 1539–1546.

MATPLOTLIB. *Matplotlib 3.5.3 documentation*. 2024. Last accessed May 15, 2024. Available at: <https://matplotlib.org/3.5.3/index.html>.

NAGY, G.; SETH, S. Hierarchical representation of optically scanned documents. In: SEVENTH INTERNATIONAL CONFERENCE ON PATTERN RECOGNITION. *Proceedings Volume 1*. Montreal, Canada: Computer Society Press, 1984. p. 347–349. ISBN 0-81860545-6.

NAVARRO, G. A guided tour to approximate string matching. *ACM Computing Surveys (CSUR)*, 2001.

Numpy. *Sorting, searching, and counting*. 2024. Last accessed Feb 3, 2024. Available at: <https://numpy.org/doc/stable/reference/routines.sort.html>.

NUMPY. *Statistics*. 2024. Last accessed May 15, 2024. Available at: <https://numpy.org/doc/stable/reference/routines.statistics.html>.

NUMPY. *What is NumPy?* 2024. Last accessed Jan 27, 2024. Available at: <https://numpy.org/doc/stable/user/whatisnumpy.html>.

OPPENHEIM, A. V.; WILLSKY, A. S.; NAWAB, S. H. *Signals Systems*. [S.l.]: Prentice Hall, 1994.

OTSU, N. A threshold selection method from gray-level histograms. *IEEE Transactions on Systems, Man, and Cybernetics*, v. 1, p. 62–66, September 1979.

PUGLIA, S. et al. *Technical Guidelines for Digitizing Archival Materials for Electronic Access: Creation of Production Master Files – Raster Images, For the Following Record Types- Textual, Graphic Illustrations/Artwork/Originals, Maps, Plans, Oversized, Photographs, Aerial Photographs, and Objects/Artifacts*. [S.l.], 2004.

PYPI. *pytesseract 0.3.10*. 2024. Last accessed March 20, 2024. Available at: <https://pypi.org/project/pytesseract/>.

PyPi. *Python-Levenshtein 0.23.0*. 2024. Last accessed April 24, 2024. Available at: <https://pypi.org/project/Python-Levenshtein/#description>.

SHANNON, C. E. A mathematical theory of communication. *Reprinted with corrections from The Bell System Technical Journal*, 1948.

SHANNON, C. E. Communication in the presence of noise. *Proceedings of the IEEE*, 1949.

SHUWANDY, M. L.; ZAIDAN, B.; ZAIDAN, A.; ALBAHRI, A.; ALAMOODI, A.; ALBAHRI, O.; ALAZAB, M. Health authentication approach based 3d touchscreen and microphone sensors for real-time remote healthcare monitoring system: Comprehensive review, open issues and methodological aspects. *Computer Science Review*, 2020.

SIEBERT, W. M. *Circuits, Signals, and Systems*. [S.l.]: MIT Press, 1986.

SONKA, M.; HLAVAC, V.; BOYLE, R. *Image Processing, Analysis, and Machine Vision*. United States of America: Cengage, 2015.

tesseract-ocr. *Tesseract documentation: A list of useful control parameters and config files*. 2024. Last accessed 29 Jan 2025. Available at: <https://tesseract-ocr.github.io/tessapi/3.x/a00362.html#aa94c8519d79413969cbf94c9a9efcbd1>.

The Digital Library Federation Benchmark Working Group. *Benchmark for Faithful Digital Reproductions of Monographs and Serials*. [S.l.], 2002.

The Library of Congress. *Guidelines for Electronic Preservation of Visual Materials*. 2014. Last accessed June 5, 2024. Available at: <https://www.loc.gov/preservation/resources/rt/guide/guid_dig.html#dig9>.

Appendix

Appendix A – CROPPING ALGORITHM

Source Code 1 – Cropping Algorithm applied in the dataset.

```python
# Selecting the image
image_file = "Home_original" #@param ["Home_original","Callidus_original", "Saltu_original"]
selected_image = "Image 01" #@param ["Image 01", "Image 02", "Image 03", "Image 04", "Image 05", "Image 06", "Image 07", "Image 08", "Image 09", "Image 10", "Image 11", "Image 12", "Image 13", "Image 14", "Image 15", "Image 16", "Image 17", "Image 18", "Image 19", "Image 20", "Image 21", "Image 22", "Image 23", "Image 24", "Image 25", "Image 26", "Image 27", "Image 28"]

# Setting destination folder based on image_file
if image_file == "Callidus_original":
    cropped_folder = "Callidus_cropped"
elif image_file == "Saltu_original":
    cropped_folder = "Saltu_cropped"
elif image_file == "Home_original":
    cropped_folder = "Home_cropped"
else:
    raise ValueError("Invalid image_file. Choose 'Home_original' or 'Callidus_original'.")

image_resolutions = ["75ppp", "150ppp", "200ppp", "300ppp", "500ppp", "700ppp", "1200ppp"]

# Creating a list of paths to the original images
images_paths = [f"{images_path}/{selected_image}/{image_file}/{res}.png" for res in image_resolutions]

# Initializing the 'images' list before the loop
images = []

# Checking if images exist
timages = []
for path in images_paths:
    img = cv2.imread(path)
    if img is None:
        print(f"Error: Image not found at {path}")
    else:
        print(f"Image {path} loaded")
        images.append(img)

# Defining the cutting parameters
top = 0  # @param {type:"slider", min:0, max:85, step:1}
bottom = 5  # @param {type:"slider", min:0, max:90, step:1}
```

```
left = 2  # @param {type:"slider", min:0, max:75, step:1}
right = 12  # @param {type:"slider", min:0, max:75, step:1}
cut_values = {"Top": top, "Bottom": bottom, "Left": left, "Right": right}

# Function to crop and save the image
def cut_and_save(image, output_path, resolution, cut_percent=(top, bottom, left,
    right)):
    if image is not None:
        top, bottom, left, right = [int(p * max(image.shape) / 100) for p in
            cut_percent]
        cut_image = image[top:image.shape[0] - bottom, left:image.shape[1] -
            right]
        cv2.imwrite(output_path, cut_image)
        return cut_image
    else:
        print(f"The image ({resolution}) is empty.")
        return None

# Function to save the cutoff values in an Excel file
def save_cut_values(cut_values, excel_path):
    df_corte = pd.DataFrame([cut_values], columns=['Top', 'Bottom', 'Left', '
        Right'])
    df_corte.to_excel(excel_path, index=False)
    print(f"Cutoff values saved in: {excel_path}")

# Creating output path list of cropped images
output_paths = [f"{images_path}/{selected_image}/{cropped_folder}/{res}.png" for
    res in image_resolutions]

# Cropping and saving images
cut_images = []
for i, image in enumerate(images):
    resolution = image_resolutions[i]
    output_path = output_paths[i]
    cut_image = cut_and_save(image, output_path, resolution)
    cut_images.append(cut_image)

# Saving Cutoff Values to an Excel File
excel_path = f"{images_path}/{selected_image}/{cropped_folder}/excel_data/
    cut_values_{selected_image}.xlsx"

# Creating the directory if it doesn't exist
os.makedirs(os.path.dirname(excel_path), exist_ok=True)
save_cut_values(cut_values, excel_path)

# Showing images
titles_originais = [f'{selected_image} - Original ({res})' for res in
```

```
    image_resolutions]
titles_cut_images = [f'{selected_image} - Coropped ({res})' for res in
    image_resolutions]
exibir_imagens(images + cut_images, titles_originais + titles_cut_images, 2, 7)
```

Source: The author (2024)

Appendix B – OTSU BINARIZATION ALGORITHM

Source Code 2 – Otsu binarization Algorithm applied in the dataset.

```
# Selecting the image
image_file = "Home_cropped" #@param ["Home_cropped","Callidus_cropped", "
    Saltu_cropped"]
selected_image = "Image 01" #@param ["Image 01", "Image 02", "Image 03", "Image
    04", "Image 05", "Image 06", "Image 07", "Image 08", "Image 09", "Image 10",
    "Image 11", "Image 12", "Image 13", "Image 14", "Image 15", "Image 16", "
    Image 17", "Image 18", "Image 19", "Image 20", "Image 21", "Image 22", "Image
     23", "Image 24", "Image 25", "Image 26", "Image 27", "Image 28"]

image_resolutions = ["75ppp", "150ppp", "200ppp", "300ppp", "500ppp", "700ppp", "
    1200ppp"]

# Creating a list of paths to the original images
images_paths = [f"{images_path}/{selected_image}/{image_file}/{res}.png" for res
    in image_resolutions]

# Initializing the 'images' list before the loop
images = []

# Checking if images exist
timages = []
for path in images_paths:
    img = cv2.imread(path)
    if img is None:
        print(f"Error: Image not found at {path}")
    else:
        print(f"Image {path} loaded")
        images.append(img)

# Function to binarize and save the image
def binarize_and_save(image, output_path, resolution):
    if image is not None:
        # Converting the image to grayscale
        gray_image = cv2.cvtColor(image, cv2.COLOR_BGR2GRAY)

        # Applying Otsu thresholding to grayscale image
        _, binarized_image = cv2.threshold(gray_image, 0, 255, cv2.THRESH_BINARY
            + cv2.THRESH_OTSU)

        cv2.imwrite(output_path, binarized_image)
        return binarized_image
    else:
        print(f"The image ({resolution}) is empty.")
        return None

# Binarizing the images and saving them to the binarized_images list
binarized_images = []
for i, image in enumerate(images):
    resolution = images_paths[i].split("/")[-1].split(".")[0]
    output_path = f"{images_path}/{selected_image}/{image_file}/binarized_{
        resolution}.png"

    binarized_image = binarize_and_save(image, output_path, resolution)

    binarized_images.append(binarized_image)

# Showing the original and binarized images
titles_originais = [f'{selected_image} - Original ({images_paths[i].split("/")
    [-1].split(".")[0]})' for i in range(len(images))]
titles_binarized = [f'{selected_image} - Binarized ({images_paths[i].split("/")
    [-1].split(".")[0]})' for i in range(len(binarized_images))]
exibir_imagens(images + binarized_images, titles_originais + titles_binarized, 2,
     7)
```

Source: The author (2024)

Appendix C – SPECTRAL ANALYSIS ALGORITHMS

Source Code 3 – Fourier Transform Algorithm applied in the dataset.

```python
# Selecting parameters
selected_image = "Image 01"  #@param ["Image 01", "Image 02", "Image 03", "Image 04", "Image 05", "Image 06", "Image 07", "Image 08", "Image 09", "Image 10", "Image 11", "Image 12", "Image 13", "Image 14", "Image 15", "Image 16", "Image 17", "Image 18", "Image 19", "Image 20", "Image 21", "Image 22", "Image 23", "Image 24", "Image 25", "Image 26", "Image 27", "Image 28"]
image_file = "Home_cropped"  #@param ["Home_cropped", "Callidus_cropped", "Saltu_cropped"]
color_image = "Color Image"  #@param ["Color Image", "Binarized Image"]

# Image resolutions for analysis
image_resolutions = ["75ppp", "150ppp", "200ppp", "300ppp", "500ppp", "700ppp", "1200ppp"]

# Image paths
images_path = "/content/drive/MyDrive/ScanImages"
if color_image == "Color Image":
    images_paths = [f"{images_path}/{selected_image}/{image_file}/{res}.png" for res in image_resolutions]
else:
    images_paths = [f"{images_path}/{selected_image}/{image_file}/binarized_{res}.png" for res in image_resolutions]

# Loading images
images = []
for path in images_paths:
    img = cv2.imread(path, cv2.IMREAD_GRAYSCALE)
    if img is not None:
        images.append(img)
    else:
        print(f"Error: Image not found at {path}")

def plot_images(images, titles, rows, cols, variables, frequencies):
    plt.figure(figsize=(18, 6 * rows))
    for i in range(len(images)):
        plt.subplot(rows, cols, i + 1)
        if i % cols == 1:  # Frequency Map
            im = plt.imshow(images[i], cmap='jet')
            plt.colorbar(im, ax=plt.gca(), fraction=0.05, pad=0.04)
        else:  # Original and Reconstructed Image
            plt.imshow(images[i], cmap='gray')
        plt.title(titles[i])
        plt.axis('off')
        if variables and frequencies and i % cols == 0 and i // cols < len(variables) and i // cols < len(frequencies):
            plt.text(0.5, 1.1, f"Variable: {variables[i // cols]}\nMax Frequency: {int(frequencies[i // cols])}",
                     horizontalalignment='center', verticalalignment='center', transform=plt.gca().transAxes)
    plt.tight_layout()
    plt.show()


def save_to_excel(variables, frequencies, excel_path):
    os.makedirs(os.path.dirname(excel_path), exist_ok=True)  # Ensure directory exists
    data = {'Variable': variables, 'Max Frequency': frequencies}
    df = pd.DataFrame(data)
    df.to_excel(excel_path, index=False)
    print(f'Data saved to {excel_path}')

def save_frequency_maps(frequency_maps, frequency_map_dir, image_variables):
    os.makedirs(frequency_map_dir, exist_ok=True)
    for i, freq_map in enumerate(frequency_maps):
        freq_map_path = os.path.join(frequency_map_dir, f"{image_variables[i]}_frequency_map.png")
        plt.imsave(freq_map_path, freq_map, cmap='jet')
    print(f'Frequency maps saved to {frequency_map_dir}')

# Fourier Transform and Frequency Analysis
def calculate_max_frequency(magnitude_spectrum):
    row_center, col_center = np.unravel_index(np.argmax(magnitude_spectrum), magnitude_spectrum.shape)
    return magnitude_spectrum[row_center, col_center]

# Configuring layout for data visualization
rows = len(images)
cols = 3  # Original Image, Frequency Map, Reconstructed Image
all_images = []
image_variables = []
frequencies = []
frequency_maps = []

for image_path in images_paths:
    image_variables.append(image_path.split("/")[-1].split(".")[0])

# Processing each resolution
for image in images:
    transform_image = np.fft.fft2(image)
    center_transform_image = np.fft.fftshift(transform_image)
    magnitude_spectrum = np.log(np.abs(center_transform_image) + 1)

    # Image Reconstruction and Frequency Map Saving
    reconstructed_image = np.abs(np.fft.ifft2(np.fft.ifftshift(
        center_transform_image))).astype(np.uint8)

    max_frequency = calculate_max_frequency(magnitude_spectrum)
    frequencies.append(max_frequency)
    frequency_maps.append(magnitude_spectrum)

    all_images.extend([image, magnitude_spectrum, reconstructed_image])

titles = ["Original Image", "Frequency Map", "Reconstructed Image"] * len(images)

# Display images and max frequency
plot_images(all_images, titles, rows, cols, image_variables, frequencies)

# Save results to Excel
output_excel_path = os.path.join(images_path, selected_image, image_file, "
    excel_data", f"{selected_image}_frequencies.xlsx" if color_image == "Color
    Image" else f"binarized_{selected_image}_frequencies.xlsx")
save_to_excel(image_variables, frequencies, output_excel_path)

# Save frequency maps
frequency_map_dir = os.path.join(images_path, selected_image, image_file, "
    frequency_maps")
save_frequency_maps(frequency_maps, frequency_map_dir, image_variables)
```

Source: The author (2025)

Source Code 4 – Spectral Density Plot Algorithm applied in the dataset.

```python
# Selecting parameters
selected_image = "Image 01"  #@param ["Image 01", "Image 02", "Image 03", "Image
    04", "Image 05", "Image 06", "Image 07", "Image 08", "Image 09", "Image 10",
    "Image 11", "Image 12", "Image 13", "Image 14", "Image 15", "Image 16", "
    Image 17", "Image 18", "Image 19", "Image 20", "Image 21", "Image 22", "Image
     23", "Image 24", "Image 25", "Image 26", "Image 27", "Image 28"]
image_file = "Home_cropped"  #@param ["Home_cropped", "Callidus_cropped", "
    Saltu_cropped"]
color_image = "Color Image"  #@param ["Color Image", "Binarized Image"]

# Image resolutions for analysis
image_resolutions = ["75ppp", "150ppp", "200ppp", "300ppp", "500ppp", "700ppp", "
    1200ppp"]
resolutions_dpi = ["75dpi", "150dpi", "200dpi", "300dpi", "500dpi", "700dpi", "
    1200dpi"]

# Create image paths
if color_image == "Color Image":
    images_paths = [f"{images_path}/{selected_image}/{image_size}/{res}.png" for
        res in resolutions]
else:
    images_paths = [f"{images_path}/{selected_image}/{image_size}/binarized_{res
        }.png" for res in resolutions]

# Load images, ensuring all are correctly loaded
images = [cv2.imread(path, cv2.IMREAD_GRAYSCALE) for path in images_paths]

# Define the default output format for images
pio.kaleido.scope.default_format = "png"

# Function to calculate spectral energy
def calculate_spectral_energy(magnitude_spectrum):
    return np.sum(magnitude_spectrum**2)

# Function to compute the maximum frequency
def calculate_max_frequency(magnitude_spectrum):
    row_center, col_center = np.unravel_index(np.argmax(magnitude_spectrum),
        magnitude_spectrum.shape)
    return magnitude_spectrum[row_center, col_center]

# Function to calculate the frequency distribution
def calculate_frequency_distribution(magnitude_spectrum):
    hist, bins = np.histogram(magnitude_spectrum.flatten(), bins=50, range=(0,
        magnitude_spectrum.max()))
    hist = hist / hist.sum()
    predominant_frequencies = bins[:-1][hist > 0.1]
    return hist, bins, predominant_frequencies

# Function to display and save frequency recurrence using Plotly
def plot_frequency_recurrence(hist, bins, title, xlabel, ylabel, save_path):
    fig = go.Figure()
    bin_width = bins[1] - bins[0]

    fig.add_trace(go.Bar(
        x=bins[:-1],
        y=hist,
        marker=dict(color='#008000', line=dict(width=0)),
        width=bin_width,
        opacity=1.0
    ))

    fig.update_layout(
        title=title,
        xaxis_title=xlabel,
        yaxis_title=ylabel,
        plot_bgcolor="#E5E5E5",
        xaxis=dict(showgrid=False),
        yaxis=dict(showgrid=True, gridcolor="white"),
        bargap=0,
        bargroupgap=0,
    )

    fig.write_image(save_path, engine="kaleido")
    fig.show()

# Directory to save the graphs
save_dir = os.path.join(images_path, "espectral_density", selected_image,
    color_image, image_size, "original")
os.makedirs(save_dir, exist_ok=True)

# Apply processing steps for each resolution
frequencies = []
energies = []
titles = [f"{selected_image} - {res}" for res in resolutions_dpi]

for i, (image, res, res_dpi) in enumerate(zip(images, resolutions,
    resolutions_dpi)):
    if image is None:
        print(f"Image {res} was not loaded correctly, skipping...")
        continue

    transform_image = np.fft.fft2(image)
    center_transform_image = np.fft.fftshift(transform_image)
    magnitude_spectrum = np.log(np.abs(center_transform_image) + 1)

    max_frequency = calculate_max_frequency(magnitude_spectrum)
    frequencies.append(max_frequency)

    energy = calculate_spectral_energy(magnitude_spectrum)
    energies.append(energy)

    hist, bins, _ = calculate_frequency_distribution(magnitude_spectrum)

    save_path = os.path.join(save_dir, f"spectral_density_{res_dpi}.png")
    print(f"Saving graph at: {save_path}")
    plot_frequency_recurrence(hist, bins, f"{image_size} | Spectral Density - {
        titles[i]}: {color_image}", "Frequency", "Recurrence", save_path)

# Create DataFrame with results
data = {
    'Resolution': resolutions_dpi,
    'Max Frequency': frequencies,
    'Energy': energies
}
df = pd.DataFrame(data)

# Path to save the Excel file
output_excel_path = os.path.join(images_path, selected_image, image_size, "
    excel_data", f"{selected_image}_spectral_analysis.xlsx")
os.makedirs(os.path.dirname(output_excel_path), exist_ok=True)
df.to_excel(output_excel_path, index=False)
```

Source: The author (2025)

Appendix D – OCR AND LEVENSHTEIN DISTANCE ALGORITHM

Source Code 5 – OCR and the Levenshtein Distance Algorithm applied in the dataset.

```python
# Selecting parameters
selected_image = "Image 18"  #@param ["Image 01", "Image 02", "Image 03", "Image 04", "Image 05", "Image 06", "Image 07", "Image 08", "Image 09", "Image 10", "Image 11", "Image 12", "Image 13", "Image 14", "Image 15", "Image 16", "Image 17", "Image 18", "Image 19", "Image 20", "Image 21", "Image 22", "Image 23", "Image 24", "Image 25", "Image 26", "Image 27", "Image 28"]
image_file = "Home_cropped"  #@param ["Home_cropped", "Callidus_cropped", "Saltu_cropped"]
color_image = "Color Image"  #@param ["Color Image", "Binarized Image"]

# Image resolutions for OCR
image_resolutions = ["75ppp", "150ppp", "200ppp", "300ppp", "500ppp", "700ppp", "1200ppp"]

# Image paths
images_path = "/content/drive/MyDrive/ScanImages"
if color_image == "Color Image":
    images_paths = [f"{images_path}/{selected_image}/{image_file}/{res}.png" for res in image_resolutions]
else:
    images_paths = [f"{images_path}/{selected_image}/{image_file}/binarized_{res}.png" for res in image_resolutions]

# Loading images
images = []
for path in images_paths:
    img = cv2.imread(path, cv2.IMREAD_GRAYSCALE)
    if img is not None:
        images.append(img)
    else:
        print(f"Error: Image not found at {path}")

# Directory to save OCR results
output_dir = f"/content/drive/MyDrive/ScanImages/OCR_Results/{selected_image}/{image_file}/{color_image}"
os.makedirs(output_dir, exist_ok=True)

# Tesseract configuration to disable dictionary
tesseract_config = "--psm 6 load_system_dawg=0 load_freq_dawg=0"
ocr_texts = []

# Performing OCR and saving results
for i, image in enumerate(images):
    if image is None:
        print(f"Error processing image at {images_paths[i]}")
        continue

    # Performing OCR
    text = pytesseract.image_to_string(image, config=tesseract_config)

    # Saving OCR result
    output_file = os.path.join(output_dir, f"{image_resolutions[i]}_nd_ocr_result
        .txt")
    with open(output_file, 'w') as file:
        file.write(text)
    ocr_texts.append(text)
    print(f"Extracted text for resolution {image_resolutions[i]} saved to {
        output_file}")

# Reading the reference text
def read_file(file_path):
    with open(file_path, 'r', encoding='utf-8') as file:
        return file.read()

reference_path = f"/content/drive/MyDrive/ScanImages/References/{selected_image}
    _reference.txt"
reference_text = read_file(reference_path)

# Computing Levenshtein distances
distances = []
for i, ocr_text in enumerate(ocr_texts):
    distance = levenshtein(reference_text, ocr_text)
    distances.append({
        'Resolution': image_resolutions[i],
        'Levenshtein Distance': distance
    })

# Saving results to Excel
output_lev_dir = f"/content/drive/MyDrive/ScanImages/Levenshtein_Dist/{
    selected_image}/{image_file}/{color_image}"
os.makedirs(output_lev_dir, exist_ok=True)
output_file_path = os.path.join(output_lev_dir, f"{selected_image}_nd_levenshtein
    .xlsx" if color_image == "Color Image" else f"binarized_{selected_image}
    _levenshtein.xlsx")
df = pd.DataFrame(distances)
df.to_excel(output_file_path, index=False)

print(f"Levenshtein distances saved to: {output_file_path}")
```

Source: The author (2025)